I. Detailed records of geomagnetic field behavior
from Death Valley and Hawaii

II. An age constraint on Gulf of California rifting
from Santa Rosalía, Baja California

Thesis by

John William Holt

in Partial Fulfillment of the Requirements
for the Degree of
Doctor of Philosophy

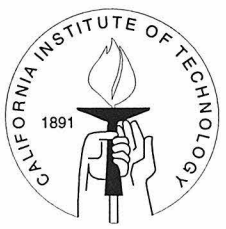

California Institute of Technology

Pasadena, California

1997

(Submitted February 5, 1997)

To my parents, Marguerite A. and William J. Holt

Science can tell us what is happening,
and how, but surely not why.

Edward Abbey

Acknowledgements

I thank Joe Kirschvink for giving me the independence to pursue science on my own terms, in my own way, and for his guidance which was always there when I asked for it. His enthusiasm and love for science was certainly a motivating factor. I also enjoyed working with Joann Stock, who always supported my interest in working in Baja California. My work with Xavier Quidelleur was one of the most rewarding aspects of my thesis research, in spite of having to travel all the way to Paris to perform the labwork. My associations with many colleagues around the world made my work more fun and interesting, and kept me on my toes. I especially thank Duane Champion, Rob Coe, Vincent Courtillot, Florence Garnier, Emilio Herrero-Bervera, Carlo Laj, Paul Renne, Warren Sharp, Brent Turrin, and Toshitsugu Yamazaki for their interest in and feedback on my work. I would also like to thank my thesis committee for taking the time to read my thesis and provide helpful comments. The committee consisted of Joe Kirschvink, Joann Stock, Dave Stevenson, Kerry Sieh, and Bruce Murray.

Bob Adams was the wise person who initially guided Joe Kirschvink to the Confidence Hills where I collected samples for much of my thesis research. We all miss him, especially when we're in his favorite environment, the desert. Many people helped me perform fieldwork in Death Valley, including my wife Liz Holt, Craig Scrivner, Ruth Warner, Jose Hurtado, several Ge124 classes, and of course Joe Kirschvink. I thank Jean Hsieh, Kathi Beratan and Bruce Murray for their important work on the sedimentology in the Confidence Hills and many discussions pertaining to my work there. Dragos Harabor and Liviu Mirica expertly measured many samples for me in the lab. I will always be indebted to and amazed by Vic Nenow, the master of everything electrical and mechanical,

for his help in my various laboratory projects. Aleen Boulatain was incredibly helpful at Caltech, expertly dealing with travel reports, accounts and purchase orders, always friendly . In the office, Ariel Anbar was a source of constant entertainment and inspiration, and he always made his window available for impromptu bottle-rocket launches. Jim "proofmaster" Spotila provided incredibly thorough reviews of several manuscripts, and Slawek Tulaczyk's insights into sedimentation processes were very helpful. I would like to thank Tim Melbourne and Rob Brady for sporadically dragging me away from work for some stress-relieving and panic-inducing rock climbing (or flailing, as the case often is). Many others, too many to list, were an important part of my experience here. I wish them the best and hope to stay in touch.

My wife Liz deserves more thanks than I can give here. My last year of graduate school was perhaps more difficult for her than for myself. Her support and love throughout the past five years made all of this much more enjoyable and much less stressful than it would have been otherwise (yes, it could have been more stressful!). Not only did she endure my preoccupation with work and my inability to relax, but she helped me with fieldwork in unpleasant conditions (read hot, dry, dusty, flooding, long hikes, heavy equipment, long hours...) in Death Valley and Baja California, and she gave me superb advice on all aspects of my research. She listened to nearly all of my presentations beforehand, giving me much-needed feedback on how to improve them. Most of all, she was always there for me.

Abstract

Detailed records of geomagnetic field behavior were produced and analyzed from Plio/Pleistocene sedimentary rocks of Death Valley, California and from Pleistocene/Holocene volcanic rocks of Hawaii. These records provide new information about geomagnetic field polarity reversals, excursions, secular variation, and the paleomagnetic recording process in sediments. In addition, a magnetostratigraphic and geochronlogic study of Mio/Pliocene marine sedimentary rocks in Baja California, Mexico was performed in order to provide a new age constraint on Gulf of California rifting.

The paleomagnetic studies in Death Valley were undertaken on siltstones, sandstones, and evaporites exposed along the southern Death Valley fault zone in the Confidence Hills. These rocks contain multiple records of the Réunion and Olduvai normal-polarity subchrons (2.15 - 2.13 Ma and 1.95 - 1.79 Ma, respectively) within rocks formed as a result of deposition in different subenvironments of a saline ephemeral lake, with an average deposition rate of ~ 30 cm/kyr. Variations in bedding attitudes between the exposed sections allow a fold test of paleomagnetic directions. Two records of the upper Olduvai polarity reversal were obtained which agree despite differences of lithology, depositional environment, and structural tilting. These records indicate several phases of polarity shifts during the transition of the geomagnetic field from normal to reversed polarity. Transitional virtual geomagnetic poles (VGP's) lie in longitudinal bands ~ 90° away from the sampling site longitude, vastly different from VGP's produced by studies in other locations around the world but consistent with site-dependent trends of VGP paths observed in global data compilations. Studies of the anisotropy of anhysteritic remanence conclude that inclination shallowing in

sediments during periods of low ambient magnetic field intensity is a possible cause for this site dependence of VGP paths. However, some aspect of the transitional geomagnetic field is recorded by the sedimentary rocks of Death Valley whether or not inclination shallowing took place.

A detailed record of the Réunion normal-polarity subchron was obtained from one of the sections in the Confidence Hills. This record shows that the Réunion subchron was a single normal-polarity event of ~ 20 kyr duration, which is a significant finding due to the lack of previous data in this time interval. The presence of a lithofacies which contains disruptive anhydrite crystals dispersed throughout the matrix creates two small gaps in the record just prior to the normal-polarity Réunion interval. Remagnetizations within this lithofacies facilitate the interpretation of the depositional environment responsible for growth of the disruptive evaporites.

Samples of the 1 km core produced by the Hawaii Scientific Drilling Project (HSDP) provided the basis for a study of geomagnetic field excursions and secular variation during the past 400 kyr at Hawaii. This core consists of over 200 lava flows erupted from Mauna Loa and Mauna Kea volcanos. In contrast to previous hypotheses that the non-dipole field has been anomalously low in the central Pacific region for the past few hundred kyrs, the results of this study show that secular variation, and hence, the non-dipole field component, at Hawaii is consistent with secular variation elsewhere on the globe for the past 400 kyr. In addition, the data show evidence for a persistent axial quadrupole in the time-averaged field. This research also resulted in the first records of geomagnetic field excurions in the central Pacific which may be correlated with those found

elsewhere on the globe, lending support to the hypothesis that these are global events rather than local perturbations of the geomagnetic field.

Paleomagnetic and geochronologic studies of marine sedimentary rocks in the Santa Rosalía basin, Baja California Sur, show that despite the presence of local copper ore deposition, primary magnetic remanence directions may be obtained from most of the marine sandstones overlying the basement in that area. Using preliminary magnetostratigraphy and an $^{40}Ar/^{39}Ar$ isotopic age of 6.76 $\pm$ 0.45 Ma (1σ) obtained for a volcanic unit interbedded with the sandstones, a correlation with the geomagnetic polarity time scale was made possible, yielding an age of 7.1 $\pm$ 0.05 Ma for the base of the marine section. This provides a new age constraint on Gulf of Califonia rifting and may help to refine models of North America – Pacific plate boundary interactions during the period 12 - 3.5 Ma.

Table of Contents

Introduction

This thesis consists of five papers, three of which are published and two of which will be submitted shortly. The first four papers describe detailed paleomagnetic records of geomagnetic field variations and some of the problems associated with such records. The last paper documents an application of paleomagnetic and geochronologic techniques to a regional tectonic problem. The research which led to each of these papers is connected by paleomagnetism and its applications. The following summarizes the findings of this thesis, which are presented in considerable detail in the papers themselves.

Geomagnetic Field Variations.

The primary goal of this research was to obtain highly detailed records of past variations of the Earth's magnetic field. The Earth's natural magnetic field at the surface varies on time scales ranging from milliseconds to millions of years, resulting from both internal and external sources. This work has focused on geomagnetic variations of internal origin, presumed to be the result of geodynamo processes in the outer core, with time scales of the order 10^3 - 10^4 years. Of course, we are only dealing with that part of the geomagnetic field which is measurable at the surface, which presently may be represented by a dipole field with some higher-order influences.

Since historical measurements of the geomagnetic field are available for only the past few hundred years, information about variations on longer time scales must be obtained from the geologic record. The geomagnetic field variations which

may be studied in the geologic record include polarity reversals, excursions (brief swings of polarity which return to the previous state), and secular variation (here limited to semi-periodic changes of the order 10^3 - 10^4 years). Indeed, it is from the geologic record that reversals of geomagnetic field polarity and excursions were discovered. A polarity reversal is generally defined as a globally observed 180° change in the dipole field averaged over a few thousand years.

For many years people have tried to understand why the Earth's magnetic field reverses polarity and what happens when it does. It is hoped that the two questions are intimately related and if one could be answered then the other answer could be deduced, but this is not yet known. The former question may be best answered through geodynamo modeling and is perhaps even a minor question compared to the overall geodynamo problem. However, these models do need real constraints, and answering the latter question may provide these constraints.

Hundreds of geomagnetic polarity reversals have occurred in the Earth's history, but since they take place in a geologically brief period of time (of the order 10^3 - 10^4 years), details of what happens during a polarity reversal are rarely preserved in the geologic record. The ambient magnetic field is generally recorded by magnetic minerals within rocks when the rocks are formed, so the ideal geologic environment to record the details of paleomagnetic field variations would be a place where rocks are formed rapidly and continuously, and are undisturbed by secondary processes which can mask the record, such as bioturbation, chemical alteration, or subsequent heating. In the course of this thesis research, two very different environments which meet several of these criteria were exploited for their paleomagnetic records of polarity reversals, excursions, and secular variation.

Another important aspect to consider for paleomagnetic records is the geographic distribution of sampling sites. Since the geomagnetic field is not everywhere uniform and does contain non-dipole components, it is imperative to obtain records of the same variations from widely spaced localities. Otherwise, in addition to natural ambiguities resulting from the recording process, the geographic extent of particular phenomena would be unknown. Death Valley and Hawaii are highly suitable in this aspect, not because of the physical separation between them (since different time periods were studied), but because the geomagnetic variations studied at each of these sites were previously studied at far removed locations.

Death Valley and the upper Olduvai reversal

The Confidence Hills in southern Death Valley is a place where in the past, rapid tectonic subsidence and a vast watershed helped to produce a sedimentary sequence of fine-grained siltstones, sandstones, and evaporites deposited in an ephemeral saline lake setting. As described in Paper 1, these sediments underwent burial and compaction before being tilted and uplifted along the southern Death Valley fault zone. Multiple stream cuts expose multiple sections of the same geologic sequence, offering different rock lithofacies from the same time period. This is important for determining the effect of sedimentary environment on the paleomagnetic record. Furthermore, these sections are tilted to different degrees, enabling us to perform a fold test which helps to establish the primary nature of the magnetic remanence. The high degree of tilt (45° - 110°) makes a present-day field overprint easy to discern from a primary magnetization. These factors enable us to check the paleomagnetic record in multiple ways, whereas

typically it is difficult to perform even one of these tests. The fact that so many internal tests are present in this location makes it one of the most unusual and promising sites ever located for such a study.

Magnetostratigraphy and the correlation of a volcanic ash with the ca. 2.1 Ma Huckleberry Ridge Ash showed that the time interval represented by the Death Valley sedimentary rocks is approximately 2.3 Ma - 1.5 Ma. During this time, the Earth's geomagnetic field was dominantly of reversed polarity (the Matuyama reversed epoch), but during the intervals 2.15 - 2.13 Ma and 1.95 - 1.79 Ma it was normal polarity (Paper 1, Fig. 6). These two intervals are called the Réunion and Olduvai subchrons, respectively (also known as C2r.1n and C2n).

Paper 1 of this thesis is a study of the upper Olduvai reversal (normal to reversed polarity, 1.79 Ma). This work reports on two detailed records of the upper Olduvai reversal, with the first-ever fold test of transitional directions from a polarity reversal. They are obtained from the two principal exposures in the Confidence Hills, separated by 1.6 km and informally named Confusion Canyon and Death March Canyon. The sedimentary environments recording the upper Olduvai transition are different in these sections. The siltstones and sandstones of Confusion Canyon were deposited episodically in a sandflat setting marginal to an ephemeral lake, while the banded anhydrites of Death March Canyon were deposited more continuously in a wetter environment of lower energy, closer to the center of the ephemeral lake [*Beratan et al.*, in press]. The average sedimentation rate was determined to be approximately 30 cm/kyr for both of these sections, which is an order of magnitude higher than most deep-marine sedimentary environments, from which the bulk of paleomagnetic records are obtained.

Therefore, these records represent a considerable improvement in resolution over most available records of polarity reversals.

Features from both the Confusion Canyon and Death March Canyon records agree quite well. They both show what appears to be an aborted reversal before the final shift of polarity from normal to reversed, followed by a small "rebound" before a stable reversed-polarity state is achieved. Virtual geomagnetic poles (VGP's) from the transition zone in both records follow paths which are fairly well confined to longitudinal bands, indicating that the transitional field was not entirely random (Paper 1, Figs. 8a and 8b).

The upper Olduvai is a reversal which has been studied relatively well, with sampling sites in Europe, China, and now North America (this work). A simple test is to compare transitional directions for the same reversal from widely separated sites. If the transitional geomagnetic field is dipolar, then VGP's from each location should match, since by definition a VGP assumes a dipolar field geometry. Furthermore, a recent analysis of many paleomagnetic records of geomagnetic field reversals had shown that there was a predominance of transitional VGP's located within certain longitudinal bands, these being over the Americas and the antipodal band [*Laj et al.*, 1991; *Valet et al.*, 1992]. This being the first clear evidence for a repeating pattern in polarity reversals, it created quite a stir. The fact that it indicated a possibly dipolar transitional field was even more startling. One flaw in the data compilation, however, was that the sampling sites were not well distributed. In fact, very few sites were actually located within the "preferred" bands of longitude. This made the Death Valley location even more interesting because it is located within one of these longitudinal bands.

The only other study of the upper Olduvai with resolution comparable to that of the Death Valley section (but without the internal tests) was performed in Italy on shallow marine sediments [*Tric et al.*, 1991]. The latitudinal variations of the transitional virtual geomagnetic poles (VGP's) from that study are vaguely similar to those from Death Valley. However, the VGP's from Italy fell in longitudinal bands over the Americas, while the Death Valley VGP's were confined to longitudinal bands over the Atlantic, and to a lesser degree, the antipodal band (Paper 1, Fig. 9). These are definitely not within the "preferred" bands of longitude, and are in fact nearly 90° away. One explanation for this discrepancy is simply that the transitional field was not dipolar during the upper Olduvai reversal. Another observation, which warranted further investigation, is that the transitional VGP's from each of these sites are located in bands approximately 90° in longitude from their respective sampling sites. In fact, all of the available data for the upper Olduvai reversal are compared to show that their transitional VGP's are better grouped when the sampling sites are shifted to a common longitude than when they are in actual geographic coordinates (Paper 1, Fig. 10).

Sediments and transitional directions

At about the same time the results of Paper 1 were being formulated, it was noted that when all available sedimentary records of geomagnetic polarity transitions were combined, there was a clear tendency for VGP's to lie in longitudinal bands approximately 90° away from the sampling site [*Quidelleur and Valet*, 1994]. This could explain the "preferred" bands of longitude since most of the sampling sites were located about 90° away from them. Since the magnetic inclination at a particular site is 0°, or horizontal, when the VGP is 90° away, and there is no plausible geomagnetic field configuration which can everywhere

produce horizontal inclinations, this observation implied that something could be causing the paleomagnetic inclinations in sediments to be drastically flattened during a polarity reversal.

Therefore, in spite of the internal tests and the strong similarity between the two records produced in the Confidence Hills, it was supposed that the paleomagnetic directions during the polarity transition could possibly be affected by a previously undetected process, and that perhaps this process could occur in many sedimentary environments.

In order to further investigate this possibility, I collaborated with colleagues from the Institut de Physique du Globe de Paris and this resulted in Paper 2. We decided to test the hypothesis that inclinations could be greatly shallowed during a polarity reversal. The theoretical basis for this hypothesis is as follows. During periods of "normal" field intensity (i.e., not during a polarity reversal) the magnetic remanence of a sediment is controlled primarily by equant magnetic grains within the sediment. These are oriented or aligned by the ambient magnetic field which dominates over the gravitational forces acting on these particles. Elongate magnetic particles are oriented somewhat by the magnetic field and somewhat by gravity (they lie flat). Their magnetism contributes to a minor overall inclination shallowing, usually observed in sediments but attributed to compaction. When the geomagnetic field has a much lower intensity (an order of magnitude less), as during a polarity reversal, the equant grains are oriented more randomly than when the magnetic field is strong. Gravity has not changed, so its relative importance increases. The flat-lying elongate magnetic grains contribute a relatively greater amount to the total magnetic remanence of the sediment than the equant grains, effectively flattening the remanent inclination.

It is very difficult to directly test for inclination shallowing in rocks which were formed in an unknown magnetic field. Since laboratory redeposition experiments do not re-create the environment or the time scales which sedimentary rocks actually experience, it is desirable to measure a parameter closely related to the inclination and compare it to the physical orientation of the elongate magnetic grains within the rock.

In a novel experiment designed for this purpose, we compared directions of the anisotropy of anhysteritic remanence (AAR) with paleomagnetic directions across the upper Olduvai reversal, using samples from the two Death Valley sections. Anhysteritic remanence is achieved by subjecting a previously demagnetized sample to an alternating magnetic field of gradually decreasing amplitude, in the presence of a constant biasing field. When this is performed and measured in multiple independent directions on a sample, the AAR can be calculated. The AAR is usually represented by an ellipsoid whose shape mimics the anisotropy of the magnetic fraction responsible for remanence. If all magnetic grains were equant, non-interacting, and distributed uniformly, the rock would magnetize equally in all directions when a magnetic field is applied to it, and the AAR ellipsoid would be a sphere. In sediments, the ellipsoid is nearly always flattened or elongated with its minimum axis oriented perpendicular to bedding (Paper 2, Fig. 1) due to the presence of elongate magnetic grains, which generally lie flat. Therefore, a comparison of remanence inclinations with AAR measurements cannot be used to test the inclination-shallowing hypothesis. The comparison of declinations could be a useful test if they are affected by the same process, however.

The results of this experiment indicated that during the upper Olduvai polarity reversal, the observed paleomagnetic declinations more closely follow the declinations of the maximum axes of AAR than before or after the reversal (Paper 2, Fig. 2). This suggests that the acquisition of remanence is affected by reduced field intensities and is influenced by the sedimentary fabric during these times. Although this is an important finding that has implications regarding the validity of all sedimentary records of geomagnetic polarity transitions, the interpretation of the results as presented in Paper 2 should be viewed with some caution. This was a very limited study with a small number of samples and there are alternative interpretations to most of the results. Furthermore, the acquisition of anhysteretic remanence is quite different from a depositional or post-depositional remanence acquired purely through the physical rotation of magnetic particles. It was nevertheless a useful study to describe the technique and should be followed by a more extensive set of experiments designed to thoroughly test the hypothesis of inclination shallowing.

Although inclination shallowing may have some effect on the paleomagnetic record of the upper Olduvai reversal in Death Valley, it is clear from our study that at least some portion of the transitional geomagnetic field is preserved. We know this because two different records of this polarity reversal from sedimentary rocks with different lithologies, environments of deposition, and structural tilting show a high degree of correlation. There is no explanation available for the features common to both of these records other than the geomagnetic field. Thus inclination shallowing cannot always completely obscure the record of the transitional geomagnetic field, and information about this geologically rare phenomenon can still be gained from such records.

The Réunion event

In addition to polarity reversals themselves, the high rate of deposition of the Confidence Hills sedimentary rocks makes possible the study of extremely brief subchrons such as the Réunion event, which took place between approximately 2.15 - 2.13 Ma (Paper 3, Fig. 6). This subchron was first detected in normal-polarity lava flows on Réunion Island [*Chamalaun and McDougall*, 1966], but has rarely been found elsewhere. The slow rate of deposition in most marine environments combined with the smoothing effects of bioturbation precludes the existence of this brief subchron in most sedimentary records that span this period of time. At most, one or two normal-polarity stratigraphic horizons represented by one or two data points have been found at any given location . Despite the lack of data (or perhaps because of it), some researchers have proposed that there were actually two brief normal-polarity events in that time period [e.g., *Mankinen and Dalrymple*, 1979; *McDougall et al.*, 1992].

In the course of this research, we identified a record of the Réunion subchron in the Death March Canyon section of the Confidence Hills. Unfortunately, this interval is disrupted by faulting both in Confusion Canyon and in a third section recently reconnoitered. The Death March Canyon record was studied in detail. The primary result, described in Paper 3, is that the Réunion subchron appears to be a single normal-polarity event approximately 20 kyr in duration. The estimated ages of the reversals associated with this subchron, based on interpolation from the Huckleberry Ridge Ash, support the ages of 2.15 Ma and 2.13 Ma recently determined by the correlation of marine marl sequences with orbital parameters of the Earth [*Lourens et al.*, 1996].

The most challenging aspect of this work, besides the clearing of a large amount of slopewash from the section in Death March Canyon, was determining the effect of certain lithofacies on the paleomagnetic record. In contrast to the upper Olduvai reversal which was recorded entirely within sandstones and siltones in one section, and entirely within banded anhydrites in the other, the Réunion interval was comprised of siltstone, banded anhydrite, and a third lithofacies termed 'gypsiferous siltstone.' The first two lithofacies are good recorders of magnetic field directions (with the possible exception of inclination shallowing in the middle of a transition), as evidenced by the upper Olduvai study and the overall magnetostratigraphy from both Death March and Confusion Canyons. The gypsiferous siltstone, on the other hand, proved to be a different sort of rock altogether. The main difference between this rock and the banded anhydrite is that evaporites in the gypsiferous siltstone appear to have grown in-situ while the sediments were undergoing burial. In the banded anhydrite lithofacies, the evaporite appears to have grown at the surface, with little post-depositional growth.

The effect of this secondary or continued growth of evaporites is essentially a re-ordering of the matrix within the sediment. Primary depositional magnetizations are lost as the sediment is disrupted by continued growth of these evaporites. This particular type of remagnetization has never before been documented, and was only discovered after erratic paleomagnetic directions and low paleointensities were correlated with paleomagnetic samples which displayed dispersed evaporites within a siltstone matrix. These evaporites are virtually undetectable in unheated samples without resorting to optical microscopy. At the outcrop, their presence is most reliably detected by the absence of significant bedding planes.

An interpretation of the sedimentary environment which produces these gypsiferous siltstones is an extension of the work of others [*Hsieh and Murray*, 1996; *Beratan et al.*, in press] in which the sedimentary environments of the various lithofacies found in the Confidence Hills are described. The paleomagnetic record actually helps to decipher the history of evaporite growth in these rocks, suggesting that they grew as late as 9 - 25 kyr after deposition, as ion-rich water was evaporatively pumped through the sediments from the subsurface to the surface.

Fortunately, it appears that no large changes of the geomagnetic field were occurring when the gypsiferous siltstones were being deposited at the surface, and thus there are no significant gaps in the Réunion record (Paper 3, Fig. 7). The analysis of additional records may help to verify what this record shows. There are two records of this subchron recently produced from shallow-marine sedimentary rocks in southern Italy and lava flows in Ethiopia, and their unpublished data agree quite well with the Réunion record in Death Valley. Since these studies are not yet published, however, fair comparisons cannot be made.

This research and our studies of the upper Olduvai reversal point out the types of difficulties encountered in high-resolution paleomagnetic records from sedimentary rocks. As the time scale of the desired geomagnetic field information decreases, the relative importance of the process of magnetization in the sediments seems to increase. Therefore, considerable attention must be given to the sedimentary environment and the geological setting of a paleomagnetic record before an interpretation of the results can be made.

Hawaii

In volcanic rocks, the process of acquiring a magnetic remanence is completely different from that which occurs in sediments. Therefore, the problems associated with obtaining detailed records of geomagnetic field variations are also completely different. Paper 4 documents a study of paleomagnetic directions obtained from a sequence of over 200 basalt flows which span the past 400 kyr. In 1993, the Hawaii Scientific Drilling Project (HSDP) recovered a core that consisted predominantly of basalt to a depth of nearly 1 km on the Big Island of Hawaii, near Hilo (Paper 4, Fig. 1). This provided an excellent opportunity to study geomagnetic field variations at Hawaii in the last half of the Brunhes normal-polarity chron. The HSDP core is azimuthally unoriented, so absolute declination determinations are not possible (relative declination changes may be obtained in some circumstances). The inclination data alone are highly useful, however, and can address many of the critical issues. Paleointensity data are also available [*Garnier et al.*, 1996], albeit in a preliminary form at this time. The lower ~ 600 m of the core was deposited rapidly, and represents ~ 100 kyr of the shield-building phase of Mauna Kea. During this period, one flow was deposited on average every ~ 600 yrs, thus this is one of the highest-resolution volcanic records ever obtained for a time interval of that duration.

Volcanic records of geomagnetic field behavior in the central Pacific rarely span more than a few thousand years at a time due to extensive resurfacing of the islands by fresh lava flows, and sedimentary records recovered from deep-sea cores in the central Pacific have not provided the resolution and/or reliability necessary to study secular variation or geomagnetic field excursions. This lack of data has led to speculation. For example, based on limited paleomagnetic

data and historically low secular variation in that region, it was hypothesized that the geomagnetic field in the central Pacific has had an anomalously low non-dipole component for several hundred kyrs. Explanations ranged from shielding by a more metallic mantle below the Pacific to interaction of the Hawaiian hot spot with the geodynamo. Additionally, having such limited data from the geographically large Pacific region has contributed to a large gap in our knowledge about the global extent of known geomagnetic field excursions.

The HSDP record shows that contrary to the previous hypotheses, the geomagnetic field in the central Pacific has not had anomalously low secular variation in the past 400 kyr. The amount of variation in inclination is in complete agreement with global data compilations for this latitude, and with models of secular variation. This finding is supported by a study which was published shortly after Paper 4 which re-analyzed previous data from Hawaii with more restrictive criteria and improved statistical techniques [*McElhinny et al.*, 1996]. However, the HSDP record suggests that the amount of secular variation is highly variable over timescales of 10 - 50 kyr. This interpretation is highly dependent on the extrusion rate of lava flows, however.

Another significant result from the HSDP core is the first evidence for geomagnetic field excursions in that region, with the exception of one land-based record of an excursion on Hawaii which has not been dated [*Holt et al.*, 1994]. Two definitive excursions are recorded in the core and their age constraints, determined primarily from isotopic dating, strongly suggest that they correlate with excursions observed in paleomagnetic records elsewhere (Paper 4, Fig. 3). This provides important evidence that excursions may be global phenomena, resulting from some fundamental process within the geodynamo rather than localized

perturbations of the geomagnetic field. The relationship between excursions and secular variation has never been understood. Rather than being an extreme form of secular variation, as has been postulated previously, at least one excursion in the HSDP record appears to interrupt a consistent trend of secular variation (Paper 4, Fig. 4, Feature C), suggesting that the two geomagnetic field variations may have different, and possibly independent sources.

The study of paleomagnetic directions from the HSDP core provides a useful contrast to the sedimentary records of Death Valley. The type of information gained is quite different, yet related to the same problem. While there are fewer unknowns associated with the acquisition of magnetic remanence in volcanic rocks than there are in sediments, there are other sources of uncertainty which must be addressed. These are described in detail in Paper 4. Unfortunately, it is not common to have such a large number of volcanic flows available at a single location. In reality, it is often very difficult to positively correlate different volcanic exposures on land without producing considerable time gaps in the paleomagnetic record. The HSDP paleomagnetic data is therefore a unique resource which may provide the basis for further studies.

Constraining the Age of Gulf of California Rifting

This aspect of my thesis research was undertaken with the goal of helping to solve a specific geologic problem with the aid of paleomagnetism and geochronology. The Gulf of California exists due to the transfer of the Baja California peninsula to the Pacific plate and the establishment of the North American – Pacific plate boundary where the present Gulf is located. The history of this process has been ascertained to some degree from seafloor magnetic lineations located in and around the southern end of the Gulf and to the west of the peninsula [e.g., *Stock and Hodges*, 1989]. The onset of rifting is constrained to have occurred sometime between plate motion changes at ~ 12 Ma and the commencement of seafloor spreading in the southern Gulf at ~ 3.6 Ma. In between, the seafloor record provides little evidence for the timing of Gulf of California rifting. The details of rifting are important to understand because the Gulf of California is one of the best examples of continental rifting and the transfer of crust from one tectonic plate to another. This process is fundamental to the division and amalgamation of continents, which is a primary product of plate tectonics and a recurrent theme in geologic history.

Constraints on the age of Gulf of California rifting may come from various sources, but some of the most promising are the numerous outcrops of marine sedimentary rocks found along the Gulf margins. The paleontological record within these sedimentary rocks provides some constraints on age and distribution, but the uncertainties are large and themselves uncertain. Paleomagnetism and geochronology have the potential to provide much tighter age constraints on the formation of these marine rocks, and magnetostratigraphy could be a useful correlation tool for those areas where direct isotopic ages are not possible.

Since little of this type of work has been performed in the Gulf region, a pilot study was undertaken to determine the feasibility of these techniques.

The area selected for this study is the Santa Rosalía basin, Baja California Sur (Paper 5, Fig. 1). One advantage of this location is that excellent geologic maps and extensive descriptions of the sedimentary rocks are available due to copper mining in that area [*Wilson*, 1948; *Wilson and Rocha*, 1955]. However, the possible presence of hydrothermal alteration could be a disadvantage for paleomagnetism. Reconnaissance sampling was undertaken in portions of all three Miocene-Pliocene sedimentary formations in the area (Paper 5, Fig. 3). The two uppermost sampled formations proved to be too coarse-grained for paleomagnetic analyses, but the lowermost formation did not. Through careful demagnetization procedures, it was discovered that remagnetizations due to copper ore deposition in this formation are confined to discrete stratigraphic zones, and primary magnetic remanences are retained elsewhere.

An approximately 30-m section directly overlying the highly-eroded basement rocks was sampled and found to be of normal polarity. A volcanic deposit interbedded in the same formation was sampled for both paleomagnetism and geochronology. It was found to be of reversed polarity, and to have an $^{40}Ar/^{39}Ar$ isotopic age of 6.76 ± 0.45 Ma (1σ), obtained from plagioclase crystals. Using this age and polarity, in addition to the normal-polarity constraint at the bottom of the formation and a reversed-polarity magnetostratigraphic constraint at the top of the formation, correlation with the geomagnetic polarity time scale (GPTS) is possible, but uncertainties exist that depend on the average sedimentation rate and the exact age used for the volcanic unit. An analysis of the probabilities associated with each of the possible correlations shows that one correlation is by

far the most likely (Paper 5, Fig. 8), and yields an age for the base of the marine sequence of 7.1 ± 0.05 Ma (Paper 5, Fig. 9 and Table 2), which is a new and useful constraint on the age of Gulf of California rifting. Since this is just a single locality, however, it is desirable to extend this to other locations around the Gulf. Given the success at Santa Rosalía, it is reasonable to expect that many other marine-sediment localities would yield useful age constraints. It is worthwhile to note that without the experience gained from detailed paleomagnetic studies of the sedimentary rocks of Death Valley, the paleomagnetism of the Santa Rosalía rocks would have been much more confounding.

References

Beratan, K., J. Hsieh and B. Murray, Pliocene/Pleistocene stratigraphy and depositional environments, southern Confidence Hills, Death Valley, California, *GSA Special Paper on Cenozoic basins of the Death Valley region*, in press.

Chamalaun, F.H. and I. McDougall, Dating geomagnetic polarity epochs in Réunion, *Nature*, 210, 1212-1214, 1966.

Garnier, F., C. Laj, E. Herrero-Bervera, C. Kissel and D.M. Thomas, Preliminary determinations of the geomagnetic field intensity for the last 450 kyr from the Hawaii Scientific Drilling Project core, Big Island, Hawaii., *Journal of Geophysical Research*, 101, (B5), 11,665-11673, 1996.

Holt, J.W., R.L. Ripperdan and J.L. Kirschvink, Paleomagnetic data from Kilauea: A comparison of preliminary results from the Hawaii Scientific Drilling Project 1 km core with surficial flows at Puu Kapukapu (abs.), *Eos Transactions, American Geophysical Union*, 75, (44), 709, 1994.

Hsieh, J.C.C. and B. Murray, A ~24,000 year period climate signal in 1.7-2.0

million year old Death Valley strata, *Earth and Planetary Science Letters*, 141, 11-19, 1996.

Laj, C., A. Mazaud, R. Weeks, M. Fuller and E. Herrero-Bervera, Geomagnetic reversal paths, *Nature*, 351, 447, 1991.

Lourens, L.J., A. Antonarakou, F.J. Hilgen, A.A.M.V. Hoof, C. Vergnaud-Grazzini and W.J. Zachariasse, Evaluation of the Plio-Pleistocene astronomical timescale, *Paleoceanography*, 11, (4), 391-413, 1996.

Mankinen, E.A. and G.B. Dalrymple, Revised geomagnetic polarity time scale for the interval 0-5 m.y. B.P., *Journal of Geophysical Research*, 84, (B2), 615-626, 1979.

McDougall, I., F.H. Brown, T.E. Cerling and J.W. Hillhouse, A reappraisal of the geomagnetic polarity time scale to 4 Ma using data from the Turkana Basin, East Africa, *Geophysical Research Letters*, 19, (23), 2349-2352, 1992.

McElhinny, M.W., P.L. McFadden and R.T. Merrill, The myth of the Pacific dipole window, *Earth and Planetary Science Letters*, 143, 13-22, 1996.

Quidelleur, X. and J.-P. Valet, Paleomagnetic records of excursions and reversals: possible biases caused by magnetization artefacts, *Physics of the Earth and Planetary Interiors*, 82, 27-48, 1994.

Stock, J.M. and K.V. Hodges, Pre-Pliocene extension around the Gulf of California and the transfer of Baja California to the Pacific plate, *Tectonics*, 8, 99-115, 1989.

Tric, E., C. Laj, C. Jehanno, J.P. Valet, C. Kissel, A. Mazaud and S. Iaccarino, High resolution record of the Upper Olduvai Transition from Po Valley (Italy) sediments: support for dipolar transition geometry?, *Physics of the Earth and Planetary Interiors*, 65, 319-336, 1991.

Valet, J.P., P. Tucholka, V. Courtillot and L. Meynadier, Paleomagnetic constraints on the geometry of the geomagnetic field during reversals, *Nature*, 356, 400-407, 1992.

Wilson, I.F., Buried topography, initial structures, and sedimentation in Santa Rosalia area, Baja California, Mexico, *Bulletin of the American Association of Petroleum Geologists*, 32, (9), 1762-1807, 1948.

Wilson, I.F. and V.S. Rocha, *Geology and Mineral Deposits of the Boleo Copper District Baja California, Mexico*, U. S. Geological Survey, Professional Paper, 273, 1955.

I. Detailed records of geomagnetic field variations from Death Valley and Hawaii

Paper 1: The upper Olduvai geomagnetic field reversal from Death Valley, California: A fold test of transitional directions

John W. Holt

Joseph L. Kirschvink

Division of Geological and Planetary Sciences

California Institute of Technology

Pasadena, California 91125

First published in:

Earth and Planetary Science Letters

vol. 133, pp. 475-491, 1995.

Abstract

High-resolution records of the upper Olduvai geomagnetic field reversal were obtained from two localities within steeply dipping lacustrine sediments of the Confidence Hills, southern Death Valley, California. The difference in bedding attitude between the two localities allowed us to perform a fold test of both transitional and non-transitional paleomagnetic directions. This is the first positive fold test obtained for transitional directions from any geomagnetic field reversal. In addition, variations in lithology allowed a comparison of transitional records from different sedimentary environments. Alternating-field and thermal demagnetization reveals that most samples have either single or simple two-component magnetizations. The low-coercivity, low-blocking temperature component is most likely held by large multidomain grains of magnetite, and aligns with the present-day field when uncorrected for bedding orientation. The high-coercivity component is held primarily by single- and pseudo-single-domain titanomagnetite, as determined from standard magnetic studies and electron microscopy. This component is interpreted as a primary magnetic signature based on the presence of stratigraphically bound reversals in the tilt-corrected data and positive reversal tests. Short-term field variations can be correlated between the two records, and differences are readily explained by the recording process inherent to the two sedimentary environments. The sampling site is located within one of the "preferred" bands of transitional virtual geomagnetic poles (VGP's) [1-3], yet the transitional VGP paths from both localities are clustered within two primary longitudinal bands which are approximately 90° away from the sampling site longitude: one lies over the Atlantic ocean (10° - 50° W), and the other, antipodal to this (130° - 170° E). These bands are also inconsistent with eight previous studies of the upper Olduvai transition [4-9,3,10]. When all reported studies of

this reversal are examined, however, no global consistency exists. Instead, the transitional VGP's are better grouped in a sampling site reference frame.

1. Introduction

One of the most exciting and controversial developments in recent geomagnetic research has been the observation that virtual geomagnetic poles (VGP's) during polarity transitions appear confined to longitudinal bands centered over the Americas and Australasia [1-3]. This has stirred much debate regarding both the statistical significance of this observation [2,11-15] and the physical mechanism responsible for it. Laj et al. [2] claim that there may be a link between these paths and structure near the core-mantle boundary. They point out seismic evidence for colder regions in the lower mantle, and models of fluid flow in the outer core which show the region underlying these proposed paths to be ones where north-south flow predominates. Such correlations have profound implications. If these links turn out to be real, then geomagnetic phenomena in the core may eventually be tied to mantle dynamics [16]. However, there are at least two important issues relevant to this debate which need to be resolved. First, Egbert noted that preferred paths could be the result of nonuniform sampling site distribution [17]. Indeed, many of the sites with detailed records of Pliocene and Pleistocene reversals tend to be located in Europe and the West Pacific, roughly 90° away from the proposed longitudinal bands. Second, and more fundamental, is whether or not the studies which are used for these compilations have provided accurate records of transitional field behavior. Few of the transition studies published so far have provided any of the classical paleomagnetic tests which can place constraints on when the magnetizations were acquired.

A recent investigation into the relationship between the anisotropy of anhysteretic remanence (AAR) and paleomagnetic remanence implied that these sediments may not accurately record magnetic field directions during periods of low field intensity [18]. While the classical paleomagnetic tests performed in the study presented here do not directly address anisotropy issues, they place important constraints on such data and may be crucial to their interpretation. In this paper, we present multiple records of the upper Olduvai reversal obtained from these sediments which agree across a distance of 1.6 km, despite folding and changes in sedimentary environments.

2. Geologic Setting

2.1 Tectonic Setting

The Confidence Hills are located in southern Death Valley, California along the eastern flank of the Owlshead Mountains (Figure 1). Death Valley is in the south-western part of the Basin and Range geological province of North America, an area of late Cenozoic extension. The deep central segment of Death Valley is interpreted to be a pull-apart structure developed as a result of tension between segments of the right-lateral Death Valley and Furnace Creek fault zones [19].

An asymmetrical anticlinorium forms the bulk of the Confidence Hills, the axis of which runs nearly parallel to the western strand of the southern Death Valley fault zone. The Pliocene to early Pleistocene sedimentary rocks exposed there have been folded and uplifted as much as 200 m above the valley floor [20,21] . Bed-

ding is well preserved with dips ranging from approximately 20° to slightly overturned.

2.2 Rocks of the Confidence Hills

The sedimentary rocks sampled for this study belong to a fine-grained part of the Funeral Formation in southern Death Valley, California [22,20], and are within the proposed Confidence Hills Formation [23]. These rocks are dominated by fine-grained siliciclastic sediment and bedded gypsum/anhydrite deposited in marginal subenvironments of a saline lake [23]. There are no fossils present in these sediments, and no indicators of bioturbation or chemical alteration. Active erosional channels which cut nearly perpendicular to the bedding strike provide fresh outcrop in which to examine the stratigraphic sequence and collect relatively unweathered samples. We concentrated our efforts on two major erosional channels 1.6 km apart, informally named Death March Canyon and Confusion Canyon (Figure 1).

Each section is bounded by the western strand of the southern Death Valley fault at its base, and an angular unconformity at the top. The measured sections begin above the most severe disruption near the fault zone. The only stratum that can be visually correlated between the two sections is a 40-cm-thick grey ash layer, located at 90 m in Confusion Canyon and at 144 m in Death March Canyon. This ash layer has been chemically fingerprinted as the Huckleberry Ridge ash [24], and provides a key time constraint for the determination of specific polarity reversals in these sections. The Huckleberry Ridge tuff has been dated at 2.057 ± 0.008 Ma using the single-crystal $^{40}Ar/^{39}Ar$ method [25].

2.3 Sedimentology of the upper Olduvai interval in Confusion Canyon

In Confusion Canyon, the upper Olduvai transition is recorded in fine- to medium-grained, well-sorted sandstone with some thin, clay-rich layers. Bedding geometry is sheet-like, without cross-lamination. Bedding thicknesses range from a few centimeters to approximately 10 cm, with the majority being 5 - 10 cm. Thin-section examination reveals that the rocks are primarily composed of angular to sub-angular grains of quartz, feldspar, and opaque minerals with no signs of weathering. These grains were probably eroded from the nearby Mesozoic granitic rocks of the Owlshead Mountains (Figure 1). Using X-ray diffraction, Beratan et al. [23] found that the dominant clay-size minerals are plagioclase feldspar (approximately An-67), quartz, and mica, with minor amounts of smectite. This is consistent with deposition in an arid environment, where physical weathering is greatly dominant over chemical weathering. The sediments in this interval are interpreted to have been deposited on a sandflat, marginal to a saline lake, supplied by a fringing alluvial fan [23]. This is a depositional environment in which floodwaters disperse as unchanneled sheetfloods across a flat sand plain. Individual beds are probably deposited in single events. The presence of mudcracks indicate that in some instances subaerial exposure occurred between events. Bedding attitude in the transition zone is S74°E/ 82°SW(overturned).

2.4 Sedimentology of the upper Olduvai interval in Death March Canyon

In Death March Canyon, the upper Olduvai transition is recorded in banded anhydrite, which is composed of very-thin- to thin-bedded (from a few millimeters to several centimeters) anhydrite interbedded with siltstone and some fine-

grained sandstone. Bedding geometry is sheet-like, without cross-lamination. Bedding thickness ranges from a few millimeters to approximately 10 cm, with the majority being less than 5 cm. The siliciclastic layers contain essentially the same mineralogy as the rocks in Confusion Canyon, with smaller grain sizes. These sediments are interpreted to have been deposited in a saline mudflat marginal to a saline lake [23]. This indicates a more continuous depositional regime than the upper Olduvai interval in Confusion Canyon. Bedding attitude in the transition zone is N64°W/45°NE.

2.5 Deposition Rates

An average sedimentation rate was determined for the Olduvai subchron (1.95 - 1.79 Ma, [26]) in each canyon from magnetostratigraphy alone, and this is 28.4 cm/ky in Confusion Canyon, and 33.1 cm/ky in Death March Canyon, without any evidence for significant hiatuses. As will be shown later in detail, we were able to match short-term field variations in the two records and estimate the relative deposition rates between the two canyons for the interval spanning the upper Olduvai reversal. This method shows that during this interval, the average deposition rate in Death March Canyon was approximately 54% higher than that in Confusion Canyon, consistent with the sedimentary environment interpretations of Beratan et al. [23].

3. Methods

3.1 Sampling

Samples were collected with a gasoline-powered drill using air-cooled, diamond-tipped, 25 mm diameter coring bits. Sample orientation was determined using a brass orienting sleeve and a magnetic compass. A sun compass was determined to be unnecessary. Broken samples were repaired in the laboratory using alumina cement, and most samples were trimmed to a maximum length of 22 mm.

3.2 Measurements

Paleomagnetic directions

Measurements were made using a computer controlled, magnetically shielded SQUID magnetometer with a background noise level of 5×10^{-12} Am^2, located within a magnetically shielded room. All samples were subjected to both static three-axis alternating field (AF) and thermal demagnetization. AF demagnetization was performed first on all samples, usually up to a maximum of 10 mT in 1.25 mT steps. Thermal demagnetization was then used, from 100°C to 400°C in 50° steps, and then from 425°C to a maximum of 625°C in 25° steps. Multiple magnetization components were isolated using least-squares principal component analysis [27]. Due to the steep dip of bedding in these sections, a present-day overprint is easily distinguished from both normal and reversed primary magnetic directions.

Rock Magnetic measurements

Rock magnetic studies were undertaken in order to constrain the mineralogy and morphology of the magnetic components of these rocks. Small portions (approxi-

mately 0.05 g) of samples throughout the transition zones were disaggregated, placed in a 1 ml plastic epindorph tube and sealed. Experiments included (1) an acquisition of anhysteritic remanent magnetism (ARM) in a 100 mT alternating field, with progressively stronger background biasing fields between 0 and 2 mT as done by Cisowski [28], (2) the progressive AF demagnetization of the ARM after the 2 mT ARM acquisition, (3) the progressive AF demagnetization of a 100 mT isothermal remanent magnetization (IRM), and (4) IRM acquisitions in pulsed fields up to 800 mT.

Magnetic material was extracted from two samples within each of the transition zones and two outside of each transition zone for direct analysis. Extraction was accomplished by gentle disaggregation, dissolution in weak acetic acid, and magnetic separation. Analysis techniques included imaging by scanning electron microscope (SEM) with energy dispersive spectral (EDS) analyses and by transmisssion electron microscope (TEM) with spot diffraction analyses. Magnetic susceptibility of all samples was measured using a Bartington M.S.2 susceptibility meter before, during, and after heating.

Paleointensity measurements

Anhysteritic remanent magnetization (ARM) was induced in samples across the upper Olduvai transition after demagnetization in order to normalize the intensity of the primary magnetic component. The samples were subjected to a 50 μT biasing field with an alternating field of 80 mT peak. Relative paleointensity was estimated by normalizing the primary magnetization component by the induced ARM. This was preferred over susceptibility normalization because the carrier of

the ARM is more likely to be the same as the carrier of the primary remanence direction[29].

4. Results

4.1 Demagnetization

The intensity of the NRM for these samples was on the order of 10^{-1} A/m. Progressive demagnetization, as described above, allowed us to resolve multiple components of magnetization. For the vast majority of the samples, there were two clear components — a primary magnetization and a present-day field overprint (Figure 2). A few samples (some reversed-polarity samples in the upper part of the Death March Canyon section) exhibited single-component primary magnetizations (Figure 2c), without any apparent overprint. The magnetization of some samples became essentially zero or random at approximately 525° - 550° C, and heating was discontinued when this condition was reached.

The overprint, which is a low coercivity, low blocking temperature component, is removed by AF demagnetization at 10 mT and thermal demagnetization at 250° C. An equal area plot showing the direction of the low-coercivity component from all samples (normal, reverse, and transitional) showing two components is shown in Figure 3. The mean direction calculated from Bingham statistics [30] is very close to the present-day field for this locality, so this component is interpreted as being a viscous remanent magnetization (VRM). The demagnetization characteristics of this component indicate that it is held primarily by multi-domain magnetite grains and partially by goethite and/or maghemite.

In Figure 4, a typical sample's magnetization versus demag step is plotted. It is apparent that there is little overlap between the coercivity spectra of the two components of magnetization. The plot shows that the overprint component is not affecting the primary magnetization after the 250° C thermal step, and there is no consistent component in the direction orthogonal to the primary and overprint directions.

4.2 Rock Magnetism

Figure 5 shows a coercivity spectrum with results of the Lowrie-Fuller test [31] measured from a typical sample. For the IRM acquisition data, roughly 95% of the intensity is acquired after exposure to peak fields of less than 300 mT. This is indicative of magnetite with a small portion of higher coercivity material, such as hematite. The positive Lowrie-Fuller test (demag of ARM > demag of IRM) indicates that the primary magnetic carrier is relatively fine-grained material (single- or pseudo-single-domain size).

The results of direct SEM and TEM analyses indicate that titanomagnetite constitutes the magnetic fraction responsible for holding the stable primary remanence. One fraction consists of single- to pseudo-single-domain sized grains [32], ranging from 50 nm to 3 μm in size. These are either equant or slightly elongate prismatic grains, or clearly equant octahedral titanomagnetite crystals (with Ti/Fe ratio of approximately 0.25, from EDS analysis). Another fraction consists of tabular magnetite and titanomagnetite grains which are approximately 30 - 100 μm across. This larger size fraction is clearly multi-domain [32], and is probably the primary carrier of the magnetically soft overprint. In support of this conclu-

sion, none of these large magnetic grains were found in extracts from reversely magnetized samples above the Olduvai subchron in Death March Canyon which exhibited no overprint.

There was no detectable correlation of magnetic susceptibility with stratigraphic position. Susceptibility changes due to heating were less than 10%, without any consistent pattern. This indicates that there were no significant changes in mineralogy during heating. In samples which exhibited erratic behavior above approximately 525 - 550° C, some minor new magnetic phases may have formed during heating at higher levels but the primary remanence directions were well established by this level.

4.3 Magnetostratigraphy

Plots showing the overall magnetostratigraphy from both canyons are shown in Figure 6 correlated with the Geomagnetic Polarity Time Scale (GPTS) adapted from Harland et al. [33] with the astronomically calibrated ages of Hilgen [26] . The Reunion event is found in the lower part of each section, and the entire Olduvai subchron is recorded above the Huckleberry Ridge ash.

4.4 Non-Transitional Directions (Fold and Reversal Tests)

Two critical tests of the primary directions were performed on these sedimentary rocks — a reversal test and a fold test. Figure 7 shows non-transitional data from each section plotted on equal-area diagrams. Non-transitional data were restricted to time-equivalent strata from each section (163 - 260 m in Death March Canyon, and 102 - 195 m in Confusion Canyon, excluding the transitional

intervals defined below). The reversal test compares the mean directions of the normally and reversely magnetized strata, in order to test for antiparallel field orientations. The formulation of McFadden and McElhinny [34] was used to characterize this test. Both sections pass the common distribution test; therefore, the null hypothesis that the directions are antiparallel cannot be rejected at the 90% confidence level. For the analytical test, with one mean reversed through the origin, Death March Canyon's means have an observed angular difference of 2.98° and a calculated critical angle (95% confidence) of 7.51°. For Confusion Canyon, the observed angular difference is 1.43° with a critical angle of 5.85°. Thus, both sections also pass the the analytical test, with a "B" quality classification [34] .

The fold test compares primary directions from each section before and after tilt-correction to determine if the remanence was acquired before structural folding of the strata. This was implemented by comparing the same non-transitional directions as used in the reversal test (Figure 7). Before tilt-correction, the means from each canyon are distinctly different. After tilt-correction, the means are statistically indistinguishable, according to the method of Fisher [35]. This verifies that the sediments in both sections acquired their remanence before tilting of the strata.

The positive results from these two stability tests, along with the fact that stratigraphically bound polarity reversals are contained within the sections, show that these directions were acquired by the sediments at or soon after deposition. Since there are no significant changes in lithology or structure across the transition zone in either canyon, it follows that the sediments deposited during the transition should also pass the fold test, assuming that they had the ability to

record ambient magnetic field directions during the period of reduced field intensity. The actual changes in field direction are used to qualitatively assess the agreement of the two records within the transition zone, as discussed below.

The expected geocentric axial dipole inclination for the latitude of the Confidence Hills is 55.3°. The mean non-transitional inclination from both sections is approximately 44° ± 6° for normally magnetized strata and -47° ± 4° for reversely magnetized strata (Figure 7). Due to the uncertainties in the expected inclination due to the non-dipole inclination anomaly [36] and the error bars on the mean inclination, we can only estimate inclination shallowing due to compaction to be in the range 0 - 15°. Therefore, the exact effect on transitional directions due to any inclination shallowing is unknown. On the other hand, even if the maximum amount is chosen there is not a significant change in the major results of this study.

4.5 Transitional Data

Detailed plots of declination, inclination, virtual geomagnetic pole (VGP) latitude, and relative paleointensity through the upper Olduvai transition zone are plotted in Figure 8 as a function of stratigraphic level.

These intervals were defined by the broad decrease in paleointensity surrounding the main part of the reversal, and also by large fluctuations in the VGP latitude. Short-term variations in the field directions were used to adjust the chosen stratigraphic intervals from each canyon in order to obtain the best match. This resulted in a 13 m section of Death March Canyon being correlated with a 7 m section of Confusion Canyon. If this match is correct, then Death March Canyon had a 54% higher sedimentation rate than Confusion Canyon during this interval.

Based on these constraints and a slightly tighter transitional zone than shown in Figure 8, estimates of the duration of the upper Olduvai reversal range from approximately 9 - 18 ky.

The primary feature, an aborted reversal, is very distinctive, so we are confident that we are not correlating random directions. This aborted reversal includes a fast jump to low VGP latitudes followed by a gradual decay of the field back to normal polarity, and then a sudden jump to reversed polarity, followed by a brief rebound. This is very similar to the general VGP latitude behavior during the upper Olduvai reversal reported by Tric et al. [3] and Lee [10]. The sudden nature of the onset and termination of this feature could be due to rapid field behavior or to depositional hiatuses. There is no field evidence for any hiatus more significant than a typical bedding plane, however, so we feel that the field must be changing at least somewhat rapidly.

On the other hand, there are differences in the way the two sections record the transitional data. The sandflat depositional environment of Confusion Canyon produces a record that shows small jumps in the field directions, most of which are correlatable to directions in the more continuous deposition of the saturated mudflat environment of Death March Canyon. The individual beds in Confusion Canyon seem to record the field direction at the time of the deposition of the bed, with “lock-in” occuring before deposition of the next bed. Similarly, the return of VGP latitudes to low negative values (rebound) after the main reversal, which occurs from 227 - 227.8 m in Death March Canyon, appears to be only partially recorded in Confusion Canyon from 168.6 - 168.8 m.

The intensity of magnetization at the 250°C thermal step (the point at which the overprint was entirely removed in most samples) is shown normalized with these ARM values across the transition in Figure 8. The period of reduced field intensity is longer than the time during which the field reverses polarity. This is in agreement with other studies of the upper Olduvai [8,3]. The most noticeable feature of intensity during the middle of the reversal is the brief rise which accompanies the gradual return of VGP's to high latitudes after the aborted reversal (168.2 - 168.6 m in Confusion Canyon; 226 - 226.5 m in Death March Canyon)

4.6 VGP Paths

The tilt-corrected transitional VGP's from each section are displayed on global projections in Figure 9. The aborted reversal produced VGP's along the path which is to the west of the sampling site, while the full reversal occured along the path to the east of the sampling site. The rebound after the main reversal, which was recorded with more detail in Death March Canyon, also transgressed along the path east of the sampling site. The similarity of the two records is quite evident when the tilt-corrected data from both sections are combined in one VGP plot (Figure 9c).

5. Discussion

5.1 Comparison with other studies

An interesting result is that this sampling location lies within one of the longitudinal bands "preferred" by VGP's during reversals [1-3], whereas transitional VGP's

trace out paths which are approximately 90° away from the sampling site longtitude in either direction. We have plotted data from all available published records [37] of the upper Olduvai in Figure 10a. VGP longitudes of Lee [10] were corrected from original data. There is no clear geographic consistency in transitional paths produced for this reversal; furthermore, they do not particularly lie along the longitudinal band of the Americas or the antipodal band. Also apparent in Figure 10a is the observation that VGP longitudes resulting from our study are distinctly different from those of other detailed studies of the upper Olduvai.

A noteworthy similarity exists between the shifts in VGP latitudes found in our study and those reported by Tric et al. [3]. In both cases, there is a pronounced drop in VGP latitudes followed by a gradual recovery which is then followed by a sudden change in polarity with a brief rebound.

The transitional data from most of these studies appear to be better correlated in sampling site coordinates than in geographical coordinates. The transitional data is plotted with a common sampling site longitude in Figure 10b, and comparison with Figure 10a shows that the data is slightly better grouped in this reference frame. The VGP paths tend to be located approximately 90° - 120° away from the sampling site longitude for this reversal, with the notable exception of the study by Clement and Kent [7]. It should be noted that all of these records were obtained from sediments except for the study by Hoffman [9], which used volcanic rocks.

5.2 Reliability of transitional directions

Mechanisms for producing this phenomenon in sediments have been proposed, and involve the reduction in field intensity which accompanies reversals. The ability of the earth's field to align elongate magnetic particles in sediments, whether before, during, or after deposition, may become insufficient to overcome the gravitational force on the particle, resulting in shallow inclinations [38,15]. A mixture of elongate and equant particles could produce the same result through a slightly different mechanism – remanence may be dominated by field-oriented equant grains during normal intensity, and by gravity-oriented elongate particles during periods of low field intensity [18].

Determining whether either of these processes are actually occurring is a difficult problem, however. A preliminary anisotropy study was performed with the goal of addressing this issue [18]. The results indicated that remanence declinations for low-latitude VGP's may follow the directions of the maximum horizontal axes of the ellipsoids of anisotropy of anhysteretic remanence (AAR) more closely than those of high-latitude VGP's. This was interpreted to mean that during the transition when the field intensity is low, remanence is dominated by elongated grains aligned by forces other than the geomagnetic field, since equant grains would be more randomly oriented. While this is a plausible mechanism for producing VGP's which are far from the sampling site meridian, it has difficulty explaining the consistent behavior of the two records. The progressive and distinctive changes in direction during the reversal are similar in both sections, recording the aborted reversal, the main polarity shift, and the brief rebound. It is possible that the inclinations were severely shallowed while the declinations remained controlled by the magnetic field; however, this is not indicated by the preliminary anisotropy report [18] since the conclusions were based on declinations only. Correlations of VGP latitude changes as seen from different sampling sites may

provide a means to assess the magnitude of a shallowing effect. This hypothesis will be addressed in detail in a separate paper.

In any case, we are left with the observation that both sections in the Confidence Hills recorded similar successive changes in the geomagnetic field during the transition. It would be difficult to argue for a mechanism other than the geomagnetic field which could align magnetic particles in these two sedimentary environments 1.6 km apart. Although one could imagine water currents similarly aligning particles across large distances in some settings, it is highly unlikely that water currents played any role in the alignment of particles in the depositional environments described by Beratan et al. [23] for the Confidence Hills sediments.

6. Conclusions

In contrast to the conclusions of a recent anisotropy study [18], traditional tests of the paleomagnetic record in the Confidence Hills show that the upper Olduvai transitional directions are representative of the geomagnetic field. A consistent pattern in the upper Olduvai transitional data is seen across changes in depositional environment, lithology, and structural tilting. VGP's lie within longitudinal bands approximately ±90° away from the sampling site longitude. These bands are substantially different from those found in other studies of the upper Olduvai transition, and do not coincide with the so-called preferred bands of VGP longitude [1-3].

A comparison of all uppper Olduvai studies indicate a consistency in the separation of VGP paths from sampling site longitudes. This site dependency lends

support to the idea that paleomagnetic inclinations in sediments are greatly shallowed during periods of low field intensity [15]. This does not require that all of these records are incorrect or that they do not record any information about the geomagnetic field during transitions. Our study shows that although VGP's are 90° away from the sampling site and that remanence declinations may follow anisotropy declinations more closely during the transition [18], some part of the geomagnetic field is clearly recorded by the sediments.

In order to resolve the contradictions arising from apparent site-dependency, potential anisotropy issues, and traditional field tests, we need the complete array of paleomagnetic tools and methods. Redeposition experiments using the sediments found in these transition zones may provide useful information about their ability to preserve magnetic directions in the presence of weak fields. In addition, there are other reversals recorded in these Confidence Hills sections (Figure 6). Comparisons of the paleomagnetic records and magnetic fabric relationships of these other reversals will certainly play a major role in this effort.

Acknowledgements

We first thank Bob Adams for leading us to the Confidence Hills and pointing out their potential. We are grateful to Kathi Beratan, Jean Hsieh and Bruce Murray for all of their important work on the sedimentary record, and to Chris Pluhar for the initial paleomagnetic survey. Special thanks are due to Liz Warner Holt for field assistance and proofreading, and to Toshitsugu Yamazaki for assisting in magnetic separations and for performing TEM work. Helpful comments on the manuscript were received from two anonymous reviewers. We appreciate the

National Park Service allowing us to take paleomagnetic samples within the former Death Valley National Monument. We made extensive use of software provided by Craig Jones (cjones@mantle.colorado.edu) for the analysis and presentation of paleomagnetic data, and the GMT package [39] for global projections of VGP's. We appreciate obtaining the reversal atlas [37] from Joanna Athanassopoulos. Work on this project was funded by NSF grant No. EAR-9019289. This is California Institute of Technology Contribution No. 5436.

References:

[1] B.M. Clement, Geographical distribution of transitional VGP's: evidence for non-zonal equatorial symmetry during the Matuyama-Brunhes geomagnetic reversal, Earth Planet. Sci. Lett. 104, 48-58, 1991.

[2] C. Laj, A. Mazaud, R. Weeks, M. Fuller and E. Herrero-Bervera, Geomagnetic reversal paths, Nature 351, 447, 1991.

[3] E. Tric, C. Laj, C. Jehanno, J.P. Valet, C. Kissel, A. Mazaud and S. Iaccarino, High resolution record of the Upper Olduvai Transition from Po Valley (Italy) sediments: support for dipolar transition geometry?, Phys. Earth Planet. Inter. 65, 319-336, 1991.

[4] K.S. Burakov, B.Z. Gurarii, A.N. Kramov, G.N. Petrova, G.V. Rossanova and V.P. Rodionov, Some peculiarities of the virtual pole positions during reversals, J. Geomagn. Geoelectr. 28, 295-307, 1976.

[5] E. Herrero-Bervera, Some aspects of the geomagnetic field during polarity transitions, Ph.D. thesis, University of Hawaii, 202 pp., 1984.

[6] B.M. Clement and D.V. Kent, A comparison of two sequential geomagnetic

polarity transitions (upper Olduvai and lower Jaramillo) from the Southern Hemisphere, Phys. Earth Planet. Inter. 39, 301-313, 1985.

[7] B.M. Clement and D.V. Kent, Geomagnetic polarity transition records from five hydraulic piston core sites in the North Atlantic, In: W. F. Ruddiman, R. Kidd and E. Thomas, ed., Initial Reports DSDP,, 831 - 852, U.S. Government Printing Office, Washington, DC, 94, 1986.

[8] E. Herrero-Bervera and F. Theyer, Non-axisymmetric behaviour of Olduvai and Jaramillo polarity transitions recorded in north-central Pacific deep-sea sediments, Nature 322, 159-162, 1986.

[9] K.A. Hoffman, Long-lived transitional states of the geomagnetic field and the two dynamo families, Nature 354, 273-277, 1991.

[10] T.-Q. Lee, Study of the polarity transition record of the upper Olduvai event from Wulochi sedimentary sequence of the coastal range, eastern Taiwan, TAO 3, 503-518, 1992.

[11] C. Constable, Link between geomagnetic reversal paths and secular variation of the field over the past 5 Myr, Nature 358, 230-233, 1992.

[12] C. Laj, A. Mazaud, R. Weeks, M. Fuller and E. Herror-Bervera, Statistical assessment of the preferred longitudinal bands for recent geomagnetic reversal records, Geophys. Res. Lett. 19, 2003-2006, 1992.

[13] J.P. Valet, P. Tucholka, V. Courtillot and L. Meynadier, Paleomagnetic constraints on the geometry of the geomagnetic field during reversals, Nature 356, 400-407, 1992.

[14] P.L. McFadden, C.E. Barton and R.T. Merrill, Do virtual geomagnetic poles follow preferred paths during geomagnetic field reversals?, Nature 361, 342-344, 1993.

[15] X. Quidelleur and J.-P. Valet, Paleomagnetic records of excursions and

reversals: possible biases caused by magnetization artefacts, Phys. Earth Planet. Inter. 82, 27-48, 1994.

[16] V. Courtillot and J. Besse, Magnetic field reversals, polar wander, and core-mantle coupling, Science 237, 1140-1147, 1987.

[17] G.D. Egbert, Sampling bias in VGP longitudes, Geophys. Res. Lett. 19, 2353-2356, 1992.

[18] X. Quidelleur, J. Holt and J.-P. Valet, Confounding influence of magnetic fabric on sedimentary records of a field reversal, Nature 374, 1995.

[19] B.C. Burchfiel and J.H. Stewart, "Pull-Apart" origin of the central segment of Death Valley, California, Geological Society of America Bulletin 77, 439-442, 1966.

[20] L.A. Wright and B.W. Troxel, Geology of the northern half of the Confidence Hills 15-minute quadrangle, Death Valley region, eastern California: The area of the Amargosa chaos, California Division of Mines and Geology, Map Sheet 34, 1984.

[21] B.W. Troxel and P.R. Butler, Multiple Quaternary deformation, central part of the Confidence Hills, Death Valley, California: an example of folding along a strike-slip fault zone, Quaternary tectonics of southern Death Valley, California field trip guide, 1986.

[22] L.F. Noble, Structural features of the Virgin Spring area, Death Valley, California, Bull. Geol. Soc. Am. 52, 941-999, 1941.

[23] K. Beratan, J. Hsieh and B. Murray, Pliocene/Pleistocene stratigraphy and depositional environments, southern Confidence Hills, Death Valley, California, GSA Special Paper on Cenozoic basins of the Death Valley region submitted.

[24] B.W. Troxel, Sarna-Wojcicki and C.E. Meyer, Ages, correlations, and sources of three ash beds in deformed Pleistocene beds, Confidence Hills,

Death Valley, California., Quaternary Tectonics of Southern Death Valley, California field trip guide, 1986.

[25] A.M. Sarna-Wojcicki and M.S. Pringle, Laser-fusion 40Ar/39Ar ages of the Tuff of Taylor Canyon and Bishop Tuff, E. California - W. Nevada, EOS Transactions, 1992 Fall Meeting 73, 633, 1992.

[26] F.J. Hilgen, Astronomical calibration of Gauss to Matuyama sapropels in the Mediterranean and implications for the geomagnetic polarity time scale, Earth Planet. Sci. Lett. 104, 226-244, 1991.

[27] J.L. Kirschvink, The least-squares line and plane and the analysis of paleomagnetic data: examples from Siberia and Morocco, Geoph. J. Royal Astr. Soc. 62, 699-718, 1980.

[28] S. Cisowski, Interacting vs. non-interacting single-domain behavior in natural and synthetic samples, Phys. Earth Planet. Inter. 26, 56-62, 1981.

[29] S.K. Banerjee, J. King and J. Marvin, A rapid method for magnetic granulometry with applications to environmental studies, Geophys. Res. Lett. 8, 333-336, 1981.

[30] T.C. Onstott, Application of the Bingham distribution function in paleomagnetic studies, J. Geophys. Res. 85, 1500-1510, 1980.

[31] W. Lowrie and M. Fuller, On the alternating field demagnetization characteristics of multidomain thermoremanent magnetization in magnetite, J. Geophys. Res. 76, 6339-6349, 1971.

[32] S. Levi and R.T. Merrill, Properties of single domain, pseudosingle domain, and multidomain magnetite, J. Geophys. Res. 83, 309-323, 1978.

[33] W.B. Harland, R.L. Armstrong, A.V. Cox, L.E. Craig, A.G. Smith and D.G. Smith, A geologic time scale, pp., Cambridge University Press, Cambridge, 1989.

[34] P.L. McFadden and M.W. McElhinny, Classification of the reversal test in

paleomagnetism, Geophysical Journal Int. 103, 725-729, 1990.

[35] N.I. Fisher, T. Lewis and B.J.J. Embleton, Statistical Analysis of Spherical Data, 329 pp., Cambridge University Press, Cambridge, 1987.

[36] A. Cox, The frequency of geomagnetic reversals and the symmetry of the non-dipole field., Rev. Geophys. Space Phys. 13, 35-50, 1975.

[37] J. Athanassopoulos, M. Fuller, R. Weeks and I.S. Williams, Atlas of reversal records, Trans. Am. Geophys. Union EOS 74, 109, 1993.

[38] A. Chauvin, P. Roperch and R.A. Duncan, Records of geomagnetic reversals from volcanic islands of French Polynesia, 2. Paleomagnetic study of a flow sequence (1.2-0.6 Ma) from the island of Tahiti and discussion of reversal models, J. Geophys. Res. 95, 2727-2752, 1990.

[39] P. Wessel and W.H.F. Smith, Free software helps map and display data, EOS Trans. AGU 72, 445-446, 1991.

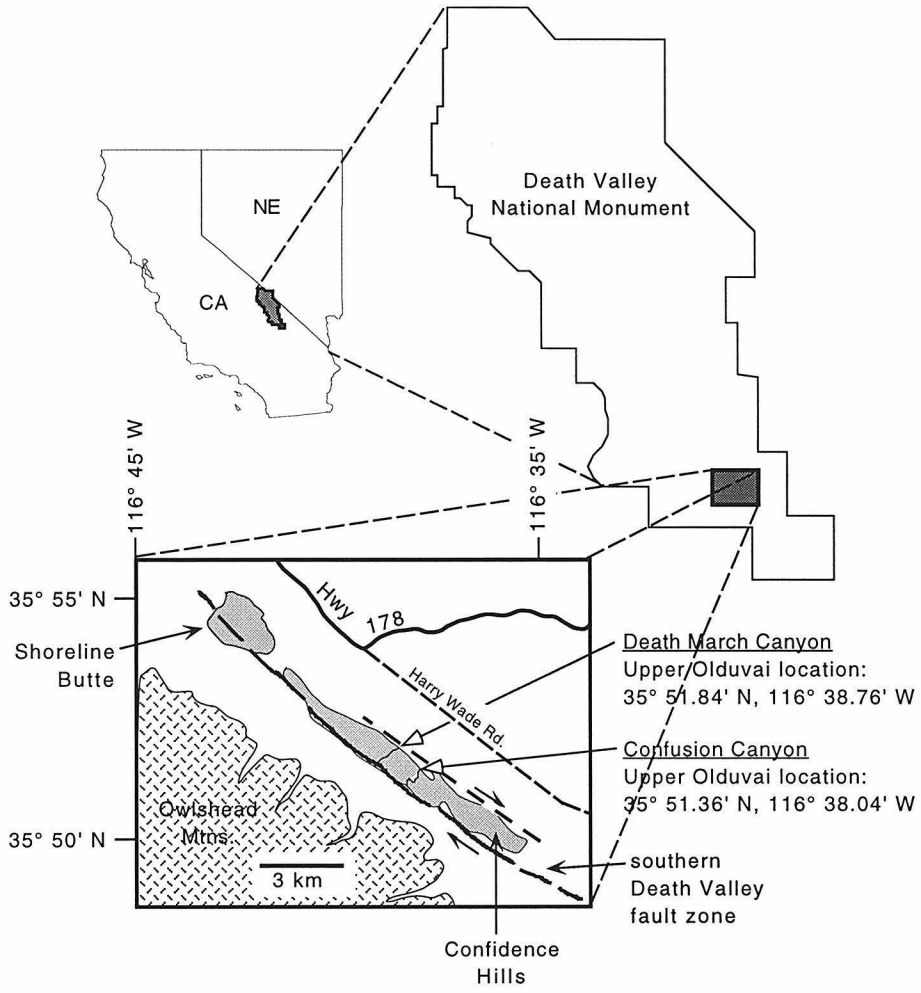

Figure 1. Location map of sampling sites within the Confidence Hills in southern Death Valley. Partially adapted from geologic map of Wright and Troxel [20].

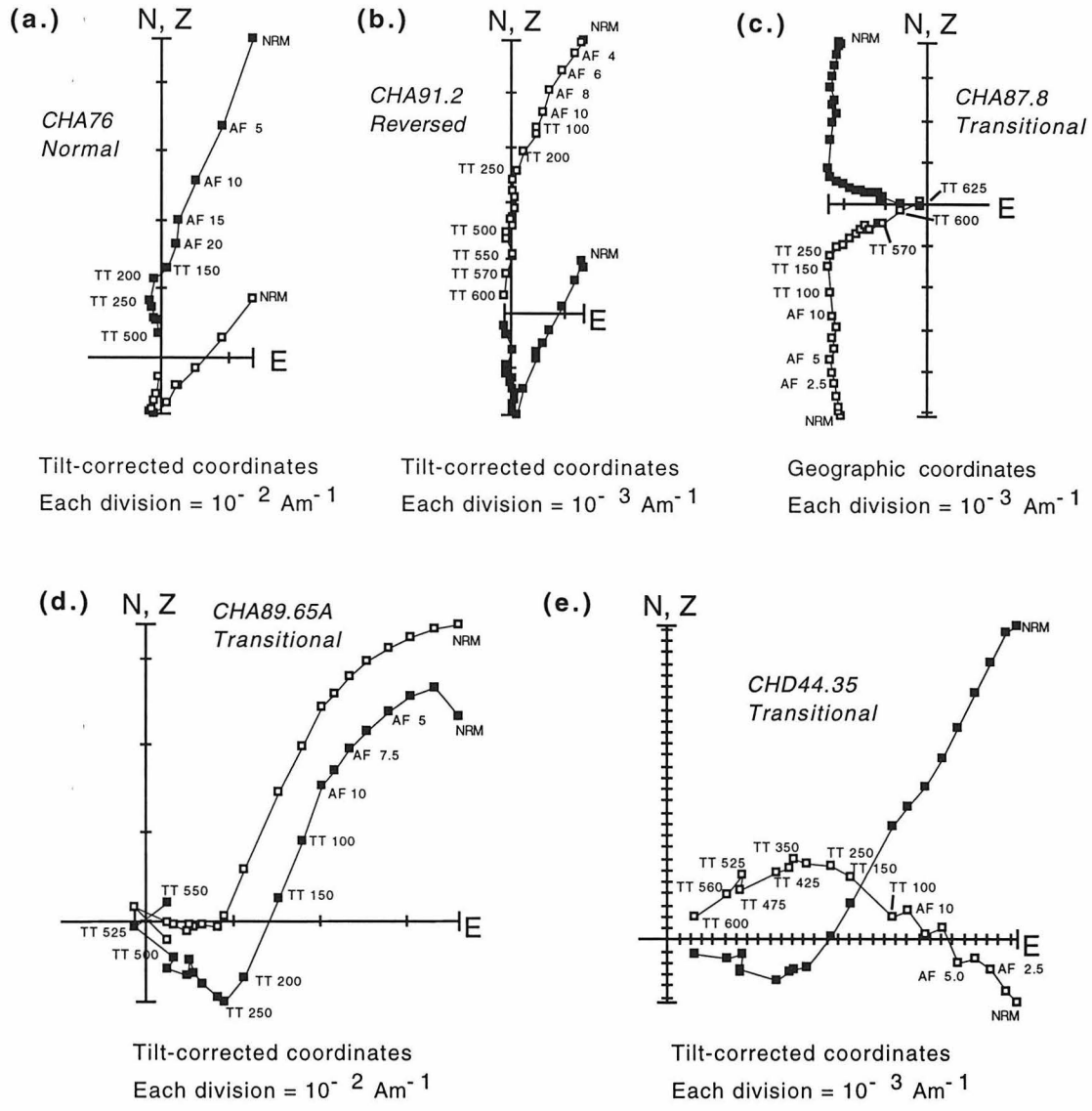

Figure 2. Sample demagnetization. Orthogonal projections of declination onto the horizontal plane (solid squares) and inclination onto the vertical plane (open squares) for typical two-component samples of (a) normal, (b) reversed, and (c- e) intermediate polarities.

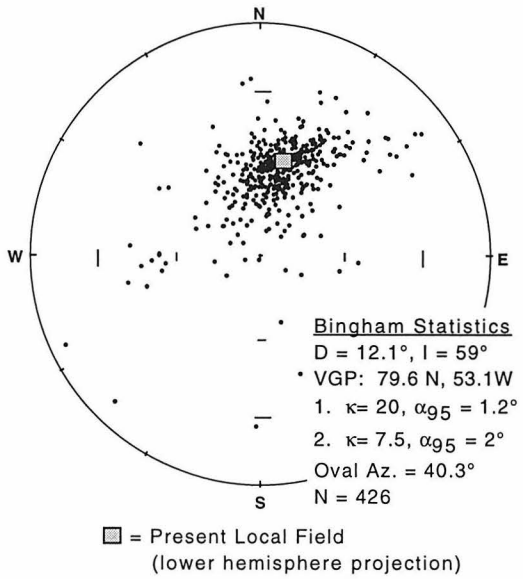

Figure 3. Overprint directions. Equal area projections of overprints from all samples which exhibited two-component magnetizations. Closed circles and PLF (present local field) represent lower hemisphere projections. Bingham statistics show that the overprint is distributed near the present-day field direction for this location. (D, declination east of north; I, inclination, positive downward; κ, precision parameter; N, number of samples) As discussed in the text, this overprint is removed after AF demagnetization to 10 mT and thermal demganetization to 250°C, and is therefore interpreted as a viscous remanent magnetization (VRM) held by multidomain magnetite and/or maghemite.

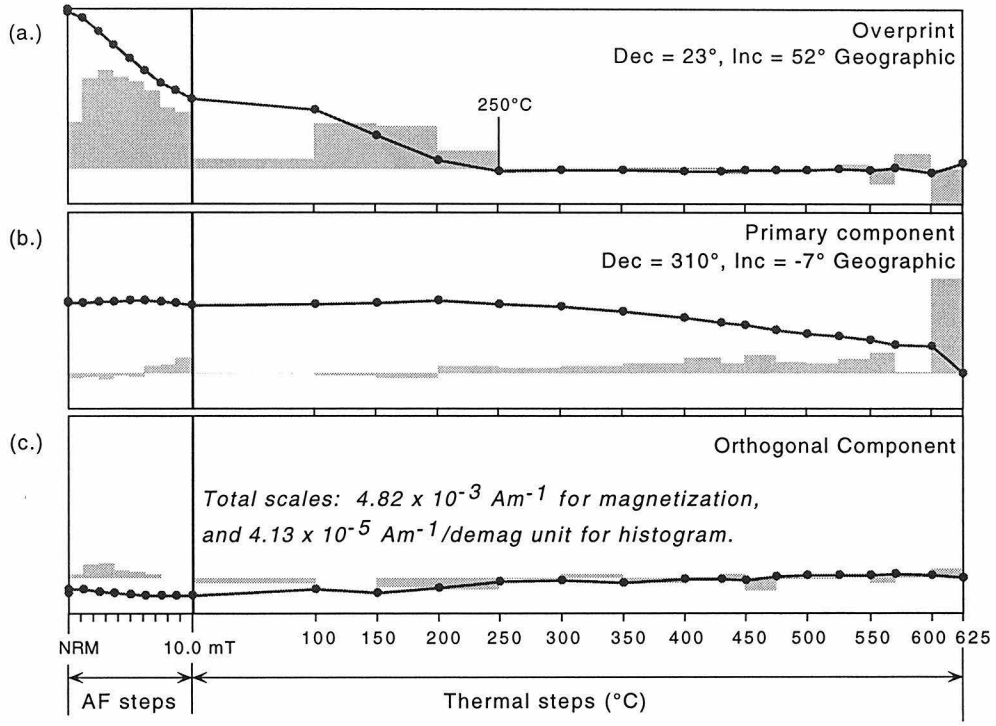

Figure 4. Sample magnetization versus demag step. The ratio of J/Jo is plotted separately for each component, as a function of demagnetization step: (a) the overprint, (b) the primary direction, and (c) a calculated component in the direction orthogonal to these two components. Erratic behavior in the orthogonal component indicates a lack of overlap between the overprint and primary directions. The removal of the overprint direction by the 250°C thermal step is apparent, as is the small amount of overlap between the coercivities of the two components. The shaded boxes represent the derivative of the J/Jo line, indicating the coercivity/blocking temperature spectrum for that component.

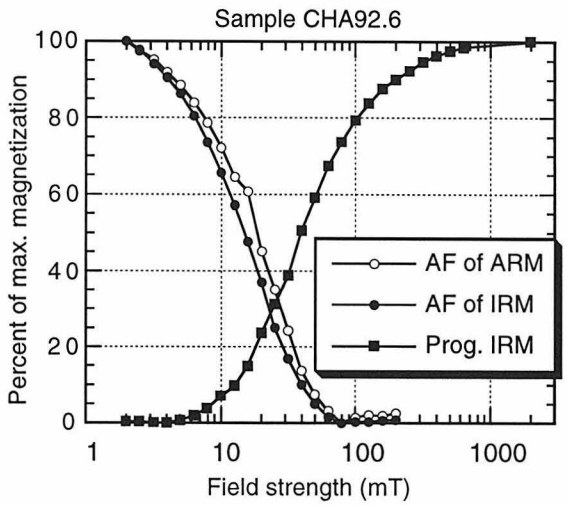

Figure 5. IRM/ARM acquisition and demagnetization. A typical coercivity distribution for a sample from Confusion Canyon. Samples from throughout the section exhibit similar patterns, as do all tested samples from Death March Canyon. Data for the IRM acquisition and AF demagnetization of the IRM are shown with open circles. The open circles show the AF demagnetization of the of the ARM acquired in a 2 mT direct current biasing field with a 100 mT (max) alternating field.

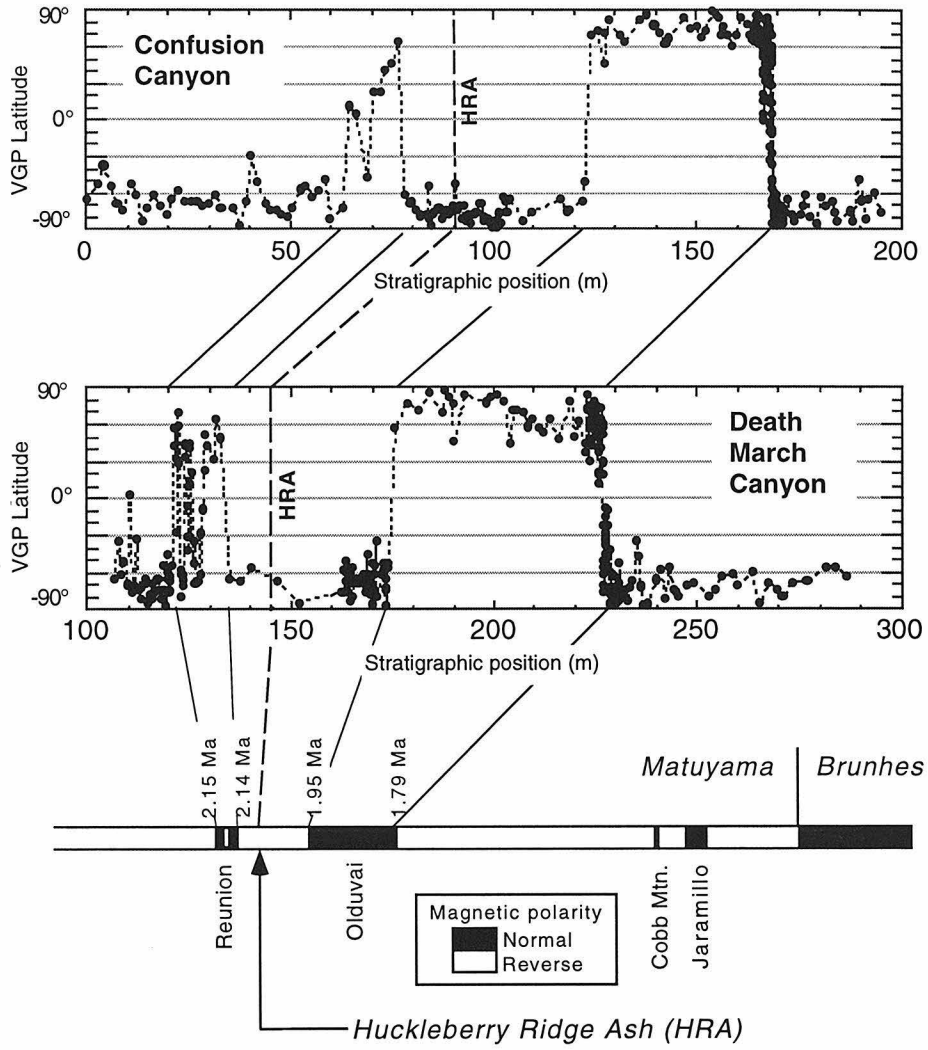

Figure 6. Magnetostratigraphy. VGP latitude as a function of stratigraphic position for both sections, compared with the Geomagnetic Polarity Timescale (GPTS), adapted from Harland et al. [33], with ages from Hilgen [26]. The location of the Huckleberry Ridge ash (~2.057 Ma, [25]) is shown for reference.

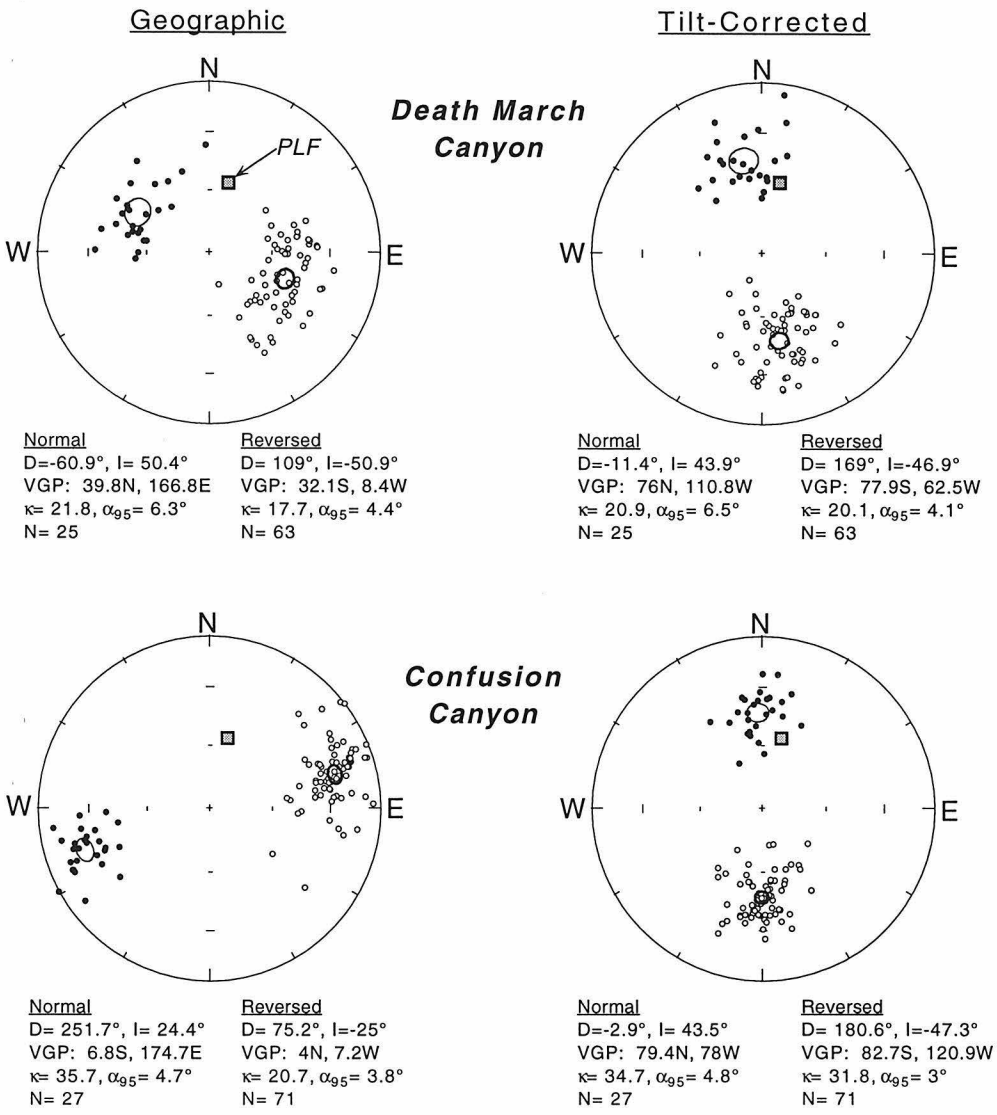

Figure 7. Non-transitional data, reversal tests, and fold test. Equal area plots of the non-transitional directions from both canyons — closed circles represent lower hemisphere projections, open circles represent upper hemisphere projections. Both sections pass the reversal tests of McFadden and McElhinny [34] , and the fold test as discussed in the text. (D, declination east of north; I, inclination, positive downward; k, precision parameter; N, number of samples)

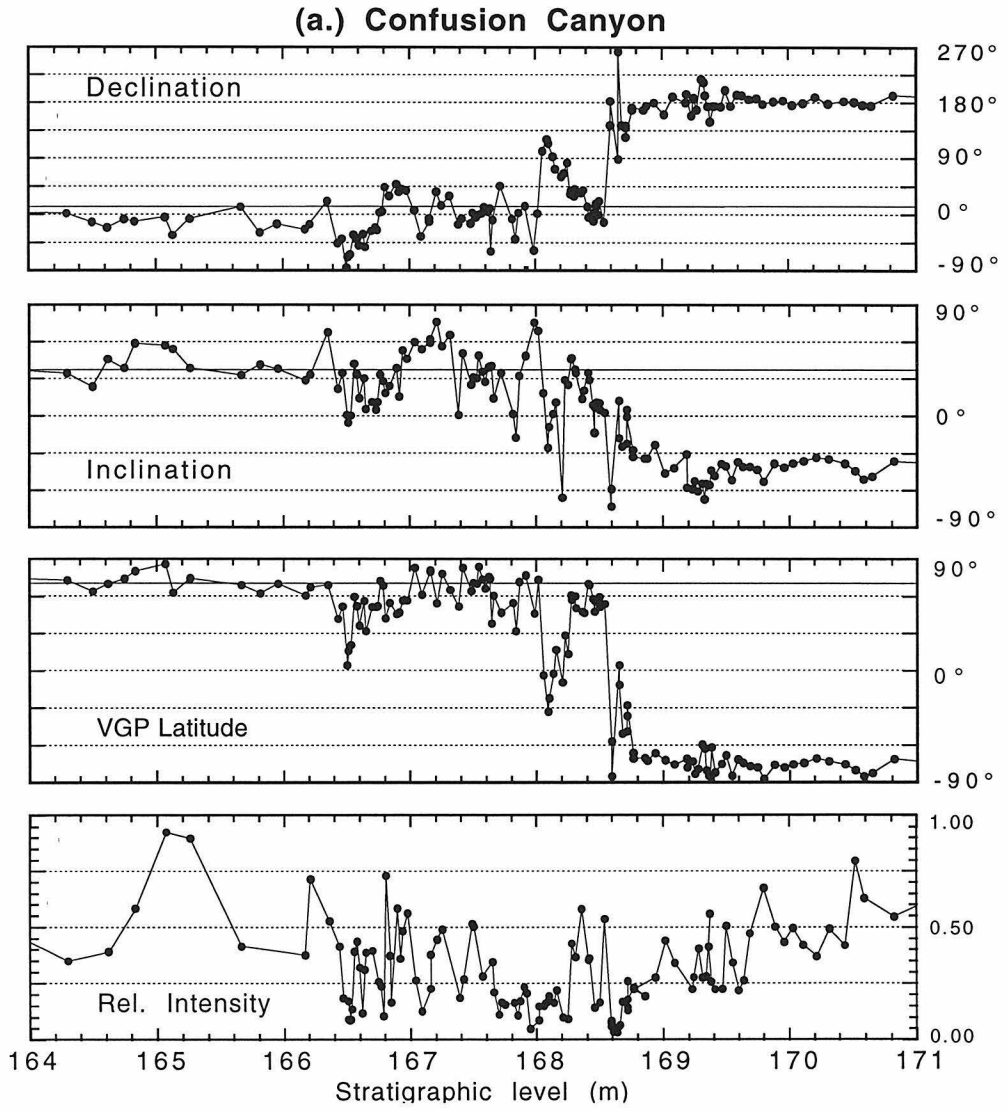

Figure 8. Transitional data. Declination, inclination, VGP latitude, and relative intensity (TT250/ ARM) plotted as a function of stratigraphic position across the upper Olduvai transition, for (a) Confusion Canyon, and (b) Death March Canyon. The intervals used in each canyon were selected in order to match the obvious central feature, which is most clearly seen in the declination record and appears to be an aborted reversal. The Death March Canyon stratigraphic interval is 54% longer for the overall transition, implying that the average sedimentation rate there during this interval was 54% higher than in Confusion Canyon.

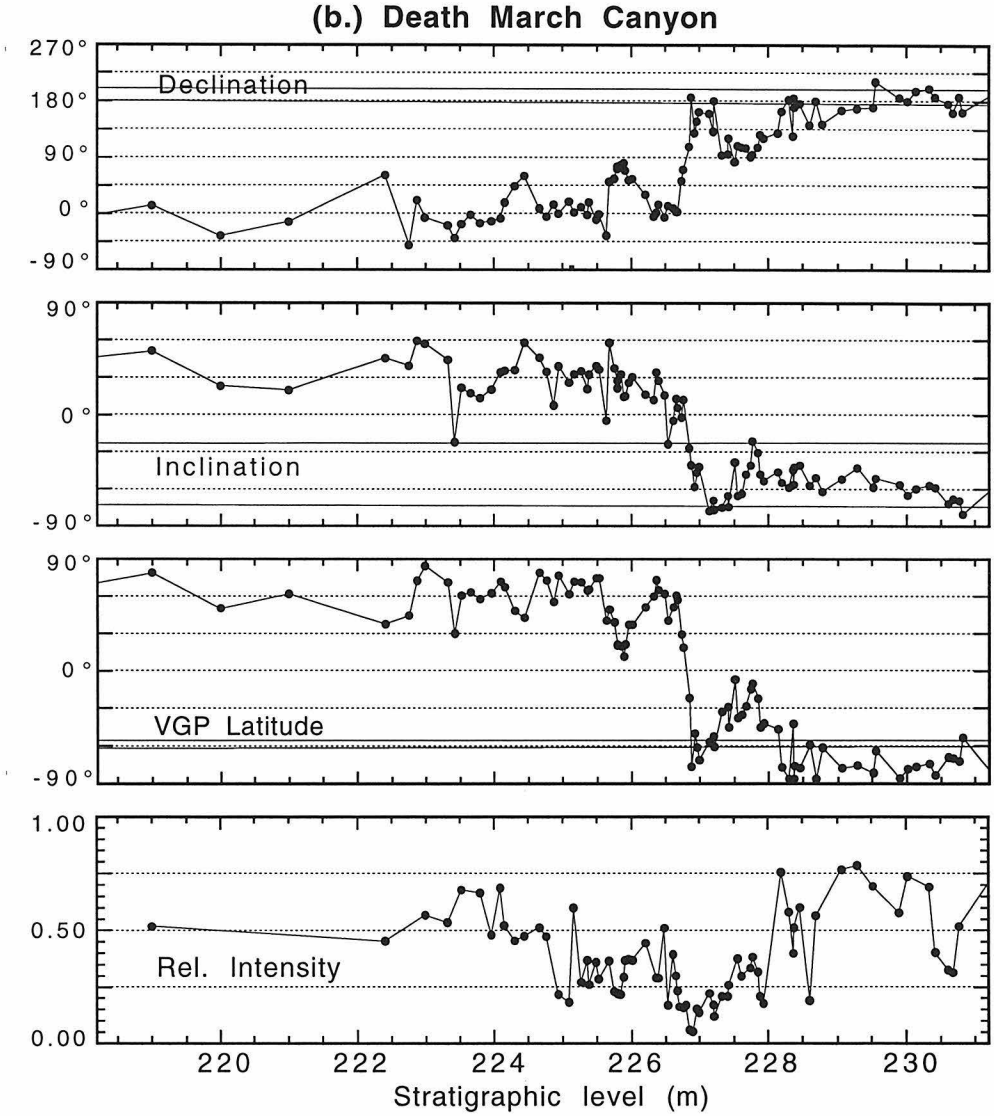
(b.) Death March Canyon
270°
180°
90°
0°
-90°
Declination
90°
0°
-90°
Inclination
90°
0°
-90°
VGP Latitude
1.00
0.50
0.00
Rel. Intensity
220
222
224
226
228
230
Stratigraphic level (m)

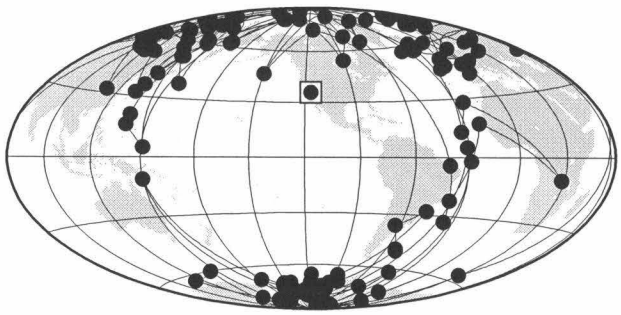

a.) Confusion Canyon

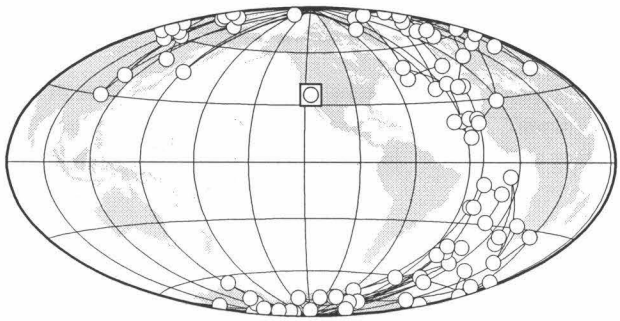

b.) Death March Canyon

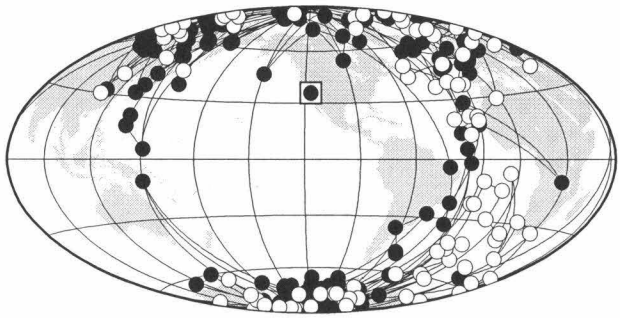

c.) Combined VGP's

Figure 9. VGP paths. VGP's are calculated for the transition zone data shown in Figure 8, and are shown here on Hammer-Aitoff projections of the earth, centered on the sampling site meridian (116.5 °W). Latitude and longitude grid spacings are 30°. Results for the individual localities are shown for (a) Confusion Canyon, and (b) Death March Canyon. (c) The combined paths illustrate the agreement of the transitional directions between the two locations. The sampling site location is indicated with a boxed data symbol.

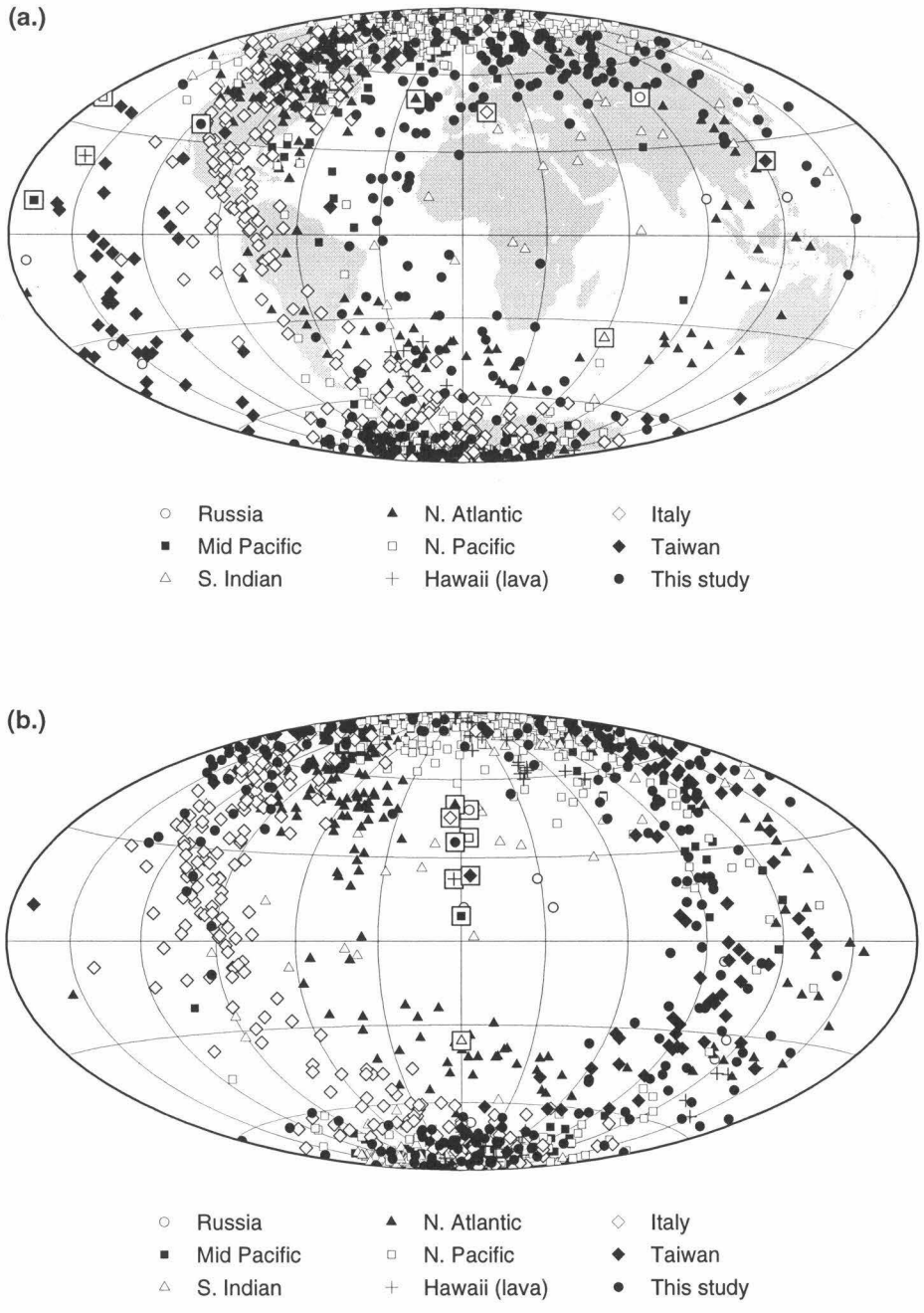

Figure 10. All upper Olduvai data. Previous data is from Russia [4], the middle Pacific Ocean [5], the Southern Indian Ocean [6], the North Atlantic [7], the North Pacific [8], Hawaii (lava) [9], Italy [3], and Taiwan [10]. VGP's from all studies in addition to those from this study are plotted together. Sampling sites are indicated by boxed data symbols for each respective study (staggered for display in order to minimize overlap). (a) Hammer-Aitoff projection centered on 0° longitude. Latitude and longitude grid spacings are 30°. (b) The same data plotted with sampling sites shifted to a common longitude, which is the center of the projection.

Paper 2: Confounding influence of magnetic fabric on sedimentary records of a field reversal

Xavier Quidelleur [1], John W. Holt [2] and Jean-Pierre Valet [1]

[1] Laboratoire de Paléomagnétisme
Institut de Physique du Globe de Paris
4, place Jussieu, 75252 Paris Cedex 05, FRANCE

[2] Division of Geological and Planetary Sciences
California Institute of Technology
Pasadena, California 91125, USA

First published in:
Nature
vol. 374, pp. 246-249, 1995

Recent compilations of geomagnetic reversals[1-8] have generated a controversy as to whether the geomagnetic field is geographically biased during polarity transitions. At the present time there is an overall agreement that the virtual geomagnetic poles (VGPs) recorded from Cenozoic sediments preferably lie over the Americas (or the antipodal longitude), yet such a preference is not statistically established[7,9]. However, it is intriguing that the claimed preferred paths lie 90° away from the site longitude[4,9]. Although this may be partly inherent to the very poor geographic distribution of the sites we prefer not to rely on fortuitous coincidences. Several authors have argued that palaeomagnetic sedimentary records may be modified by artefacts linked to the acquisition of magnetization[10-13]. Here we report that in two sedimentary records of the upper Olduvai reversal from Confidence Hills, California, the delincations of the remanent magnetization recorded during the reversal are similar to the directions of the maximum horizontal axes of the ellipsoids of magnetic anisotropy. This supports the idea that, at times of low geomagnetic intensity (such as during a reversal), factors other than the geomagnetic field influence the orientation of elongated grains.

High-resolution records of the Upper Olduvai geomagnetic reversal were recently obtained from two adjacent sections of lacustrine deposits (Death March Canyon, hereafter referred to as section 1, and Confusion Canyon, or section 2) in the Confidence Hills of southern Death Valley, California[14]. These sediments are characterized by a high deposition rate, 33 and 28 cm/ky, for sections 1 and 2, respectively. The difference in bedding attitude between the two sections (strike/dip for section 1 is N50°W/45°NE, whereas section 2 is N60°W/98°NE) allowed the first fold test[14] of transitional directions and was used to recognize present-day field overprints. It was thus possible to assess the primary origin of the characteristic

component of magnetization carried by single domain titanomagnetite. The virtual geomagnetic pole (VGP) paths, which cluster over the Atlantic and the western Pacific oceans, show no consistency with other records of the same transition. The most obvious characteristic is the tendency for VGPs to lie ~90° away from the site meridian. It has been suggested[9,15] that this feature, commonly observed in sedimentary records, could reflect the tendency for elongated particles to be deposited with their long axes aligned parallel to the horizontal plane when the field strength is not large enough, a process that would result in low magnetic inclinations which in turn cause deviations of the VGP paths from the site meridian. We thus found it useful and interesting to investigate the relationship between the magnetic fabric and the directions of the remanent magnetization for transitional and non-transitional samples from the Confidence Hills. Due to the high level of detail present in these records, they are particularly suitable for studies of acquisition processes of magnetization in sediments during transitions.

The anisotropy of magnetic susceptibility (AMS)[16-21] has long been used as a method for quantifying sedimentary fabrics. However, this technique is most sensitive to coarse magnetite grains which do not carry the characteristic remanent magnetization. It is therefore difficult to interpret AMS data when dealing with the anisotropy of the carriers of magnetic remanence. This problem can be overcome by measuring the anhysteretic remanent magnetization (ARM) which is carried preferentially by single domain and pseudo-single domain grains[22-24]. The ARM anisotropy (AAR), using the ARM acquisition ability of a given sample[24] has been shown to be a useful complement to standard AMS measurements. In addition, there is no contribution to AAR from paramagnetic and diamagnetic grains. Therefore, we used AAR in addition to AMS in order to fully characterize the magnetic fabric.

Seventy-four oriented cylindrical samples (41 from section 1 and 33 from section 2) were collected across the Upper Olduvai transition zone. The measurements of AMS were performed at the laboratory of Parc St Maur (France) with a Kappabridge KLY-2 (Geofyzica Brno). The AAR was determined from measurements performed in the shielded room of the I.P.G.P. using the following procedure: 1) the specimen was demagnetized in a peak alternating field of 90 mT; 2) an ARM was imparted along a specific sample axis in a peak alternating field of 80 mT with a direct field of 0.1 mT; 3) the ARM was partially demagnetized with a peak alternating field of 20 mT along the same sample axis; 4) the ARM was measured with a CTF cryogenic magnetometer using a multi-orientation sample holder so that the induced ARM could always be measured along the z-axis of the magnetometer; 5) the sample was then demagnetized along three axes with a peak alternating field of 90 mT in order to remove the previous ARM; 6) another ARM was then imparted along a different axis of the sample. This procedure was repeated for 9 different orientations using the same conventions as for the AMS determinations. The best-fit anisotropy tensor and its eigenvalues and eigenvectors were computed with the method of Jelinek[25]. This allows a precise determination of the anisotropy tensor. In order to rule out any secondary effect the very small component remaining after demagnetization was substracted from any imparted ARM.

The maximum and minimum axes of AMS and AAR are shown in equal area stereograms in Figure 1. Both sections show a well defined AMS foliation with the minimum axes perpendicular to the bedding plane and maximum AMS axes with a tendency for NW-SE preferential orientation. The maximum AAR axes are also parallel to the bedding plane. However, the AAR K_{max} declinations from section 1 are quite scattered while they show a NW-SE lineation in section 2. The K_{min} axes are vertical in section 1 but deviate from 90° in section 2. The percentages of AAR

are greater than for those of AMS (H=9.9 ± 5.4 and 7.9 ± 4.3 for sections 1 and 2 respectively versus 3.8 ± 1.9 and 2.5 ± 1.4, where $H = 100((K_{max}-K_{min})/K_{int})$). The values of the shape parameter for the AAR ($F = (K_{max}-K_{int})/(K_{max}-K_{min})$) are typical of oblate ellipsoids (F= 0.31 ± 0.22) in section 1 and closer to prolate structure (F=0.47 ± 0.19) in section 2. These anisotropy parameters show no apparent correlation with directional changes.

Thus, there are obviously some differences between the two sections. In the absence of deformation the AMS in sediments[26] is linked to the shape of the elongated grains that come to rest during deposition with their long axes parallel to the bedding plane and eventually azimutally oriented by bottom currents. Shape anisotropy is common for single or pseudo-single domain grains of magnetite and is reflected by the AAR[27]. The fact that the inclinations of the K_{min} axes (of both anisotropies) remain tightly grouped close to 90° in section 1 while the K_{max} are widely scattered (Figure 1) in the bedding plane indicates that the original depositional fabric has been preserved, unaffected by deformation. Although this appears to be much less apparent in the AMS, the dispersion of the AAR K_{min} axes in section 2 and the preference of the K_{max} axes to lie closer to the direction of the bedding strike (300°) indicates that deformation could be more significant than in the previous section. Indeed, in presence of intense folding the orientation of the K_{max} axes is expected to be parallel to the fold axis while the inclinations tend to be scattered away from the horizontal plane[28,29]. The anisotropy measurements (especially the AAR) are thus quite consistent with the field observations which show that section 1 (45° dip) experienced less folding than section 2 (110°). On the other hand, these differences in AAR K_{max} scatter could be explained by the different sedimentary environments characterizing these sections[14]. Section 2 is a high energy environment while section 1 has quieter depositional conditions which would produce more scattered directions of the AAR K_{max} axes. One can speculate that

both of these mechanisms of non-magnetic origin should have a limited affect upon the remanence directions outside the transition. This is because they mostly influence orientation of elongated grains whereas remanence is carried primarily by equant grains in these sediments[14].

In Figure 2 we compare the directions of the AAR K_{max} axes with the declinations of the remanence. K_{max} has no polarity, and, hence, the axes define two declinations 180° apart. We plotted the declinations of K_{max} with the minimum deviation from the direction of the remanence. The most striking feature is that in both sections the declinations of the AAR-K_{max} axes more closely match the remanence declinations during the transition (220 to 228 m in section 1 and 167 to 169 m in section 2) than outside this interval. Furthermore, it can be noted that there is a good agreement if only directions associated with a low latitude VGP are considered. There are several possible interpretations for the apparent correlation between the transitional declinations and the orientation of the AAR K_{max} axes. First of all, significant effects of smoothing of the transitional directions by post-depositional reorientations of the grains seem unlikely because of the very high deposition rates and the large directional jumps observed during both transitional intervals. The fold test also eliminates the possibility of overprinting by the present geomagnetic field. The AAR could reflect preferential orientation of the long axes of single domain and/or pseudo-single domain grains by the geomagnetic field. However in this case, the inclinations of the AAR axes should also coincide with those of the remanence, particularly outside the transition interval where the geomagnetic field intensity is much higher. In both sections the inclinations of the K_{max} axes remain close to 0° and thus strikingly different from those of the remanence outside the transitional intervals. It seems thus difficult to invoke only a geomagnetic origin for the AAR.

We may first find it surprising that under such conditions similar directional changes have been recorded at both sections. Although there is an overall similarity between the two records, there are large swings and abrupt variations of declination in section 2 which contrast with the much smoother behavior of the declination in section 1 (Figure 2). In both cases this different character is duplicated by the declinations of the AAR K_{max} axes. The similarity between the orientations of the transitional directions and the K_{max} axes of the AAR suggests that the anisotropy effects may have played a significant role in the records of the transitional directions.

One may thus wonder in this case why the orientations of the K_{max} axes of the AAR do not match those of the characteristic component of magnetization outside the transition zone. Also puzzling is the fact that the inclinations of the remanence do not match exactly those of the K_{max} axes during the transition, although it is noticeable that the largest similarities occur for transitional directions with VGPs at the lowest latitudes. However, if we assume that the orientations of the elongated grains dominate the remanent magnetization during the transition, this should not necessarily be so outside the reversal because most of the characteristic remanent magnetization is carried by single domain equant grains without shape anisotropy. This is supported by TEM experiments on fine grain separates that confirmed the presence of equant single domain grains of titanomagnetite and detected also the presence of non-equant grains[14]. During periods of stable polarity the fraction of elongated grains lying with their long axes parallel to the bedding eventually introduces a bias into the remanence which is usually described as an inclination error[31] and observed at Confidence Hills[14]. When the external field reaches a weak intensity as during a geomagnetic reversal, the alignment of the equant particles by the geomagnetic field becomes much weaker so that the contribution of the fraction of

elongated particles to the remanence may be considerably enhanced if not dominant. The resultant magnetization is thus much more sensitive to grains with their moments more or less parallel to the horizontal plane. This process induces significant inclination shallowing which in turn causes deviations of the VGP paths from the site meridian. It can be noted that this hypothesis is slightly different than one previously proposed[9], in which only elongated grains were involved.

Although we cannot preclude that these results could be specifically inherent to these sediments, they imply some degree of inability of sediments in general to accurately record the field direction during periods of low field intensity. This clearly emphasizes the importance of anisotropy measurements before any interpretation of transitional directions in terms of geomagnetic field behavior can be carried out.

Acknowledgements

We are pleased to thank J.P. Cogné and C. Laj for helpful suggestions and discussions, R. Warner and C. Scrivner for field assistance, and B. Henry for help with measurements and interpretations of the AMS. This work was supported by the French program CNRS INSU DBT Terre Profonde and the US NSF.

References

1. Clement, B.M. *Earth Planet. Sci. Lett.* **104**, 48-58 (1991).
2. Tric, E., Laj, C., Jehanno, C., Valet, J.P., Kissel, C., Mazaud, A. & Iaccarino, S. *Phys. Earth Planet. Inter.* **65**, 319-336 (1991).
3. Laj, C., Mazaud, A., Fuller, M., Weeks, R. & Herrero-Bervera, E. *Nature* **351**, 447 (1991).
4. Valet, J.P., Tucholka, P., Courtillot, V. & Meynadier, L. *Nature*e**356**, 400-407 (1992).
5. Hoffman, K.A. *Nature* **359**, 789-794 (1992).
6. Bogue, S.W. & Merrill, R.T. *Annu. Rev. Earth Planet. Sci.* **20**, 181-219 (1992).
7. McFadden, P.L., Barton, C.E. & Merill, R.T. *Nature* **361**, 342-344 (1993).
8. Prévot, M. & Camps, P. *Nature* **366**, 53-57 (1993).
9. Quidelleur, X. & Valet, J.P. *Phys. Earth. Planet. Int.* **82**, 27-48 (1994).
10. Rochette, P. *Earth Planet. Sci. Lett.* **98**, 33-39 (1990).
11. Van Hoof, A.A.M. & Langereis C.G. *Nature* **351**, 223-225 (1991).
12. Langereis, C.G., van Hoof, A.A.M. & Rochette, P. *Nature* **358**, 226-230 (1992).
13. Kent, D.V. & Schneider, D.A. C *EOS* **75**, 119 (1994).
14. Holt, J.W. & Kirschvink, J.L. *Earth Planet. Sci. Lett* (submitted).
15. Chauvin, A., Roperch, P. & Duncan, R.A. *J. Geophys. Res.* **95**, 2727-2752 (1990).
16. Ising, G. *Astron. Och Fysils.* **29A**, 1-37 (1942).
17. Graham, J. W. *Geol. Soc. Am. Abstr. Prog.* **65**, 2257 (1954).
18. Granar, L. *Ark. Geofys.* **3**, 1-40 (1958).
19. Rees, A.I. *Sedimentology* **4**, 257-271 (1965).

20. Hamilton, N. & Rees, A.I. *In Runcorn, S.k.,* ed., Paleogeophysics, Academic Press, New York, 445-464 (1970).
21. Kent, D.V. & Lowrie, W. *Earth Planet. Sci. Lett.* **28**, 1-12 (1975).
22. Banerjee, S.K., King, J. & Marvin, J. *Geophys. Res. Lett.* **8**, 333-336 (1981).
23. King, J., Banerjee, S.K., Marvin, J. & Özdemir, Ö. *Earth Planet. Sci. Lett.* **59**, 404-419 (1982).
24. McCabe, C., Jackson, M. & Ellwood, B.B. *Geophys. Res. Lett.* **12**, 333-336 (1985).
25. Jelinek, V. *Geofyzika*, Brno (1977).
26. Ellwood, B.B. *Mar. Geol.* **34**, 83-90 (1980).
27. Jackson, M., Gruber, W., Marvin, J. & Banerjee, S.K. *Geophys. Res. Lett.* **15**, 440-443 (1988).
28. Hrouda, F. *Geophys. Surv.* **5**, 37-82 (1982).
29. Borradaile, G. *Tectonophys.* **156**, 1-20 (1988).
30. Beratan, K., Hsieh, J. & Murray, B. *GSA Special Volume* (Submitted)
31. Opdyke, N.D. & Henry, K.W. *Earth Planet. Sci. Lett.* **6**, 138-151 (1969).

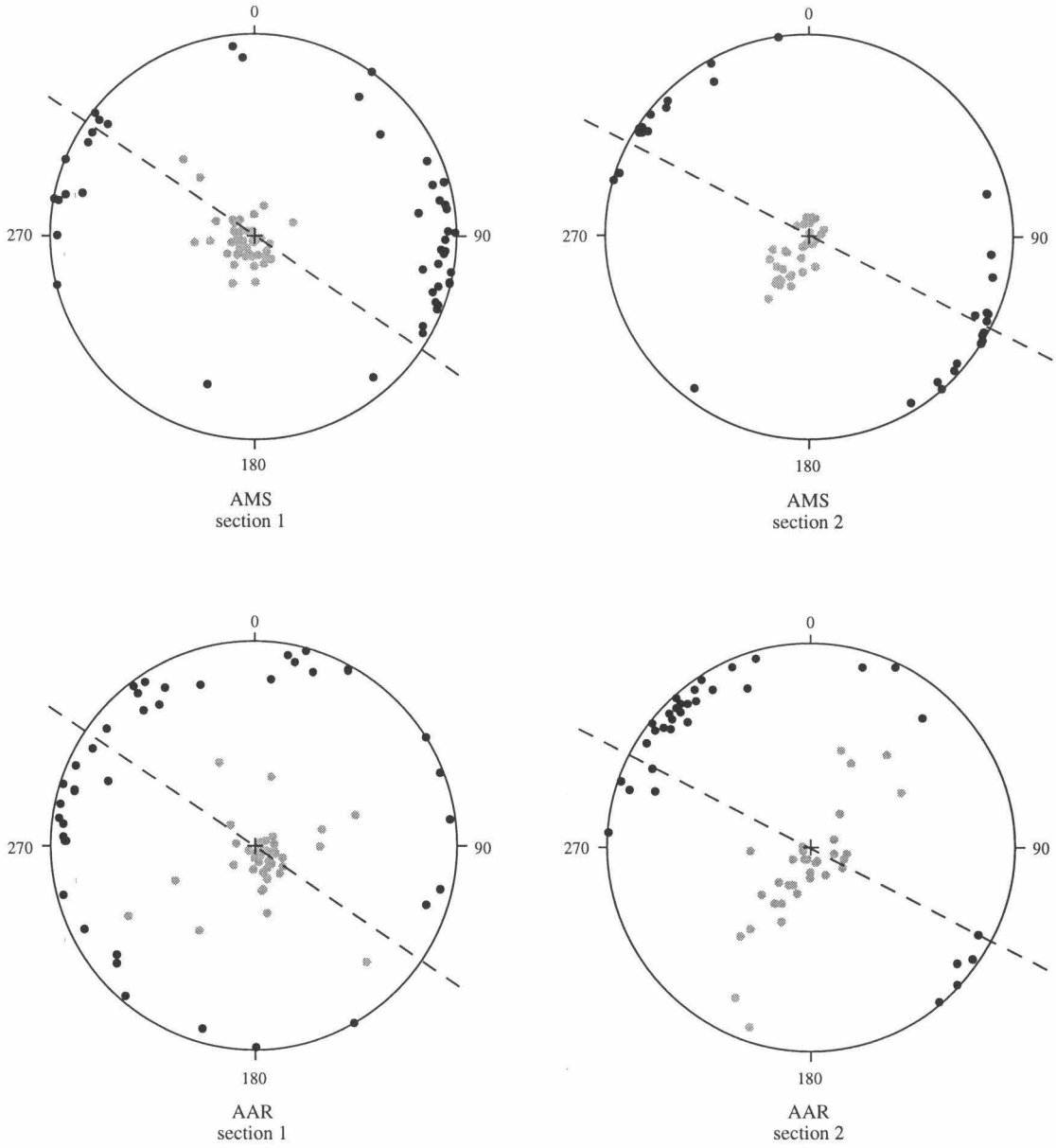

Figure 1: Top, equal area stereo plots of the directions of the K_{max} (black dot) and K_{min} axes (grey dot) of magnetic susceptibility (AMS) for samples from section 1 (left) and section 2 (right). Bottom, the Kmax and Kmin axes of the anhysteretic remanence (AAR). Dotted lines show the directions of the bedding strike.

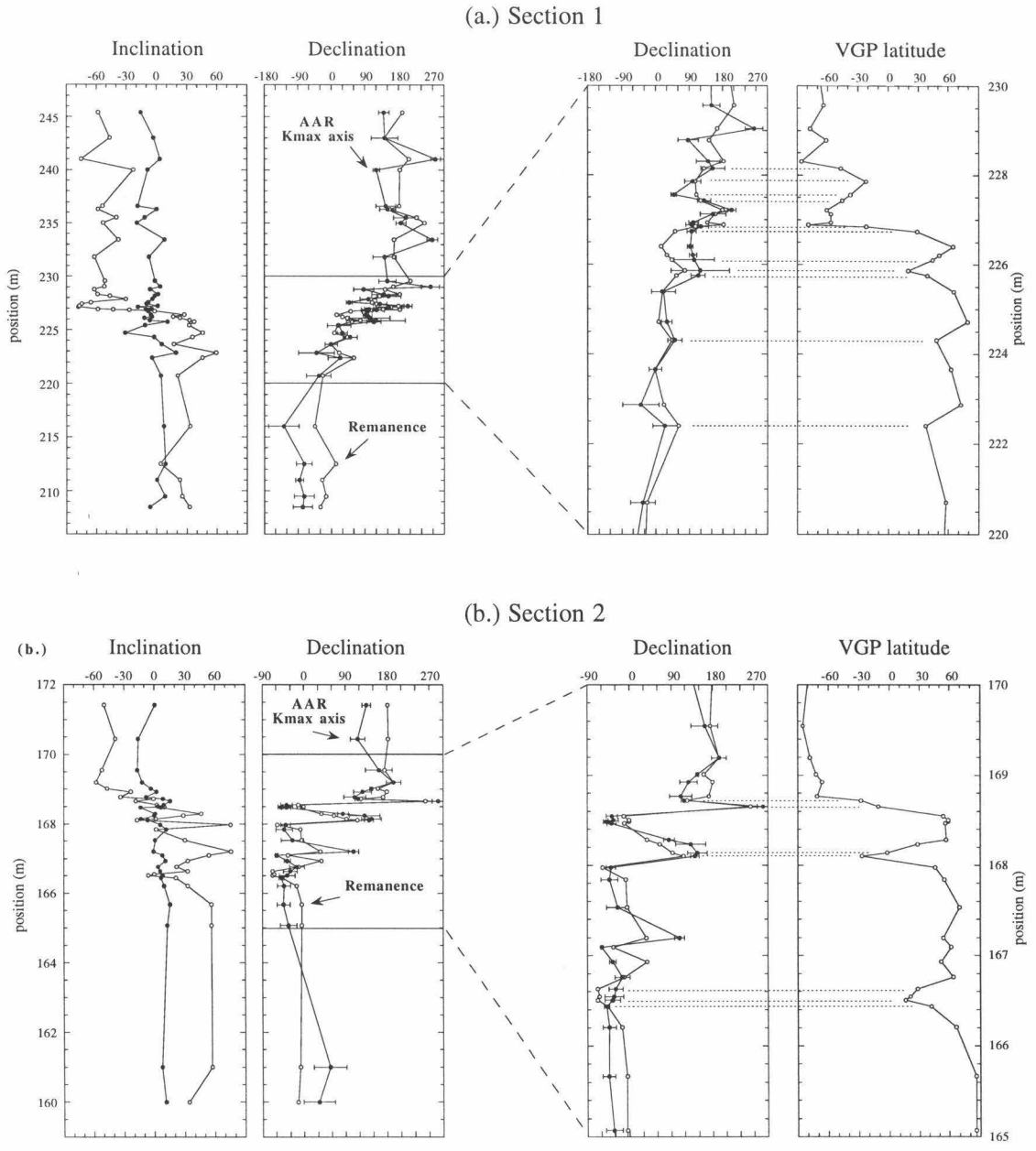

Figure 2: (a.) The two left-hand plots show inclinations and declinations (in degrees) of the AAR K_{max} axes (filled circles) compared with the declinations of the remanence (open circles) as a function of the stratigraphic height in section 1 deposits. The two right-hand plots show an enlarged view of the declinations and VGP latitudes across the transition zone. (b.) same as (a) for section 2.

Paper 3: A Death Valley Réunion event

John W. Holt and Joseph L. Kirschvink

Division of Geological and Planetary Sciences

California Institute of Technology, Pasadena, CA 91125

To be submitted to:

Journal of Geophysical Research

Abstract

A detailed record of the Réunion normal-polarity geomagnetic subchron was obtained from fine-grained ephemeral lake sediments with an average sedimentation rate of approx. 30 cm/kyr exposed along the southern Death Valley fault zone. Alternating-field and thermal demagnetizations revealed that most samples have two-component magnetizations, a primary component acquired at or soon after the time of deposition and a normal-polarity secondary component acquired after structural tilting of the rocks. The primary magnetization is probably held primarily by magnetite and/or titanomagnetite, while the secondary component is likely held by multi-domain magnetite and goethite. All samples exhibiting stable magnetizations with consistent paleomagnetic directions are from siltstone or banded anhydrite lithofacies. Most samples which did not exhibit stable magnetizations, and all samples exhibiting erratic directions are from a gypsiferous siltstone lithofacies. This lithofacies is characterized by displacive evaporite crystals disseminated throughout the matrix. These crystals were growing approx. 9 - 25 kyr after deposition while the sediments were undergoing burial and compaction. This process disrupted primary magnetizations, rendering useless the remanent magnetic directions from this lithofacies. Due to the confinement of this lithofacies to two specific stratigraphic zones, only two small gaps exist in the record. They are located just below a normal polarity interval which, according to average sedimentation rates and extrapolation from the Huckleberry Ridge ash, existed from approx. 2.15 - 2.13 Ma, in agreement with recent astronomically calibrated ages for the Réunion subchron. Transitional directions from the reversals trace virtual geomagnetic pole (VGP) paths which are roughly 90° east of the sampling site.

Introduction

In recent years, high-precision radiometric dates for several geomagnetic polarity time scale (GPTS) boundaries have been reported which support ages determined by astronomical calibration (Baksi et al., 1992; Tauxe et al., 1992; Renne et al., 1993). The astronomical method is based on the correlation of geologic proxies for climatic variation with periodic changes in the earth's orbital parameters (e.g., Hays et al., 1976; Shackleton et al., 1990; Hilgen, 1991b; Hilgen, 1991a; Lourens et al., 1996), and appears to be the most accurate and precise method of calibrating the GPTS for at least the past 5 myr (Cande and Kent, 1995). However, the correlation of astronomically calibrated ages with geomagnetic polarity reversals is only as accurate or precise as the magnetostratigraphy produced from the sedimentary sequence containing the climatic proxy.

One of the most enigmatic polarity intervals in the early time scale is the Réunion subchron (C2r.1n) which in a recent GPTS compilation (Cande and Kent, 1995) has been listed as a single normal-polarity interval spanning the 10 kyr interval 2.14 - 2.15 Ma. It has been shown in various other time scales as either one or two normal polarity intervals which lasted from 30 - 160 kyr, anywhere in the range 2.01 - 2.27 Ma (e.g., Mankinen and Dalrymple, 1979; Harland et al., 1982; Harland et al., 1989; McDougall et al., 1992).

The dates used in the GPTS of *Cande and Kent* (1995) for the Réunion subchron are based on an astronomical calibration (Hilgen, 1991a). In the magnetostratigraphy used for this calibration, the Réunion subchron is represented by a single normal-polarity lithostratigraphic unit with two samples (Zijderveld et al., 1991). An updated astronomical calibration (Lourens et al.,

1996) for the past 5 myr is based on a more detailed magnetostratigraphic record (Langereis, unpublished data) as yet unpublished. According to this calibration, the Réunion is expanded to a 20 kyr interval from 2.149 Ma to 2.129 Ma.

The initial discovery of the Réunion subchron was made by Chamalaun and McDougall (1966) in ~2.0 Ma lava flows on Réunion Island in the southern Indian Ocean. While many detailed records of the Olduvai normal-polarity subchron (1.95 - 1.69 Ma, Cande and Kent, 1995) have been described (e.g., Grommé and Hay, 1971; Clement and Kent, 1985; Herrero-Bervera and Theyer, 1986; Tric et al., 1991; Lee, 1992; Liu et al., 1993; Holt and Kirschvink, 1995), few records with any data representing the Réunion subchron have been found (McDougall and Watkins, 1973; Brown and Shuey, 1976; Zijderveld et al., 1991). Reasons for ambiguity in the Réunion subchron are threefold: (1) The lack of complete, detailed records of this time interval from either volcanic or sedimentary rocks. (2) Radiometric dates from normal-polarity volcanic rocks in this time interval cluster into two groups, ~2.05 Ma and ~2.15 Ma (Grommé and Hay, 1971), which appear to be distinct, yet may be the result of some K/Ar dates being too young (Shackleton et al., 1990; Hilgen, 1991a; Baksi et al., 1993). (3) The Réunion subchron is so brief that sedimentary records with typical marine deposition rates may miss it entirely or smooth multiple closely-spaced events into the appearance of one event.

In this paper we present a detailed paleomagnetic record of the Réunion subchron obtained from an unfaulted, continuous stratigraphic section of non-marine sedimentary rocks with a high rate of deposition (~30 cm/kyr).

Geologic Setting

Tectonic history

The sampling area for this study is located in the Confidence Hills of southern Death Valley, California (Fig. 1). Playa lake sediments were deposited in a physical setting similar to present-day Badwater Basin in central Death Valley, and after undergoing burial and compaction, were later uplifted and tilted by tectonic forces acting along the southern Death Valley fault zone (Troxel and Butler, 1986). The axis of tilting is nearly perpendicular to the prevailing drainage patterns. This has caused erosional channels to cut across the strike of bedding, revealing continuous stratigraphic sections of the sedimentary rocks (Gomez et al., 1992).

Two of these sections, informally named Death March Canyon and Confusion Canyon, have been the focus of previous paleomagnetic (Holt and Kirschvink, 1995) and stratigraphic (Hsieh and Murray, 1996; Beratan et al., in press) studies. Small-scale faulting may have disrupted the record of the Réunion subchron in Confusion Canyon; therefore, this study is focused on the record of the Réunion subchron in Death March Canyon, where the bedding strike and dip are approximately N45W, 55°NE. After extensive cleaning and detailed examination of the section there, no faulting has been observed.

Environment of deposition

The sedimentology and stratigraphy of the Confidence Hills have been described previously in detail (Hsieh and Murray, 1996; Beratan et al., in press). The sedi-

ments relevant to this study are within the Confidence Hills Formation and are interpreted to have been deposited in subenvironments of an ephemeral saline lake and/or salt pan within a closed basin (Beratan et al., in press). The primary source area for these sediments was the granitic Owlshead mountains to the southwest of the Confidence Hills (Fig. 1). The two sections studied are comprised primarily of siltstone, fine-grained sandstone, massive anhydrite ($CaSO_4$), and banded anhydrite. The banded anhydrites consist of alternating layers of primary anhydrite (or anhydrite after gypsum) and silt. These layers are < 1 mm to 1 cm in thickness, while the siltstones and sandstones consist of beds ~ 1 cm to 10 cm thick (averaging ~ 3 cm). There is no fossil evidence (macro- or microscopic) for any life within these sediments [*R. E. Reynolds*, written communication, 1993].

The siltstones and fine-grained sandstones are well-sorted, and were carried by thin sheets of water flowing out onto the playa as a result of precipitation within the ancestral Death Valley watershed (Hsieh, 1993). Sedimentation was therefore episodic in nature, rather than being continuously fed by a standing water column. Sedimentation rates for the different lithologies were probably quite similar over ~ 10^3 yr time scales due to the extremely low relief of the playa and/or saltpan which tended to keep sedimentation well distributed across the surface (Hsieh, 1993).

In addition to these primary lithologies, there are a few minor lithofacies present in the Confidence Hills sections. One of these is *gypsiferous siltstone*, a siltstone containing crystals and/or nodules of gypsum or anhydrite disseminated throughout the matrix (Beratan et al., in press). The evaporites appear to have grown *in-situ* while ductile flow was still possible in the sediment, destroying all primary

depositional structure (Beratan et al., in press). This lithofacies was not present within the upper Olduvai interval in either Death March Canyon or Confusion Canyon, where the lithologies were banded anhydrite and siltstone/fine-grained sandstone, respectively (Holt and Kirschvink, 1995). In each section, however, the Réunion subchron is found within similar sediments which are dominated by siltstone and banded anhydrite, with gypsiferous siltstone being found in discrete zones nearby.

The calcium-sulfates found in all of the evaporite-bearing lithofacies were probably formed at or near the surface of the ephemeral lake or salt pan by precipitation from evaporating groundwater (Hsieh, 1993). In this type of environment, groundwater may be drawn up through the sediments via evaporative pumping. Changes in the water table height, the amount and type of dissolved ions, or climate (which may all be related) can therefore affect the deposition of evaporites. Calcium carbonates were not found in any of the rocks, however.

During the Olduvai subchron, stratigraphically above the Réunion, the average sedimentation rate is 33.7 cm/kyr (updated from 33.1 cm/kyr (Holt and Kirschvink, 1995) to reflect the most recenty determined age for the Olduvai reversals (Lourens et al., 1996)).

Data Acquisition

Sampling

Paleomagnetic sampling was performed in essentially the same manner as in the

previous study at this location (Holt and Kirschvink, 1995), the main difference being the type of drill used. An electrically-powered rotary drill was employed (in lieu of a gasoline-powered drill) with a standard diamond-tipped coring bit, using compressed air or CO_2 for cooling. Samples were oriented in the field using only a magnetic compass, as a sun compass was determined to be unnecessary.

A total of 187 samples were collected within 33.6 m of section encompassing the Réunion subchron, of which 140 were located within a 15 m zone of primary interest. Sample spacing ranged from ~ 1 cm to 30 cm, controlled primarily by lithology and bed thickness, i.e., some layers cracked apart too easily to obtain an oriented sample. This corresponds to theoretical time intervals of ~ 30 to 900 years while a single sample would average 75 years, with an average sedimentation rate of 33.7 cm/kyr.

Demagnetization

Magnetic direction and intensity were measured in a μ-metal shielded, 2G-modified SCT cryogenic magnetometer located within a μ-metal shielded room. The intensity of the natural remanent magnetization (NRM) for most samples was on the order of 10^{-1} A/m. After measurements of the NRM, samples were subjected to stepwise, automated alternating field (AF) demagnetization in 2 - 5 steps to 10 mT. This was followed by thermal demagnetization in 3 - 6 steps to 400°C, followed by steps of 25° - 75° to a maximum of 625°C.

Magnetization directions were determined using least-squares principal component analysis (Kirschvink, 1980). For the vast majority of samples, there were two clear components of magnetization – a primary magnetization and a second-

ary overprint (Figs. 2a-c). Due to the dip of bedding in this section, a present-day overprint can easily be distinguished from both normal and reversed primary magnetic directions. The magnetization usually became unmeasurable or random at approximately 550° - 625°C, with the greatest drop in intensity occurring at the 600°C or 625°C heating steps in many samples (Figs. 2c, 3a).

The overprint, which is a low coercivity, low blocking temperature component, is removed by AF demagnetization at 10 mT and thermal demagnetization to approximately 300° C (Figs. 2a-c, 3b). As evident in the component J/Jo plot (Fig. 3b), there is little overlap of coercivity between the two components. The mean direction of these overprints is between an axially-symmetric dipole normal-polarity direction and the present-day field direction for this locality (as in Fig. 3, Holt and Kirschvink, 1995), so this component is interpreted as being a combination of chemical remanent magnetization (CRM) and viscous remanent magnetization (VRM). The demagnetization characteristics of this component, in conjunction with rock magnetic studies (discussed below), indicate that the VRM is held by multi-domain magnetite grains and the CRM by goethite.

Samples which did not reach a stable, linear demagnetization path (Fig. 2d) were not used. This included 28 samples of the gypsiferous siltstone lithofacies and 7 from siltstone. The 44 remaining gypsiferous siltstone samples produced primary directions distinct from an overprint in a similar manner to the 89 samples from siltstone and the 19 from banded anhydrite (Fig. 2c), but with lower relative intensities and higher average values of maximum angular deviation (MAD, Kirschvink, 1980) determined from the least-squares analyses. Due to the process of evaporite growth within gypsiferous siltstones, paleomagnetic directions

obtained from this lithofacies are considered unreliable and will be treated separately in the results.

Rock magnetism

Rock magnetic experiments were undertaken in order to constrain the mineralogy and morphology of the magnetic remanence carriers, and to identify any major variations within the sampled section. Experiments included (1) an acquisition of anhysteritic remanent magnetism (ARM) in a 100 mT alternating field, with progressively stronger background biasing fields between 0 and 1 mT, after *Cisowski* (1981), (2) the progressive AF demagnetization of the ARM after the 1 mT ARM acquisition, (3) the progressive AF demagnetization of a 100 mT isothermal remanent magnetization (IRM), and (4) IRM acquisitions in pulsed fields up to 800 mT.

The magnetic susceptibility of most samples was measured after each heating step using a Bartington MS2 susceptometer located within the shielded room.

Fig. 4 is a coercivity spectrum plot which includes a modified Lowrie-Fuller test (Lowrie and Fuller, 1971) for a typical sample. The positive Lowrie-Fuller test (the ARM having a higher coercivity than the IRM) suggests that the primary magnetic carrier is of single- or pseudo-single-domain size. For the IRM acquisition data, roughly 95% of the intensity is acquired after exposure to peak fields of less than 300 mT. This is indicative of magnetite with a small portion of higher coercivity material, such as hematite. Samples from throughout the Réunion interval and spanning the observed range of susceptibility showed virtually identical results for these tests, indicating the magnetic fraction is the same throughout. This is supported by evidence from thin-section examinations and X-ray

diffraction studies which demostrated that the composition of the clastic component in the Confidence Hills strata is similar throughout all observed lithofacies (Beratan et al., in press).

The results of direct scanning electron microscope (SEM) and transmission electron microscope (TEM) analyses on rocks of the Olduvai interval in the same section and in the Confusion Canyon section (Holt and Kirschvink, 1995) indicate that titanomagnetite constitutes the magnetic fraction responsible for holding the stable primary remanence. Some of these magnetic grains are from 50 nm to 3 μm in size, which is in the range of single- to pseudo-single-domain grains (Levi and Merrill, 1978). The morphology of this size fraction is either equant to slightly elongate prismatic grains or clearly equant octahedral titanomagnetite crystals (with Ti/Fe ratio up to approximately 0.25, from energy dispersive spectral analyses). Other magnetic grains are of tabular magnetite and titanomagnetite grains which are approximately 30 - 100 μm across. This larger size fraction is clearly multi-domain (Levi and Merrill, 1978), and is probably the primary carrier of the magnetically soft overprint. It is assumed that rocks of the Réunion interval have very similar magnetic properties to those of the Olduvai interval due to the similarity of lithology, the continuity of the section without any significant depositional hiatus, identical demagnetization characteristics, and the similarity of IRM and ARM acquistions and demagnetizations.

Susceptibility measurements were performed on a Bartington MS2 susceptometer located within the shielded room during the course of thermal demagnetization. Results are shown for samples which span the observed range of intial susceptibility in Fig. 5. There are no large changes in susceptibility until the last heating step at 625°C. This is accompanied by a marked increase

in the amount of red coloration in the sample, probably indicating a sudden increase in the oxidation of Fe-bearing minerals.

Results

Magnetostratigraphy of Death March Canyon

The overall magnetostratigraphy of the section used in this study is shown in Fig. 6, which compares virtual geomagnetic pole (VGP) latitudes with the GPTS. There are three stratigraphic zones of reversed geomagnetic field polarity separated by two zones of normal polarity. Absolute age control is provided by a 40-cm-thick, grey volcanic ash. Chemically correlated with the Huckleberry Ridge Ash (Troxel et al., 1986), this tephra unit has been dated at 2.09 $\pm$ .008 Ma (Sarna-Wojcicki and Pringle, 1992) using the $^{40}Ar/^{39}Ar$ method on samples from the source region at Yellowstone caldera (recalculated from their original age of 2.06 Ma using a new standard (Sarna-Wojcicki, unpublished data)). The correlation and age were confirmed by $^{40}Ar/^{39}Ar$ analyses of ash samples from the Confidence Hills (Renne, unpublished data).

The two major normal-polarity intervals are therefore correlated with the Olduvai and Réunion subchrons. Paleomagnetic directions obtained from samples of the gypsiferous siltstone lithofacies are indicated with different symbols. The few samples of this type found within the Olduvai subchron (at ~ 190 m - 195 m) have highly discordant paleomagnetic directions from other Olduvai normal-polarity samples. In addition, these anomalous directions are not observed in the Confusion Canyon section, where the time-equivalent section is comprised of siltstone

and banded anhydrite (Beratan, 1992; Holt and Kirschvink, 1995).

Magnetostratigraphy of the Réunion interval, Death March Canyon

The abrupt changes of polarity recorded between the stratigraphic levels of 120 m and 135 m are shown in detail in Figs. 7a-c along with variations of lithology. Paleomagnetic directions obtained from siltstones and banded anhydrites display a smooth transition from reversed polarity to normal polarity between 127.5 m and 129 m, stable normal-polarity (although somewhat low latitude) VGP's for the following 3 m, and then a more abrupt transition back to reversed polarity from 132.5 m to 133 m. Paleomagnetic directions from gypsiferous siltstones (plotted separately) display erratic behavior, and are associated with high average MAD values (Fig. 7d).

All normal- and reversed-polarity directions (excluding those from gypsiferous siltstone samples) are plotted on an equal-area diagram (Fig. 8), both before and after tilt-correction. These were chosen on the basis of their VGP latitude being greater than 60°, in order to avoid transitional samples. The mean inclinations for both normal- and reversed-polarity samples is lower than the 55.3° expected at the sampling site latitude for a geocentric axial dipole (GAD), even if a time-averaged non-dipole term (e.g., Cox, 1975; Constable and Parker, 1988) is added to reduce the expected inclination by a few degrees. Normal directions are significantly shallower than reversed directions, indicating that compaction is not the only cause of these shallow inclinations. Normal- and reversed-polarity directions from higher in the same section pass the reversal test (McFadden and McElhinny, 1990) as shown in Holt and Kirschvink (1995), whereas those from the Réunion interval do not. Reversed-polarity directions from the upper part of

the section are the same as those from the Réunion interval, within uncertainty. Due to the scatter of Réunion normal-polarity inclinations the primary difference in normal directions is due to declinations. The Réunion declinations are signifiantly eastward of either Olduvai declinations or a GAD declination.

There are several possible explanations for both the slightly eastward Réunion declinations and shallow inclinations in the normal samples relative to the reversed samples. The first is merely a lack of adequate sampling of the Réunion subchron. With such a brief time interval of normal polarity, short-term variations in the sedimentation rate could result in a more detailed record of the lower transition and less resolution during the normal polarity state and upper transition. Another possibility is that normal-polarity, post-tilting overprints have not been completely removed from normal-polarity samples. This might suggest a difference between the magnetic fraction found in the rocks of the Réunion interval and those of the Olduvai in the same section, a difference which has not been detected otherwise. Furthermore, given the geometry of tilting, this effect would produce significantly steeper reversed directions. In the upper part of the section, where there are many more normal data, normal and reversed inclinations are not significantly different (Holt and Kirschvink, 1995). These observations could also indicate that the Réunion subchron did not achieve a stable, fully opposite state of polarity with enough secular variation to produce a geocentric axial dipole over its short duration.

Age and duration of the normal event

Reliable age controls on the polarity reversals associated with the Réunion subchron independent of the astronomical calibrations have been difficult to

obtain. A reassessment of earlier K/Ar ages on normal-polarity lava flows of Réunion Island (McDougall and Watkins, 1973) using the $^{40}Ar/^{39}Ar$ method yielded four ages which were indistinguishable, with a weighted mean of 2.14 ± 0.03 Ma (Baksi et al., 1993).

Using average sedimentation rates for the Death March Canyon section, we can estimate the ages of the polarity reversals by extrapolating from the Huckleberry Ridge Ash which is 10 m above the upper Réunion transition. The obvious drawback to this method is that variations in the sedimentation rate, and hence uncertainties of the estimated ages, cannot be determined. Also, this is not entirely independent of the astronomically calibrated ages, since at this point we only have one isotopically determined age in the section, and at least two ages are needed to determine an average sedimentation rate. However, if we use the Huckleberry Ridge Ash in conjuction with the upper Olduvai reversal, this method may provide a useful approximate estimate of the age and duration of the Réunion subchron for comparison with other methods.

Results of this extrapolation are compared in Table 1 with ages of the Réunion subchron determined by several previous studies. Our ages are shown for two estimates of average rates of sedimentation. One is determined for only the time period of the Oludvai subchron (33.7 cm/kyr) and another for the interval between the Huckleberry Ridge Ash and the upper Olduvai reversal (27.5 cm/kyr). These ages and the overall duration are remarkably consistent with the latest astronomical calibration (Lourens et al., 1996) of the Réunion subchron.

Intensity variations

The low-coercivity, low-blocking-temperature overprint is most consistently removed by the 300°C demagnetization step. Therefore, the intensity of magnetization measured at this step is used to estimate variations of relative paleointensity during this interval. Plotted without any normalization (Fig. 7f), there do not appear to be any significant changes which correlate with paleomagnetic directional changes. Bulk susceptibility (measured before heating) is normalized by mass (Fig. 7e) and this is used to normalize intensity, as shown in Fig. 7g.

The lowest intensities throughout the Réunion interval occur in the same stratigraphic zones as the gypsiferous siltstones, even after normalization for susceptibility/mass (Figs. 7e-g). This supports the hypothesis that the evaporite crystals disrupted the sedimentary fabric of the rock during and/or after initial acquisiton of depositional remanence. The alignment of magnetic grains was more randomized as a result, producing a new "primary" magnetization which is much weaker. These intensities are therefore not representative of geomagnetic field behavior.

There is an interval of low intensity from 127 m - 129 m which is surrounded by higher intensities and centered on the lower Réunion transition (Figs. 7c and 7g). This could be the result of decreased geomagnetic field intensity related to the transition, but it might also be related to lithology. The higher intensities correlate with the banded anhydrite lithologies. The changes do not appear to correlate with susceptibility/mass measurements, however (Fig. 7e), as would be expected if it were related to lithology. The most transitional sample in the upper transition zone has a low normalized intensity (132.8 m, Fig. 7g) but it also has both a very

low unnormalized intensity and susceptibility/mass ratio, indicating that the normalized intensity is not representative of true geomagnetic field behavior.

Transitional directions

The lower Réunion reversal, which spans ~ 1.5 m of section, is represented by 13 transitional samples. The upper reversal appears to be very abrupt or is not recorded with as much resolution as the lower reversal due to variations in sedimentation rate. Three transitional directions are recorded between 132.2 m and 132.8 m.

Paleomagnetic directions spanning the interval from ~ 115 m - 137 m (as shown in Fig. 7) are shown plotted in VGP space in Fig. 9. Pre- and post-Réunion reversed-polarity samples are plotted separately for comparison. The majority of transitional directions are from the lower reversal, but the three samples from the upper transition plot in the same general transitional path, over western Europe, western Africa, and the southern Atlantic. This path is very similar to the one observed for the upper Olduvai transition in the Confidence Hills (Holt and Kirschvink, 1995), and is approximately 90° away from the sampling site in longitude. Many sedimentary records of geomagnetic field reversals show a tendency for transitional VGP's to be located approximately 90° away from the sampling site in longitude (Quidelleur and Valet, 1994). This could be due to the inability of the sediments to accurately record inclinations during low field intensities (Quidelleur et al., 1995), but the VGP paths observed in this study could also be the result of smoothing between non-antipodal field directions before and after the reversal.

Discussion

Interpretation of paleomagnetic directions

In order to be certain that this record is accurate, the relationship between gypsiferous siltstone and erratic directions must be understood in more detail. The siltsone and banded anhydrite lithofacies have already been proven to accurately record geomagnetic field directions in the Olduvai subchron and in the upper Olduvai transition zones within both Confidence Hills sections (Holt and Kirschvink, 1995). As in any sedimentary record, there is the possibility that inclinations are greatly shallowed during periods of extremely low field intensity (Quidelleur and Valet, 1994; Quidelleur et al., 1995). However, polarity is undoubtedly recorded quite well, and upper Olduvai transitional directions from the two sections agree in spite of the fact that they are recorded in banded anhydrites in the Death March Canyon section and siltstones and fine-grained sandstones in Confusion Canyon.

The correlation between erratic directions in the Réunion interval and the presence of the gypsiferous siltstone lithofacies is definitive (Fig. 7). In addition, lithofacies without dispersed evaporites do not show this behavior. Since many of the gypsiferous siltstone samples did contain a recognizable, seemingly primary component of magnetization (although weak), we must consider this magnetization to either be originally spurious or a remagnetization which took place in-situ, affecting only that lithofacies. From observation of the composition and texture of this lithofacies, it appears to be related to the growth and/or regrowth of evaporite crystals within the matrix of these rocks. The extremely low intensity (Figs. 7f,g) relative to samples of other lithofacies supports the hypothesis that

displacive evaporites deformed the sediment during their growth (Beratan et al., in press), randomizing the orientation of clastic grains and allowing some realignment of magnetic grains with the ambient field within water-saturated pore spaces.

Given the fact that this phenomenon is limited to particular stratigraphic horizons, and the clastic sediments contained within these horizons are identical to those which do not contain displacive evaporites, it is reasonable to assume that the growth of these evaporites is related to their depositional environment (occurring soon after deposition) and not to a recent weathering effect. Since many of the samples seem to have acquired a direction of normal polarity (Figs. 7a-c), the earliest it could have occurred was during the Réunion subchron. This is reasonable given their stratigraphic position relative to the Réunion subchron and the environment of deposition. The sediments furthest from that subchron would have been ~ 7 m below the surface. The stratigraphically highest gypsiferous siltstones in this zone are ~ 2.5 m below the bottom of the Réunion subchron and ~ 7 m below the top of the Réunion subchron. Therefore, if the siltstones and banded anhydrites recording the normal-polarity Réunion subchron acquired remanence at or near the surface, the evaporites in the gypsiferous siltstones must have been growing between 9 - 25 kyr after deposition.

At this point, further explanation of the evaporite deposition process is in order. In the playa or salt pan environment, a water table exists which may be at or above the surface, but is usually at some depth below the surface. When it is below the surface, evaporative pumping causes water to move up through the sediment from the water table, carrying calcium and sulfate ions (among others) which precipitate as they become saturated in the water (Hsieh and Murray,

1996). This activity is regulated to some degree by groundwater recharge from the margins of the playa or salt pan, which in turn is related to local climatic conditions. If the water table is too deep, evaporative pumping is not sufficient to activate water movement and no deposition of evaporites takes place. During periods of wetter climate (or at locations closer to the center of the basin) more water is available, and hence more ions are supplied. If the supply of dissolved ions and groundwater is sufficient, evaporites may form at the surface, resulting in banded or massive anhydrite. Under some conditions (slightly less water or ions), evaporites may form only as crystals dispersed within sediment near the surface. This could be the origin of the gypsiferous siltstones encountered in this study.

We can apply this interpretation to the stratigraphy of the Réunion section. Climatic factors were such that evaporite crystals precipitated within the sediments now located between ~ 121 m - 126 m while they were near the surface, during evaporative pumping of groundwater. During an interval when the groundwater recharge was insufficient or the water table was too low for evaporative pumping to be effective, the evaporite-free zone between ~ 123 m - 124 m was created. As these sediments were buried, the existing evaporites continued to grow at times when groundwater rich in dissolved ions again flowed upward through the sediment column on its way to the surface. Calcium sulfate preferentially precipitated on the existing crystals due to the lower energy requirements relative to forming new crystals in the evaporite-free zones. The presence of the existing evaporites also acted to buffer the groundwater, helping to prevent new crystals from forming. As this growth took place, the clastic matrix surrounding the evaporite crystals was disturbed and magnetic directions were realigned, but with

much less efficacy than near the surface, due to the rapidly decreasing pore space.

The presence of banded anhydrite within the normal-polarity zone above the gypsiferous siltstones (Fig. 7a) is clear evidence that groundwater and dissolved ions were available in sufficient quantities during that time. As the sediments were buried, the potential for evaporite precipitation diminished due to the decreasing availability of ions (the concentration of ions in the groundwater decreases with depth due to the evaporative pumping from the surface) and/or dewatering of the sediment from compaction.

It is imperative to be able to confidently identify those samples whose directions may have been affected by the growth of dispersed evaporites. The presence of these dispersed evaporites within the matrix is the determining factor, and this can be checked visually. In unheated samples or in the actual outcrop, this can be difficult due to the similarity in texture and color between siltstones which contain evaporites and those which do not. Upon heating the samples to high temperatures (ca. 600°C) , however, the color contrast between evaporites and the clastic components is remarkably enhanced. The evaporites remain white while the originally light-tan clastic material becomes a dark reddish-brown color, so it is a simple matter to identify samples which contain disperesed evaporites. The most obvious difference in outcrop between the gypsiferous siltstone and siltstone lithofacies is the absence of bedding in the gypsiferous siltstone. Primary depositional structures are destroyed by the evaporite growth (Beratan et al., in press).

Comparison with previous studies

The studies on Réunion Island revealed normal-polarity lava flows in two locations (Chamalaun and McDougall, 1966; McDougall and Chamalaun, 1966; McDougall and Watkins, 1973). One section records a R-N transition, normal-polarity directions, and what appears to be a transitional direction at the very top of the section. The other section records only a N-R transition. This second section was assumed to overlie the first, and therefore it was not possible to say for certain whether one or two events occurred, as there could be a time gap between the sections. The precision of isotopic dating of rocks from the two sections was insufficient to discern whether such a gap did indeed exist (McDougall and Watkins, 1973; Baksi et al., 1993).

In eastern Africa, normal polarity rocks were found in a section of sedimentary rocks of the Shungura Formation (Brown and Shuey, 1976; Brown et al., 1978). Only a few samples recorded what appeared to be the Réunion subchron. There were many samples within the section which exhibited unusual, unexplained paleomagnetic directions, and very limited demagnetization procedures were employed.

A few deep-marine sediment cores have recorded an anomalous direction or two at about the level of the Réunion subchron (e.g., Tauxe et al., 1984; Zhao et al., 1996), but in most cases, the sedimentation rate of marine sediments combined with bioturbation effects causes this brief subchron to be missed (Opdyke, 1972).

The shallow-marine sedimentary record of Zijderveld et al. (1991) from southern

Sicily shows a single normal-polarity lithostratigraphic unit interpreted as the Réunion subchron. The average sedimentation rate for their section is of the order 13 cm/kyr, while their average sample spacing in the Réunion interval is 1.25 m (Zijderveld et al., 1991). This yields an average sampling interval of ~ 9 kyr, leaving considerable room for undetected variations of the geomagnetic field during the interval of the Réunion subchron. A more detailed study of a similar, nearby section reveals a single normal polarity event spanning ~ 20 kyr (Langereis, unpublished data), and this is the magnetostratigraphic basis for a recent update to the astronomical age of the Réunion subchron (Lourens et al., 1996) which our estimated ages match very well (Table 1).

A single normal-polarity zone comprised of 9 lava flows has been found in ca. 2.0 Ma rocks of eastern Africa (Courtillot, 1996). This has the potential to provide new, independent isotopic ages for the Réunion, although it is unlikely that a significant difference in age for the upper and lower boundaries of the interval can be obtained by that method. Another disadvantage of volcanic rocks is the discontinuous nature of deposition, which places large uncertainties on the duration of polarity events. However, volcanic rocks do not suffer from diagenetic side-effects as sedimentary rocks do, so it is extremely useful to have detailed records from volcanic rocks for comparison.

Conclusions

This study shows that the reliability of paleomagnetic directions from fine-grained sediments deposited in ephemeral lake environments may be highly sensitive to environmental conditions after initial deposition and subsidence. Under certain conditions, secondary or continued growth of evaporites accompanied by deformation of the sediment may occur while the sediments are as much as 7 m below the surface. This process can randomize pre-existing magnetic directions and allow partial realignment of some magnetic grains.

We have also found that the gypsiferous siltstone lithofacies is easily recognizable, the boundaries of such zones are quite sharp, and stratigraphically adjacent layers are not affected. The siltstone and banded anhydrite lithofacies appear to produce reliable, stable paleomagnetic directions, and from them we were able to obtain a detailed record of the Réunion subchron which shows a single normal polarity interval approximately 20 kyr in duration, from ~ 2.15 Ma - 2.13 Ma. Transitional VGP's fall in a fairly confined band which is located approximately 90° east of the sampling site in longitude. There are two brief gaps in the record due to the presence of gypsiferous siltstone in the stratigraphic column, but because these intervals are short and they straddle a section of definitive reversed-polarity directions, it is unlikely that another normal-polarity interval was missed.

Acknowledgements

The authors would like to thank the Caltech Ge124 class of 1993 for preliminary fieldwork, undergraduates of Ricketts House, Christopher DuPuis, Mark Wanek, Hiroshi Ishii and Dragos Harabor for field assistance, Laura Serpa and Terry Pavlis for use of the Shoshone Convention Center, and the National Park Service for permission to sample within a National Park wilderness area. The first author is also grateful to Liz Warner Holt, Jean Hsieh, Slawek Tulaczyk, Andre Sarna-Wojcicki and Cor Langereis for helpful discussions. We made extensive use of software provided by Craig Jones (cjones@mantle.colorado.edu) for the analysis and presentation of paleomagnetic data, and the GMT package (Wessel and Smith, 1991) for global projections of VGP's. This research was funded by NSF grant EAR-9419041. This is contribution no. 5814 of the Caltech Division of Geological and Planetary Sciences.

References

Baksi, A. K., Hoffman, K. A., and McWilliams, M., 1993, Testing the accuracy of the geomagnetic polarity timescale (GPTS) at 2-5 Ma, utilizing $^{40}Ar/^{39}Ar$ incremental heating data on whole-rock basalts: Earth and Planetary Science Letters, v. 118, p. 135-144.

Baksi, A. K., Hsu, V., McWilliams, M. O., and Farrar, E., 1992, $^{40}Ar/^{39}Ar$ dating of the Brunhes Matuyama geomagnetic field reversal: Science, v. 256, p. 356-357.

Beratan, K., 1992, Stratigraphy and depositional environments, southern Confidence Hills, Death Valley, California: San Bernardino County Museum Asso-

ciation Quarterly, v. 39, no. 2, p. 7-11.

Beratan, K., Hsieh, J., and Murray, B., in press, Pliocene/Pleistocene stratigraphy and depositional environments, southern Confidence Hills, Death Valley, California: GSA Special Paper on Cenozoic basins of the Death Valley region.

Brown, F. H., and Shuey, R. T., 1976, Magnetostratigraphy of the Shungura and Usno Formations, lower Omo valley, Ethiopia, *in* al., Y. C. e., ed., Earliest man and environments in the Lake Rudolf Basin: Chicago, University of Chicago, p. 64-68.

Brown, F. H., Shuey, R. T., and Croes, M. K., 1978, Magnetostratigraphy of the Shungura and Usno Formations, southwestern Ethiopia: new data and comprehensive reanalysis.: Geophysical Journal of the Royal Astronomical Society, v. 54, p. 519-538.

Cande, S. C., and Kent, D. V., 1995, Revised calibration of the geomagnetic polarity timescale for the Late Cretaceous and Cenozoic: Journal of Geophysical Research, v. 100, no. B4, p. 6093-6095.

Chamalaun, F. H., and McDougall, I., 1966, Dating geomagnetic polarity epochs in Réunion: Nature, v. 210, p. 1212-1214.

Cisowski, S., 1981, Interacting vs. non-interacting single-domain behavior in natural and synthetic samples: Physics of the Earth and Planetary Interiors, v. 26, p. 56-62.

Clement, B. M., and Kent, D. V., 1985, A comparison of two sequential geomagnetic polarity transitions (upper Olduvai and lower Jaramillo) from the Southern Hemisphere: Physics of the Earth and Planetary Interiors, v. 39, p. 301-313.

Constable, C. G., and Parker, R. L., 1988, Statistics of the geomagnetic secular variation for the past 5 m.y.: Journal of Geophysical Research, v. 93, p. 11569-11581.

Courtillot, 1996, Identification of the Réunion event in Ethiopian Afar: EOS Trans. AGU (abstract), v. 77, no. 46, p. 166.

Cox, A., 1975, The frequency of geomagnetic reversals and the symmetry of the non-dipole field.: Reviews of Geophysics and Space Physics, v. 13, no. 3, p. 35-50.

Fisher, N. I., Lewis, T., and Embleton, B. J. J., 1987, Statistical Analysis of Spherical Data: Cambridge, Cambridge University Press, 329 p.

Gomez, F., Hsieh, J., Holt, J., Murray, B., and Kirschvink, J., 1992, Outcrop geology of Plio-Pleistocene strata of the Confidence Hills, southern Death Valley, California: San Bernardino County Museum Association Quarterly, v. 39, no. 2, p. 3-6.

Grommé, C. S., and Hay, R. L., 1971, Geomagnetic polarity epochs: age and duration of the Olduvai normal polarity event: Earth and Planetary Science Letters, v. 10, p. 179-185.

Harland, W. B., Armstrong, R. L., Cox, A. V., Craig, L. E., Smith, A. G., and Smith, D. G., 1989, A geologic time scale: Cambridge, Cambridge University Press.

Harland, W. B., Cox, A. V., Llewellyn, P. G., Pickton, C. A. G., Smith, A. G., and Walters, R., 1982, A geologic time scale: Cambridge, Cambridge Univ. Press, 131 p.

Hays, J. D., Imbrie, J., and Shackleton, N. J., 1976, Variations in the Earth's orbit: Pacemaker of the ice ages: Science, v. 194, p. 1121-1132.

Herrero-Bervera, E., and Theyer, F., 1986, Non-axisymmetric behaviour of Olduvai and Jaramillo polarity transitions recorded in north-central Pacific deep-sea sediments: Nature, v. 322, p. 159-162.

Hilgen, F. J., 1991a, Astronomical calibration of Gauss to Matuyama sapropels in the Mediterranean and implications for the geomagnetic polarity time scale:

Earth and Planetary Science Letters, v. 104, p. 226-244.

Hilgen, F. J., 1991b, Extension of the astronomically calibrated (polarity) timescale to the Miocene/Pliocene boundary: Earth and Planetary Science Letters, v. 107, p. 349-368.

Holt, J. W., and Kirschvink, J. L., 1995, The upper Olduvai geomagnetic field reversal from Death Valley, California: a fold test of transitional directions: Earth and Planetary Science Letters, v. 133, p. 475-491.

Hsieh, J., 1993, Continental climate change from 2.4 Ma to 1.6 Ma: A high resolution record from lake beds in Death Valley, California: GSA Annual Spring Meeting, Abstracts with Programs, v. 25, no. 6, p. A456.

Hsieh, J. C. C., and Murray, B., 1996, A ~24,000 year period climate signal in 1.7-2.0 million year old Death Valley strata: Earth and Planetary Science Letters, v. 141, p. 11-19.

Kirschvink, J. L., 1980, The least-squares line and plane and the analysis of paleomagnetic data: examples from Siberia and Morocco: Geoph. J. Royal Astr. Soc., v. 62, p. 699-718.

Lee, T.-Q., 1992, Study of the polarity transition record of the upper Olduvai event from Wulochi sedimentary sequence of the coastal range, eastern Taiwan: TAO, v. 3, no. 4, p. 503-518.

Levi, S., and Merrill, R. T., 1978, Properties of single domain, pseudosingle domain, and multidomain magnetite: Journal of Geophysical Research, v. 83, p. 309-323.

Liu, H., An, J., and Wang, J., 1993, Preliminary study of the Olduvai termination recorded in the red loam in southeast Shanxi Province, China: Journal of Geomagnetism and Geoelectricity, v. 45, no. 4, p. 331-338.

Lourens, L. J., Antonarakou, A., Hilgen, F. J., Hoof, A. A. M. V., Vergnaud-Grazzini, C., and Zachariasse, W. J., 1996, Evaluation of the Plio-Pleistocene

astronomical timescale: Paleoceanography, v. 11, no. 4, p. 391-413.

Lowrie, W., and Fuller, M., 1971, On the alternating field demagnetization characteristics of multidomain thermoremanent magnetization in magnetite: Journal of Geophysical Research, v. 76, p. 6339-6349.

Mankinen, E. A., and Dalrymple, G. B., 1979, Revised geomagnetic polarity time scale for the interval 0-5 m.y. B.P.: Journal of Geophysical Research, v. 84, no. B2, p. 615-626.

McDougall, I., Brown, F. H., Cerling, T. E., and Hillhouse, J. W., 1992, A reappraisal of the geomagnetic polarity time scale to 4 Ma using data from the Turkana Basin, East Africa: Geophysical Research Letters, v. 19, no. 23, p. 2349-2352.

McDougall, I., and Chamalaun, F. H., 1966, Geomagnetic polarity scale of time: Nature, v. 212, p. 1415-1418.

McDougall, I., and Watkins, N. D., 1973, Age and duration of the Réunion geomagnetic polarity event: Earth and Planetary Science Letters, v. 19, p. 443-452.

McFadden, P. L., and McElhinny, M. W., 1990, Classification of the reversal test in paleomagnetism: Geophysical Journal Int., v. 103, p. 725-729.

Opdyke, N. D., 1972, Paleomagnetism of deep-sea cores: Reviews of Geophysics and Space Physics, v. 10, no. 1, p. 213-249.

Quidelleur, X., Holt, J., and Valet, J.-P., 1995, Confounding influence of magnetic fabric on sedimentary records of a field reversal: Nature, v. 374, p. 246-249.

Quidelleur, X., and Valet, J.-P., 1994, Paleomagnetic records of excursions and reversals: possible biases caused by magnetization artefacts: Physics of the Earth and Planetary Interiors, v. 82, p. 27-48.

Renne, P., Walter, R., Verosub, K., Sweitzer, M., and Aronson, J., 1993, New data from Hadar (Ethiopia) support orbitally tuned time scale to 3.3 Ma: Geo-

physical Research Letters, v. 20, no. 11, p. 1067-1070.

Sarna-Wojcicki, A. M., and Pringle, M. S., 1992, Laser-fusion 40Ar/39Ar ages of the Tuff of Taylor Canyon and Bishop Tuff, E. California - W. Nevada: Eos Trans., AGU, Fall Meeting Supp., v. 73, no. 43, p. 633.

Shackleton, N. J., Berger, A., and Peltier, W. R., 1990, An alternative astronomical calibration of the lower Pleistocene timescale based on ODP Site 677: Transactions of the Royal Society of Edinborough: Earth Sciences, v. 81, p. 21-261.

Tauxe, L., Deino, A. L., Behrensmeyer, A. K., and Potts, R., 1992, Pinning down the Brunhes/Matuyama and upper Jaramillo boundaries: A reconciliation of orbital and isotopic time scales: Earth and Planetary Science Letters, v. 109, p. 561-572.

Tauxe, L., Tucker, P., Peterson, N. P., and LaBrecque, J. L., 1984, Magnetostratigraphy of Leg 73 sediments, *in* Hsü, K. J., and LaBrecque, J. L., eds., Init. Repts. DSDP: Washington, U.S. Govt. Printing Office, p. 609-621.

Tric, E., Laj, C., Jehanno, C., Valet, J. P., Kissel, C., Mazaud, A., and Iaccarino, S., 1991, High resolution record of the Upper Olduvai Transition from Po Valley (Italy) sediments: support for dipolar transition geometry?: Physics of the Earth and Planetary Interiors, v. 65, p. 319-336.

Troxel, B. W., and Butler, P. R., 1986, Multiple Quaternary deformation, central part of the Confidence Hills, Death Valley, California: an example of folding along a strike-slip fault zone, Quaternary tectonics of southern Death Valley, California field trip guide: Friends of the Pleistocene, Pacific Cell: Shoshone, CA, Bennie W. Troxel Publications.

Troxel, B. W., Sarna-Wojcicki, and Meyer, C. E., 1986, Ages, correlations, and sources of three ash beds in deformed Pleistocene beds, Confidence Hills, Death Valley, California., Quaternary Tectonics of Southern Death Valley,

California field trip guide: Pacific Cell, Friends of the Pleistocene: Shoshone, CA, B.W. Troxel Publications.

Wessel, P., and Smith, W. H. F., 1991, Free software helps map and display data: EOS Trans. AGU, v. 72, no. 441, p. 445-446.

Wright, L. A., and Troxel, B. W., 1984, Geology of the northern half of the Confidence Hills 15-minute quadrangle, Death Valley region, eastern California: The area of the Amargosa chaos: California Division of Mines and Geology, scale Wright1984.

Zhao, X., Milkert, D., Liu, L., and Kanamatsu, T., 1996, Magnetostratigraphy of Cenozoic sediments recovered from the Iberia abyssal plain, *in* Whitmarsh, R. B., Sawyer, D. S., Klaus, A., and Masson, D. G., eds., Proc. ODP, Scientific Results: Washington, U.S. Govt. Printing Office, p. 315-334.

Zijderveld, J. D. A., Hilgen, F. J., Langereis, C. G., Verhallen, P. J. J. M., and Zachariasse, W. J., 1991, Integrated magnetostratigraphy and biostratigraphy of the Upper Pliocene - Lower Pleistocene from the Monte Singa and Crotone areas in Calabria, Italy: Earth and Planetary Science Letters, v. 107, p. 697-714.

Polarity Reversal	K/Ar MK79 Age, Ma	Anom. Ha89 Age, Ma	Sed. MD92 Age, Ma	Astron. Lo96 Age, Ma	Sed. rate (cm/kyr) 33.7 Age, Ma	27.5 Age, Ma
Réunion 2						
Top	2.01	-	2.11	-	-	-
Bottom	2.04	-	2.15	-	-	-
Réunion 1						
Top	2.12	2.06	2.19	2.129	2.12	2.13
Bottom	2.14	2.09	2.27	2.149	2.14	2.15
Duration (kyr)	*130*	*30*	*160*	*20*	*20*	*20*

Table 1. Comparison of results with selected previous studies. Age and duration of Réunion subchron are shown for: MK79 [*Mankinen and Dalrymple*, 1979], based on K/Ar isotopic ages; Ha89 [*Harland et al.*, 1989], based on seafloor magnetic anomalies; MD92 [*McDougall et al.*, 1992], based on sedimentary extrapolation from tephras; and Lo96 [*Lourens et al.*, 1996], based on astronomical calibration of sapropel-bearing sediments. The two right-hand columns are results from this study, using average sedimentation rates determined for only the Olduvai subchron (33.7 cm/kyr, using dates of *Lourens* [1996]) and for the interval between the Huckleberry Ridge Ash [2.09 ± 0.008 Ma, *Sarna-Wojcicki and Pringle*, 1992; *Sarna-Wojcicki*, unpublished data] and the upper Olduvai (27.5 cm/kyr, using date from *Lourens* [1996]). Estimated ages determined for this study are rounded to nearest 0.01 Ma.

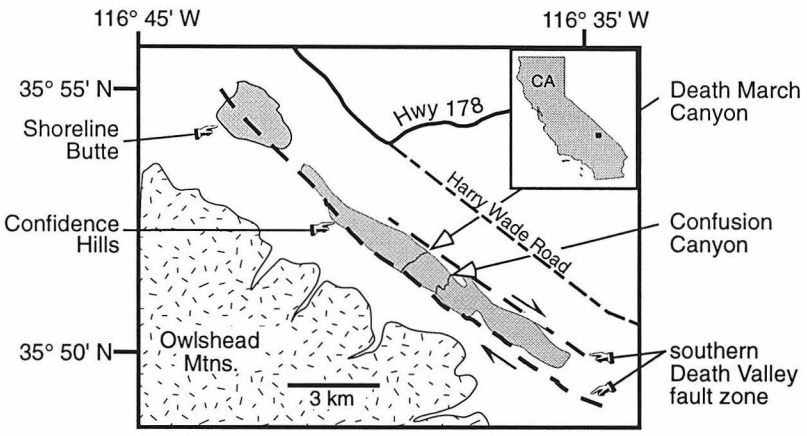

Figure 1. Location map. Sections sampled within the Confidence Hills in southern Death Valley are indicated, along with the eastern and western strands of the southern Death Valley fault zone [*Wright and Troxel*, 1984]. Adapted from *Holt and Kirschvink* [1995].

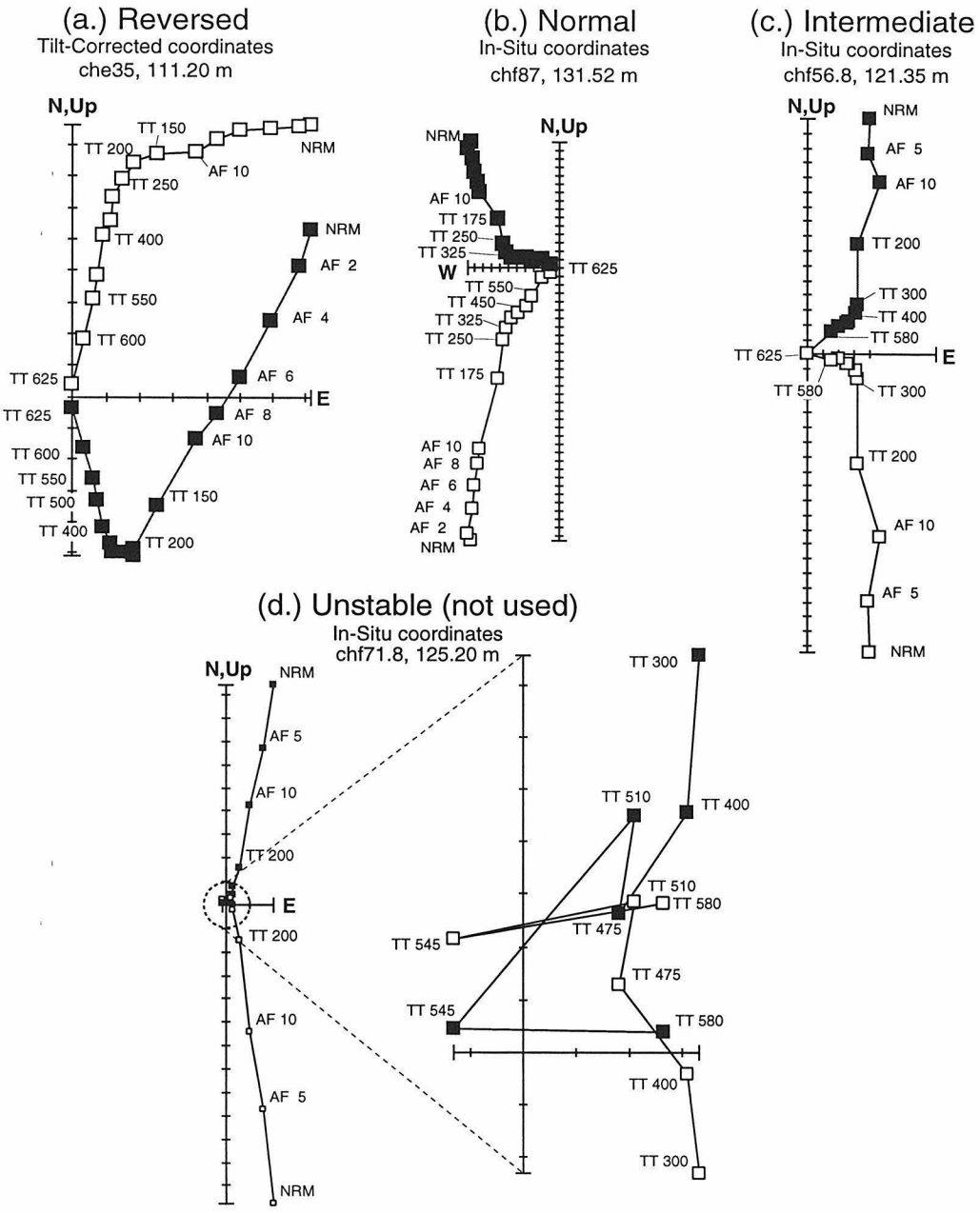

Figure 2. Sample demagnetization. Orthogonal projections of declination onto the horizontal plane (filled squares) and inclination onto the vertical plane (open squares) for typical samples of (a.) reversed polarity (siltstone) (b.) normal polarity (siltstone), (c.) intermediate polarity (gypsiferous siltstone), and (d.) an example of a sample which did not reach a stable, linear demagnetization path (gypsiferous siltstone). Each division along the axes is 10^{-3} A/m except for (d.) which has divisions of 10^{-4} A/m.

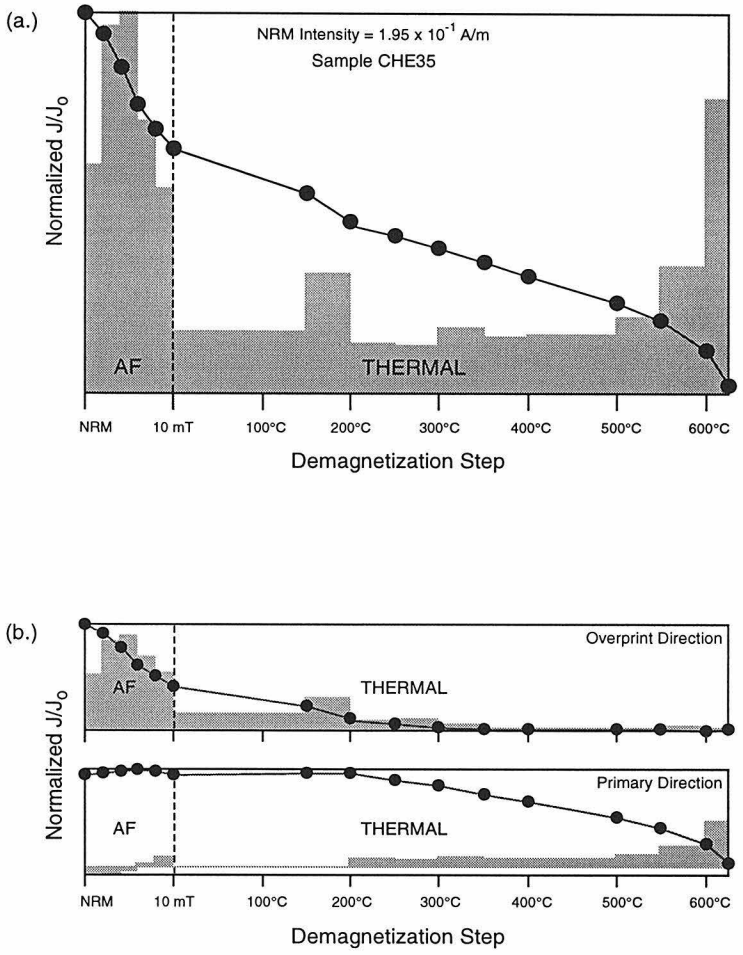

Figure 3. Sample magnetization versus demag step. The ratio of J/Jo is plotted as a function of demagnetization step for a representative sample as (a.) total J/Jo, and (b.) J/Jo separately for each component. The removal of the overprint direction by the 300°C thermal step is apparent, as is the small amount of overlap between the coercivities of the two components. The shaded boxes represent the derivative of the J/Jo line, indicating the coercivity/blocking temperature spectrum for that component.

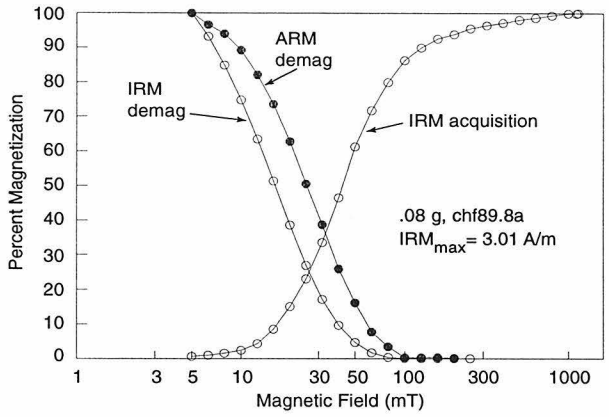

Figure 4. IRM/ARM acquisition and demagnetization. A typical coercivity distribution for a sample from the Réunion interval. Samples from throughout the interval exhibit virtually identical patterns, as do all tested samples from Death March Canyon. Data for the IRM acquisition and AF demagnetization of the IRM are shown with open circles. The filled circles show the AF demagnetization of the of the ARM acquired in a 1 mT direct current biasing field with a 100 mT (max) alternating field.

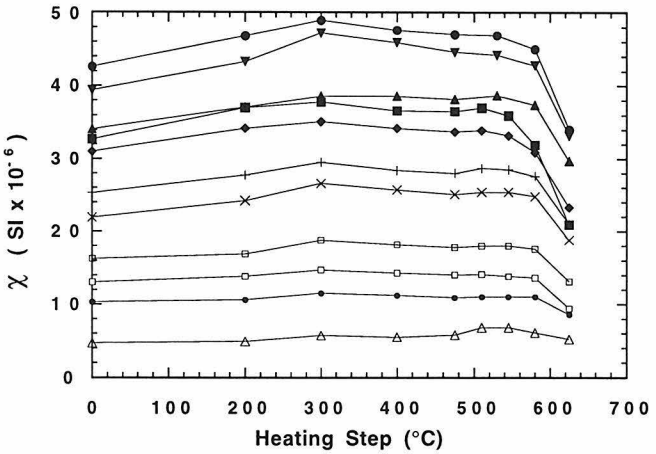

Figure 5. Susceptibility vs. demag step. Susceptibility was measured after each thermal demag step and plotted for samples which span the observed range of initial susceptibility. The greatest change occurs upon heating the samples to 625° and also corresponds to the greatest color change during heating, wherein the clastic component of the samples becomes reddish-brown.

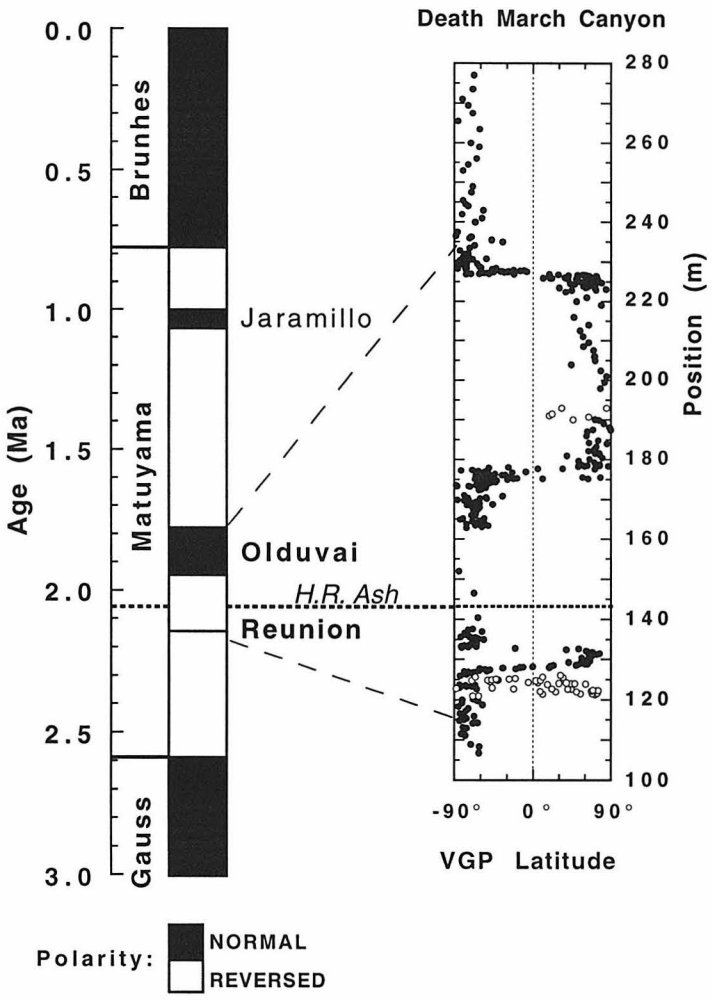

Figure 6. Magnetostratigraphy. VGP latitude as a function of stratigraphic position for the Death March Canyon section, compared with the Geomagnetic Polarity Timescale (GPTS) from *Cande and Kent* [1995]. VGP latitudes obtained from the gypsiferous siltstone lithofacies are plotted as open circles as they are considered unreliable (see text for discussion), those from other lithofacies are plotted as filled circles. The Huckleberry Ridge ash (~2.09 Ma [*Sarna-Wojcicki and Pringle*, 1992], recalculated for new standard [*Sarna-Wojcicki*, unpublished data]) is the primary tiepoint with the GPTS. VGP Latitude plot is updated from *Holt and Kirschvink* [1995].

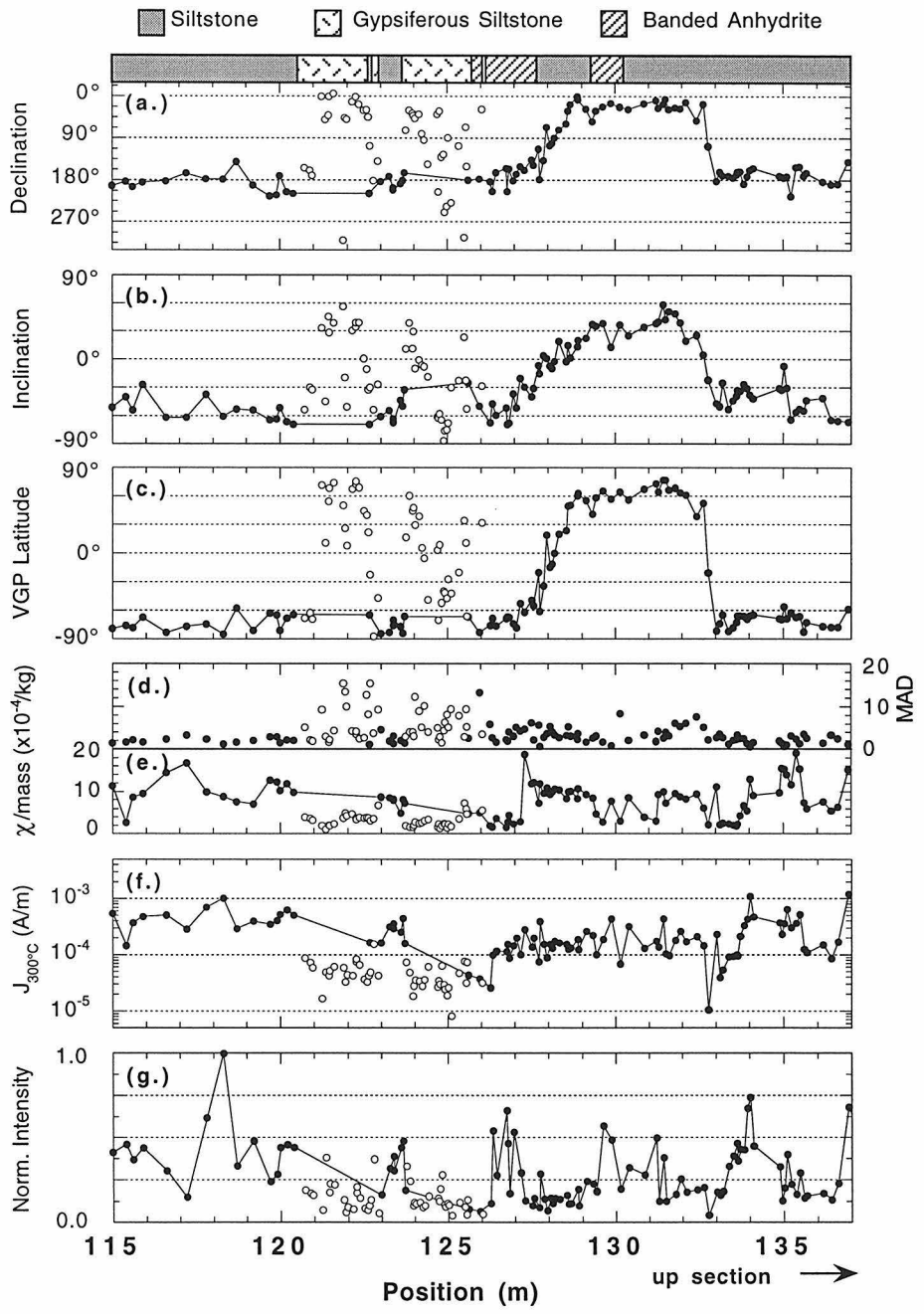

Figure 7. Réunion interval data and lithostratigraphic column. (a.) Declination, (b.) inclination, (c.) VGP latitude, (d.) maximum angular deviation (MAD), (e.) susceptibility/mass, (f.) intensity at the 300°C demag step, and (g.) normalized intensity are plotted as a function of stratigraphic position in the interval of the Réunion subchron. Data obtained from the gypsiferous siltstone lithofacies are plotted as open circles as they are considered unreliable (see text for discussion), those from siltstone and banded anhydrite are plotted as solid circles. Direction of younger section is to right.

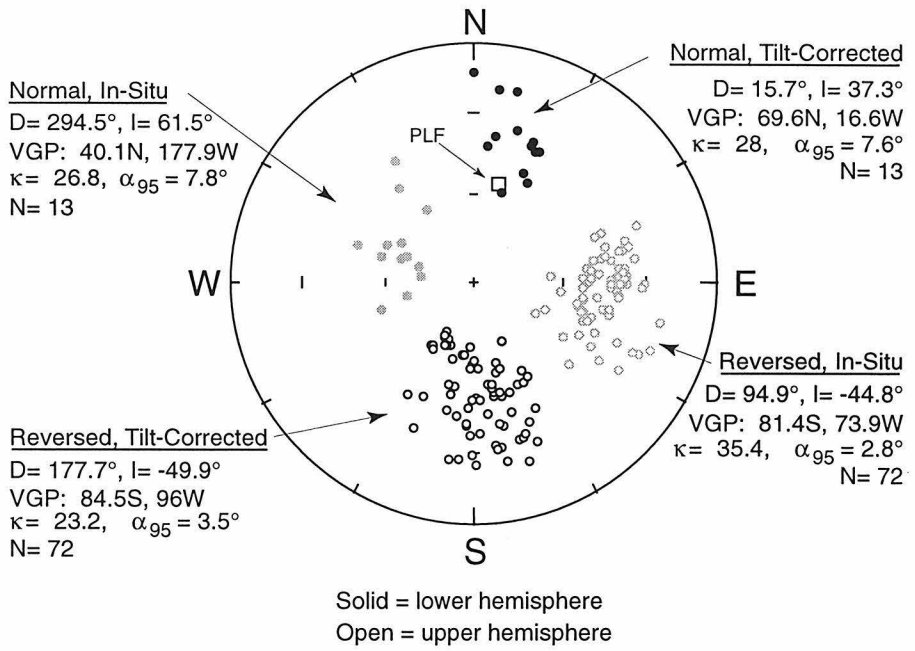

Figure 8. Non-transitional data. Equal area plots of the non-transitional directions from the same stratigraphic interval shown in Fig. 7. Filled circles represent lower hemisphere projections, open circles represent upper hemisphere projections. Fisher statistics [*Fisher et al.*, 1987] for each group are shown for pre- and post-tilt-corrected data (D, declination east of north; I, inclination, positive downward; κ, precision parameter; N, number of samples). The data fail the reversal test of *McFadden and McElhinny* [1990]. See text for discussion.

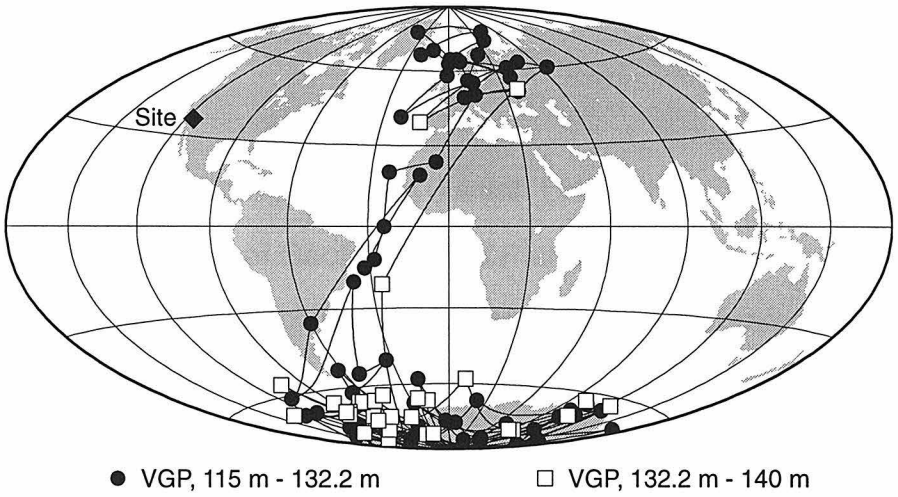

Figure 9. Virtual Geomagnetic Poles. VGP's are shown for the stratigraphic interval of Fig. 7 on a Hammer-Aitoff projection of the Earth, centered on 0° N, 0° E. Latitude and longitude grid spacings are 30°. VGP's for samples up to and including the normal-polarity zone of the Réunion subchron are shown as filled circles, while those from the upper Réunion transition and above are shown as open squares.

Paper 4: Geomagnetic field inclinations for the past 400 kyr from the 1 km core of the Hawaii Scientific Drilling Project

John W. Holt and Joseph L. Kirschvink

Division of Geological and Planetary Sciences

California Institute of Technology, Pasadena, California 91125

Florence Garnier

Centre des Faibles Radioactivites, CEA-CNRS, 91198 Gif-sur-Yvette Cedex, France

First Published in:

Journal of Geophysical Research

vol. 101 (B5), pp. 11655-11663, 1996

Abstract

A volcanic record of geomagnetic field inclination for the past ~400 kyr at Hilo, Hawaii has been obtained from the 941.5 meters of core recovered by the Hawaii Scientific Drilling Project. The analysis of 195 lava flows reveals six instances of near-zero inclination and two instances of fully negative inclination (reverse polarity) within an otherwise normal-polarity core. In particular, flow unit 23 (~178 m depth) records a horizontal inclination and may be associated with the Laschamp event; flow units 40 and 42 (~260 m depth) record negative inclinations and are close in age to the Blake event; flow unit 55 (~320 m depth) records a negative inclination with a relative declination change of ~75° with respect to the overlying flow, and is probably the Jamaica/Biwa I/Pringle Falls event. The five instances of shallow inclination found below 400 m depth appear to have resulted from long-term secular variation as they are part of inclination swings between ~0° and ~60° with a periodicity of ~10 - 50 kyr. In contrast, the inclination shifts at ~178 m and ~320 m depths significantly deviate from long-term trends, suggesting the existence of at least two independent processes producing time variations of the geomagnetic field. The secular variation has a mean of 30.9° (α_{95} = 2.27°), which is significantly shallower than the expected dipole mean of 36°. The dispersion (σ = 12.5°) agrees with global paleosecular variation data for 0 - 5 Ma and secular variation models.

Introduction

The Hawaii Scientific Drilling Project (HSDP) [*Stolper et al.*, this issue] was conceived in order to study the nature and evolution of a mantle plume hot spot by drilling through the flank of an active ocean island volcano. The initial phase of

this program was a "pilot hole," drilled at Hilo, Hawaii (Figure 1). In addition to the petrologic, geochemical, and volcanological information afforded by the recovered core [*Stolper et al.*, this issue], this project provided the unprecedented opportunity to obtain a record of geomagnetic field inclination for the last ~ 400 kyr from a continuous sequence of lava flows at one location in the central Pacific.

Paleomagnetic studies on the island of Hawaii (known as the "Big Island", Figure 1) have established that Hawaiian basalts record the ambient field direction extremely well [*Doell and Cox*, 1963, 1965; *Hagstrum and Champion*, 1994] and that all flows exposed on the surface were deposited during the Brunhes normal polarity chron [*Doell and Cox*, 1965]. In addition, detailed studies of hundreds of lava flows [*Doell and Cox*, 1971; *Doell*, 1972; *McWilliams et al.*, 1982; *Holcomb et al.*, 1986; *Mankinen and Champion*, 1993; *Hagstrum and Champion*, 1994] and lake sediments [*Peng and King*, 1992] have produced paleosecular variation records as far back as 13,000 years. These records show that the subdued nature of the present geomagnetic field's non-dipole component may have persisted for the past several thousands of years and possibly longer, although *Mankinen and Champion* [1993] pointed out that despite attempts at correction [e.g., *McWilliams et al.*, 1982], this may still be the result of sampling very short time intervals. While these and other studies have provided valuable information on recent lava flows and geomagnetic field behavior, continuous records extending into the Pleistocene are difficult to obtain since most of the island is covered by flows less than a few thousand years old.

Although the HSDP core is azimuthally unoriented, the paleomagnetic inclination record may address several important issues regarding geomagnetic field behav-

ior. Sudden polarity changes or excursions, paleointensity, and secular variation of the zonal components of the geomagnetic field can in principle be measured or detected with inclination data alone. This core is particularly interesting because the HSDP record spans the upper half of the Brunhes magnetochron [*Harland et al.*, 1989], a period in which several departures from the stable normal polarity of the field have been previously observed (reviewed by *Champion et al.* [1988] and *Jacobs* [1994]). Volcanic records are not as continuous as sedimentary records and may miss excursions of the geomagnetic field, which are often less than a few thousand years in duration [e.g., *Courtillot and Lemouel*, 1988]; however, volcanic records do not suffer from the time-averaging effect of sedimentary acquisition of remanence which may also cause short-lived events to be missed [e.g., *Thouveny and Creer*, 1992]. When sudden changes of geomagnetic field direction are found in volcanic records, there is the opportunity to constrain their ages using geochronologic techniques, as well as to obtain an absolute measurement of the field intensity at that time. The former is required to establish global correlation of geomagnetic field excursions or events, while the latter permits a discussion of the geomagnetic regime responsible for the rapid directional changes.

Unfortunately, there are few volcanic records available which span more than one of these relatively rare events. According to our paleomagnetic studies, the 208 lava flow units comprising the HSDP pilot core record three sudden, large shifts of geomagnetic field inclination and five instances of extremely shallow inclination. $^{40}Ar/^{39}Ar$ and K/Ar dating of basaltic samples from the core [*Sharp et al.*, this issue] as well as radiocarbon dating of volcanic ashes [*Beeson et al.*, this issue] provide age constraints for several of these geomagnetic phenomena.

Core Description

The 1056-m-deep HSDP hole was drilled through ~280 m of Mauna Loa flows into the flank of Mauna Kea volcano. Core recovery rate was 90%, with the unrecoverable portion being comprised of unconsolidated sediments and rubble [*Stolper et al.*, this issue]. Most flow units sampled by the core resulted in at least one or two sections of continuous core approximately 0.3 m in length, and occasional reconstructions of 1 - 2 m in length were possible. As previously mentioned, the core was not azimuthally oriented. Vertical orientation of the core was preserved immediately after each core run (retrieval of ~3 m of core) by two blue/red line pairs (each pair consisting of blue on left, red on right) drawn along opposite sides of the retrieved core section. The section was then cut into ~0.6 m lengths for boxing and split lengthwise into one archive sample and one sample for subsequent study [*Stolper and Baker*, 1994].

Core logging identified 227 distinct lithologic units, 208 of which are individual or compound lava flows; the remainder being ash beds, sediments, and soils [*Stolper and Baker*, 1994; *Stolper et al.*, this issue]. The term "unit" refers to either a single lava flow or a compound flow erupted in a short time. "Flow" could therefore be synonomous with "unit," or could be a subdivision of a compound flow unit. The 27 Mauna Loa flows, extending from the surface to 280 m depth and were deposited on shallow slopes (~1°) of lava deltas. Mauna Kea flows, constituting the bulk of the core, were deposited on the relatively steeper slope (~3° - 6°) of the volcano [G.P.L. Walker, unpublished manuscript, 1995]. As a result, Mauna Loa flows in the core are generally thicker than those of Mauna Kea and contain more intercalated sediment and soil horizons. The boundary between Mauna Loa and Mauna Kea flows is distinguished by major- and trace-

element compositions [*Rhodes*, this issue]. Detailed petrography and petrology of HSDP samples is reported by *Baker et al.* [this issue]. Lava flows from both volcanoes are exceptionally unaltered due to their location away from active hydrothermal areas [*Stolper et al.*, this issue].

Sampling and Measurements

Four to six 2.5-cm-diameter samples were drilled from 195 flows within the HSDP core using a diamond-tipped, water-cooled coring bit. A vertical orientation line was drawn parallel to the sides of the HSDP core segment on the flat face of the HSDP core split. Samples were then drilled, centered on this line, perpendicular to the HSDP core axis at various azimuths (due to the azimuthally unoriented nature of the core). When continuous sections of core were encountered, samples were drilled with the same azimuth. After drilling, a longitudinal orientation mark was drawn along the top of each paleomagnetic samples before being trimmed to a length of 2.2 cm. End chips were tagged and saved for possible future use.

Measurements were made using a computer controlled, magnetically shielded cryogenic magnetometer with a background noise level of 5×10^{-12} Am^2, located within a magnetically shielded room at the Caltech Paleomagnetics Laboratory. 618 samples were subjected to progressive, static, three-axis, alternating-field (AF) demagnetization to 80 mT in steps ranging from 2.5 to 15 mT. Inclination data for 104 samples were also obtained by *Garnier et al.* [this issue] as part of their paleointensity analyses, which employed thermal demagnetization techniques. The inclination data resulting from their study is used in the flow averages along with our data obtained from AF demagnetization. Progressive ther-

mal demagnetization using 50 °C steps was performed on seven samples of our study in order to determine relative declination changes between multiple components of magnetization in partially remagnetized flow units, as discussed below.

Rock magnetic investigations of HSDP core samples were also undertaken by *Garnier et al.* [this issue]. Their high field thermomagnetic analyses and magnetic hysteresis measurements indicate that the primary carrier of magnetic remanence in these samples is pseudo-single-domain magnetite and/or titanomagnetite.

Sources of Uncertainty

With any volcanic rock core there is the possibility that apparent large shifts of paleomagnetic directions are the result of sample misorientation, inverted segments of core, block rotation, slumping, local magnetic anomalies, or self-reversing magnetic components. Sample and core segment orientations were the first factors checked when apparent polarity reversals were found in the data. This eliminated six apparent "events" which were highly suspect because they occurred within flows with otherwise normal inclinations. Since sample end pieces could be matched to the sample using the longitudinal orientation mark, and end pieces could be matched with the outer core surface using vesicles, fractures, and/or one or both of the blue/red orientation lines, sample orientation could be verified. If there was any doubt then new samples were drilled in the same segment. In four of the six cases of core inversion, comparison of the blue/red vertical orientation lines with the orientation marks made during our sampling revealed that short segments of the core (typically < 0.3 m) were inverted during

packaging or subsequent handling. In order to confirm this, we carefully examined the broken ends of adjacent segments and compared lithologic and structural variations (grain size, olivine content, vesicles, fractures, flow boundaries, etc.) in adjacent sections. Continuity of these variations could be used independently of the orientation lines to reconstruct the vertical orientation of questionable segments. In two cases, segments of broken core were clearly inverted before the lines were drawn.

In all cases of inclination change described in this paper, the relevant core sections can be unambiguously fitted to adjacent core segments with normal inclinations and all lithologic/structural variations are oriented consistently within the context of that particular region of the core. When present, the partial thermal overprints from normal-polarity overlying flows rule out multiple-flow slumps and self-reversing magnetic components. Thermomagnetic experiments and determinations of paleointensity did not reveal evidence for self-reversing mineralogy [*Garnier et al.*, this issue].

During the drilling operation, the position of the hole at depth was obtained by magnetic single-shot surveys to determine the direction and angle of the drill hole. This was used to test the validity of our assumption that the sides of the core were positioned vertically. These measurements show that the hole was an average of 1.7° from vertical, with a surface projection of the bottom of the hole located 31.32 m from the top of the hole at an azimuth of 248° (Table 1). Individual depth intervals between measurements smoothly ranged from 0.5° to 2.5° from vertical. Based on these data we can assign a specific uncertainty to samples from each depth interval (Table 1).

Detailed studies of the sources of error in outcrop-based paleomagnetic studies of Hawaiian lava flows have been performed by *Doell and Cox* [1963] and *Holcomb et al.* [1986]. Given the results of their studies and the circumstances of this study, the two largest presumed sources of error in our data are the possible rotation of blocks or intraflow deformation after individual flows have cooled below their blocking temperatures and the influence of magnetic anomalies existing over the paleosurface where the flow was deposited. Block rotations are difficult to detect, but in general the upper portions of some flows show the most evidence for possible small-scale block rotations during cooling. These areas, identified by their rubbly, blocky appearance were avoided by sampling the interiors of flows. The shifts in inclination reported here are typically recorded in only one or two flow units. It would be unlikely for large-scale block rotation or slumping to affect these units without affecting immediately underlying or overlying units. Flow contacts in units suspected of rotation were examined for this, as large rotations of individual units should drastically alter the continuity of flow contacts. The error due to intraflow deformation measured by *Holcomb et al.* [1986] was ~2.0°.

The uncertainties arising from local magnetic anomalies are perhaps the largest unknown factor, and according to some workers [*Baag et al.*, 1995] could render paleomagnetic data from highly magnetic rocks such as basalts completely uninterpretable. On the other hand, *Doell and Cox* [1963] performed comparisons of paleomagnetic measurements and geomagnetic observatory data for historic flows, and discrepancies were estimated to be 1° - 1.5°. An analysis of hundreds of paleomagnetic sampling sites by *Holcomb et al.* [1986] led to an estimate of 2.2° for the error due to local magnetic anomalies, and *Hagstrum and*

Champion [1994] found that paleomagnetic directions recorded by historic flows were not significantly affected by local magnetic anomalies.

We computed the 1 σ error for individual lava flows by assuming ± 2° of error from intraflow deformation and ± 2.2° of error from magnetic anomaly effects [*Holcomb et al.*, 1986] along with the appropriate value of vertical uncertainty from Table 1. These uncertainties were added in a root-mean-squared fashion to the within-flow dispersion inherent in the paleomagnetic data. The resulting 1 σ error for all 195 lava flows has a mean value of 4.96°, which is consistent with the estimate of ~ 5° for intraflow variations by *Hagstrum and Champion* [1994]. Some flows with high dispersion may actually be compound flows comprised of distinct subunits. This is the case for flow unit 15, which we subsequently divided into two flows for this study. While uncertainties of this magnitude may be significant for highly detailed secular variation studies for short time periods [e.g., *Holcomb et al.*, 1986; *Hagstrum and Champion*, 1994], they are relatively insignificant for the purposes of this study, where the relevant inclination shifts are of the order 25° - 80° and long-term secular variation changes are of the order 60°.

General Results

Nearly all samples exhibited stable demagnetization behavior, with highly linear demagnetization paths occurring after AF levels of 0 - 40 mT (Figure 2a). Inclinations for individual samples were determined by principal-components, least-squares analyses [*Kirschvink*, 1980] and were averaged for each of the 195 sampled flows along with inclination data from thermal demagnetizations of single samples from 104 of the same flow units [*Garnier et al.*, this issue] . Of the flow units which have both types of data, thermal and AF demagnetizations

produced nearly identical results. Twenty-four samples near the tops of flow units showed strong evidence for partial remagnetization by the overlying flow, and these were removed for computing flow averages, leaving 705 total samples. The inclination data may be downloaded directly from the HSDP World Wide Web site (http://expet.gps.caltech.edu/Hawaii_project.html) or the Caltech Paleomagnetics Laboratory site (http://www.gps.caltech.edu/MagLab/) and will be updated as more samples are analyzed.

Flow inclination means and their $\pm$ 1 σ total uncertainties are shown in Figure 3 as a function of depth and interpolated age. The age interpolation was performed as three separate linear fits (0 - 180 m, 180 - 416 m, and 416 - 1050 m), based on K/Ar and $^{40}Ar/^{39}Ar$ dates on whole-rock samples [*Sharp et al.*, this issue], one radiocarbon date based on two ashes at 178 m depth [*Beeson et al.*, this issue], and the constraint that the top of the core is approximately zero age. This is intended to provide a crude approximation of paleomagnetic inclination as a function of age down the core. This also aids in estimating the approximate time-resolution of the data, although rates of deposition could be highly variable on short timescales. If rates are assumed to be linear, the three intervals described above would have average deposition rates of one lava flow per every 3 kyr from the present to ~ 40 ka, every 7 kyr from ~ 40 ka to ~ 285 ka, and 0.6 kyr from ~ 285 ka to ~ 400 ka, respectively. Such variations are expected due to changes in eruptive style from the early shield-building stage of Mauna Kea to a slowdown in growth, followed by a transition to volcanics from Mauna Loa, which is now growing more rapidly than Mauna Kea [*DePaolo and Stolper*, this issue; *Lipman and Moore*, this issue].

To a first order, the paleomagnetic inclination record in the HSDP core shows large, mostly continuous inclination swings, ranging from approximately 0° - 65°. However, there are also short flips of polarity and sudden shifts of inclination away from consistent trends to shallow values. Some of these features are followed by a continuation at the same trend of inclination as before the departure. If this is of geomagnetic origin, it could have very important consequences to our understanding of the relationship between secular variation and excursions of the geomagnetic field. In the following sections we present details of the specific geomagnetic phenomena and discuss the secular variation recorded by the HSDP core.

Geomagnetic Phenomena

Feature A

Beginning with the topmost feature, there is an abrupt change of paleomagnetic inclination at 177 m depth (Figure 4) from a steady trend of high positive inclinations (~45°) in units 30 through 27 to a very shallow inclination of 0.9° ± 3.2° in unit 23. This unit is a 10-m-thick, massive, aphyric basalt which spans three different core runs. The pattern of inclination variation surrounding unit 23 is one of steadily increasing values from +43.8° ± 6.0° in unit 30 (205.1 m) to +54° ± 3.37° in unit 20 (160.9 m). The jump to shallow inclination in unit 23 is followed by a return to the same trend. There is the possibility that there are substantial changes in the field direction between successive lava flows, and that unit 23 is merely "catching" a typical swing of secular variation. However, it would be difficult to achieve the consistent trend of inclination recorded between flows 30 and 20 by randomly sampling a distribution of secular variation with a dispersion

equal to that seen in the overall core. If the shallow inclination of unit 23 is the result of "normal" secular variation occurring briefly during an extended time of subdued variation, then this becomes a matter of definition. Shallow inclinations could also result from a large-scale rotation of a block of unit 23 subsequent to cooling. This would produce highly irregular flow contacts, especially at the top of the unit. Examination of the core material shows uniform, gradational flow contacts at both the top and bottom of this unit, indicating that significant block rotation did not occur. The anomalously shallow inclination of unit 23 thus appears to not be a feature of secular variation or block rotation.

Units 24 - 26, directly underlying unit 23, were not sampled. Unit 25 is a thin (0.3 m) basalt; units 24 and 26 (with an average depth of 178 m), are volcanic ashes and have a weighted average radiocarbon date of 38.6 ± 0.6 ka [*Beeson et al.*, this issue]. This date is also consistent with the island submergence curve of *Lipman and Moore* [this issue]. These data constrain the shallow inclination of unit 23 to have occurred very close in time to the Laschamp event, first discovered by *Bonhommet and Babkine* [1967] and K/Ar dated at 42.9 ± 7.8 ka [*Levi et al.*, 1990]. The sedimentary record of *Levi and Karlin* [1989] from the Gulf of California (7° higher latitude) displays a sudden shift of paleomagnetic inclination from normal steep values to +3° in this time period, which they infer to be correlative with the Laschamp event.

Preliminary paleointensity measurements on HSDP core samples [*Garnier et al.*, this issue] indicate that this feature may be associated with a low geomagnetic field intensity. Low paleointensities have been associated with anamalous paleomagnetic directions in volcanics of this approximate age in Iceland [*Levi et al.*, 1990] and France [*Roperch et al.*, 1988; *Chauvin et al.*, 1989], and in sediments

of this age from the western Pacific [*Yamazaki and Ioka*, 1994], to name a few examples. The coincidences of age, preliminary paleointensity determinations, and anomalous inclination behavior lead us to interpret this feature as possibly being associated with the Laschamp event.

Feature B

At 261.5 m depth, paleomagnetic inclination changes from +46.4° ± 5.5° in unit 43 to - 32.6° ± 3.7° in unit 42 (Figure 4). Unit 43 is an 18.3-m-thick moderately olivine phyric basalt, while unit 42 is a 0.25-m-thick aphyric basalt. Unit 41, directly overlying unit 42, is a 0.25-m-thick weathered ash which was not sampled. Unit 40 is a 1.7 m thick highly olivine phyric basalt and records a negative inclination of approximately -44° (single sample) which is fully opposite the pre-reversal value. Moving upward, there is an erosional surface within unit 39 (at 258.8 m depth) including a baked sand layer on top. We obtained a reversed magnetization for a sample just below this contact, suggesting that unit 39 is a compound flow and the bottom of unit 39 is a distinct flow approximately 0.3 m thick (designated in Figure 4 to be unit 39.5). This unit yielded a shallow, negative inclination (-7°), which may be either a transitional direction or the result of partial remagnetization by unit 39 above. Unit 39, a 1-m-thick sparsely olivine phyric basalt, records a positive inclination (22.8° ± 7.8°) immediately above the contact with unit 39.5.

This polarity shift is especially interesting because it falls very close to the boundary between Mauna Kea flows (below) and Mauna Loa flows (above) at ~280 m depth [*Stolper et al.*, this issue]. Beach sands present in unit 38 indicate that these units were deposited very close to sea level. The island submergence

curve of *Lipman and Moore* [this issue] provides an approximate upper constraint on the age of this boundary at 95 ka. The lack of adequate potassium in lava flows from this region of the core has hampered dating efforts, although *Sharp et al.* [this issue] have produced an $^{40}Ar/^{39}Ar$ age of 132 ± 32 ka for unit 43 (268.2 m depth, Figure 4).

The most widely documented excursion or event near that time is the Blake event. This event has been reported from studies of deep sea sediments [e.g., *Smith and Foster*, 1969; *Creer et al.*, 1980; *Tric et al.*, 1991], lacustrine sediments [*Eardley et al.*, 1973; *Yaskawa*, 1974], and loess deposits [*Zhu et al.*, 1994] . A whole-rock K/Ar age of 128 ± 33 ka was obtained by *Champion et al.* [1988] from a basalt flow in New Mexico which displays a transitional paleomagnetic direction and low paleointensity. This age is consistent with those obtained for the Blake event from sedimentary extrapolations of deposition rate, which range from 105 ka [*Ryan*, 1972] to 161 ka [*Aksu*, 1983]. The global nature of the Blake event has been fairly well established, and it appears to have lasted 4 - 16 kyr based on average sedimentary deposition rates. Using the rough estimates of time-resolution described above, the average time between flows which we have sampled is of the order 3 - 7 kyr. Although the short-term rates of lava deposition could be highly variable, the fact that 3 - 4 flows in the HSDP core recorded negative inclinations indicates that the event we observe at 260 m may have lasted for several thousands of years. Due to the strong evidence for reversed directions and the available dating constraints, we correlate this event with the Blake event.

Feature C

At ~ 320 m depth, inclinations jump from +31.5° ± 6.4° in unit 56 to a fully reversed -48.2° ± 4.6° in unit 55, which is a 5.4 m thick moderately- to highly-olivine phyric basalt spanning two core runs (Figure 4). The reversed inclinations of unit 55 are followed by a return to positive inclinations in unit 54. This feature is surrounded by a gradually decreasing trend of positive inclination (Figures 3 and 4) which continues after the jump in unit 55.

Potassium content in this region of the core was much more favorable to $^{40}Ar/^{39}Ar$ dating techniques. This feature is well bracketed by the four dates [*Sharp et al.*, this issue] between 299 m and 416 m shown in Figure 3. Since unit 55 was clearly deposited between two of the dated flows, even the most conservative approach yields the useful constraint of 191 - 236 ka by taking the extreme limits for the ages immediately above and below. The lava deposition in this interval has resulted in a linear relationship between age and depth (or flow unit) within analytical uncertainty, yielding an estimate for unit 55 of 226 ± 7 ka [*Sharp et al.*, in press].

Ryan [1972] identified several brief polarity reversals in sedimentary cores from the Caribbean and Mediterranean, one of which he estimated to be ~200 ka old. He named it the Jamaica event and since that time there have been other studies (reviewed by *Champion et al.* [1988]) identifying reversed-polarity rocks of similar age, including the Lake Biwa record of *Yaskawa* [1974]. Recently, *Herrero-Bervera et al.* [1994] have produced multiple records of a reversed-polarity interval which they dated at 218 ± 10 ka and named the Pringle Falls event. This matches the estimated age of feature C within uncertainties. The dates (with

associated errors) reported for the published records of events near this time cannot rule out the possibility that there is only one event near 200 ka, and we observe only one event in this period. While our record could have missed other nearby events, it does provide support for at least one global polarity event occurring in the time period 191 - 236 ka. We will refer to this as the Jamaica/ Biwa I/Pringle Falls event.

In order to further characterize this event, we undertook progressive stepwise thermal demagnetizations of samples from near the top of flow unit 55 and the top of flow unit 56. This was done with the goal of finding partial thermal overprints produced by the emplacement of a hot flow unit on top of the already cooled flow. Stepwise demagnetization enables measurement of the relative declination change between the primary magnetization and the partial overprint [*Champion et al.*, 1988], which is important in discerning excursions or polarity events from large swings of secular variation.

For this experiment, seven samples were taken 1.65 m – 2.98 m from the top of flow unit 55 (below an altered zone of rubble), and five samples were taken 0.2 m – 0.5 m from the top of flow unit 56. These samples were thermally demagnetized in ~50° C increments up to 405° C. There was no detectable overprint in unit 56 from reheating by unit 55. For the samples from unit 55, blocking temperatures of the overprint increased from essentially 0° C for the top sample (no overprint) to ~250° C for the lowest sample. The lower four samples yielded overprints sufficient for least-squares principal component analysis [*Kirschvink*, 1980] and comparison with primary magnetizations. A representative thermal demagnetization is shown in Figure 2b. The phenomenon of stronger overprinting toward the center of the flow may be related to a change in coercivity of the

carriers of remanence as a function of cooling rate, which has been noted previously in Hawaiian basalts [*Doell and Cox*, 1963, 1965]. The top of the flow, which cools more quickly than the middle, is typically finer grained and can result in magnetic domains of higher coercive force. A detailed study of a 30 m - 60 m thick basaltic lava flow in the northwestern United States [*Audunsson and Levi*, 1992] also showed that there can be extensive zonation of magnetic properties in a lava flow with the central section being less magnetically stable than the upper.

An equal-area diagram showing both components from the four lowest samples in unit 55 is shown in Figure 5. The inclination of the overprint matches that determined from samples of unit 54, within error. Based on these preliminary results, the relative declination change from the primary component to the overprint component is 75.4° ± 10°. This confirms that unit 55 recorded a drastic change in total paleomagnetic direction at ~226 ka. The detailed correlation of this event with published records of the Jamaica/Biwa I/Pringle Falls event will be addressed in a separate paper.

Other shallow-inclination features

The remainder of the HSDP core below feature C is characterized by a higher rate of lava flow deposition and fewer sudden changes of inclination. Although there are no reversely magnetized samples in this part of the record (Figure 3), there are five instances below feature "C" where the inclination approaches horizontal: unit 90 at 465 m depth, units 139 - 141 at ~ 685 m, unit 168 at 826 m, units 182 and 186 at ~ 895 m, and unit 214 at 1000 m. The age at the bottom of the core is fairly well constrained to be ~400 ka [*Sharp et al.*, this issue]. These inclinations are within the limits of secular variation and tend to occur within

continuous inclination swings, similar to the shallow inclination located at 300 m depth (unit 49, Figure 4) which occurs immediately after feature C and at the end of a long swing of inclination from much higher values (Figure 4). It is possible that one or more of these periods of shallow inclination may be related to previously recorded excursions or events, but without declinations or more precise age control, any attempts to perform such a correlation or to even claim that they are excursional would be highly speculative.

Secular Variation

Much has been written concerning the hypothesis of a lack of non-dipole geomagnetic field components in the central Pacific region [*Doell and Cox*, 1971, 1972; *McWilliams et al.*, 1982; *Peng and King*, 1992; *Mankinen and Champion*, 1993]. This has not been extended back in time more than ~15 kyr due to the paucity of older data sequences. Although the HSDP core data are inclination-only, they may be used to address several important questions regarding secular variation and non-dipole field components in general. The mean inclination for all flows, excluding those with reversed inclinations, is 30.9° as calculated according to *McFadden and Reid* [1982] for inclination-only data, with an α_{95} radius of 2.27°. This is significantly lower than the 35.6° expected from a geocentric axial dipole, and consistent with a time-averaged field including an axial quadrupolar (g_2^0) component [*Wilson*, 1970, 1971]. The dispersion of the inclination data about the mean is 12.5°, which agrees with the dispersion of inclination dispersion data for 0 - 5 Ma from global secular variation databases [e.g., *Quidelleur et al.*, 1994] and the predictions of simple secular variation models [e.g., *Constable and Parker*, 1988; *Quidelleur and Courtillot*, in press]. Hence, there is a significant non-dipole field contribution when averaging over the past ~400 kyr. How-

ever, the inclination data (Figure 3) show considerable variation in their mean and dispersion over timescales of ~ 10 - 50 kyr. This may indicate that there are large variations in the amount of non-dipole contribution to the geomagnetic field, or possibly even variations in the dipole component, over these timescales.

The data show a pattern of inclination swings which result in a series of repeating shallow inclination values below 400 m depth (Figure 3). This pattern appears to be a feature of secular variation with a periodicity of the order ~ 10 - 50 kyr. Typical secular variation has periodicities less than ~ 10 kyr [*Courtillot and Lemouel*, 1988]. Geomagnetic field variations on a longer timescale were recently reported by *Yamazaki and Ioka* [1994], who found inclination variations of several degrees amplitude with a periodicity of 40 - 50 kyr in sedimentary inclination records from the western Pacific. They suggest that orbital forcing may be the ultimate source of their long-term inclination variations. This follows the work of *Negrini et al.* [1988] who performed a spectral analysis of sedimentary paleomagnetic records from the northwest United States and found peaks with periodicities close to those of orbital parameters. In sediments, however, there is the possibility that fluctuations of inclination with this periodicity may be the result of periodic changes in lithology which affect the degree of compaction-induced inclination shallowing. The record from the HSDP core demonstrates the existence of a real component of secular variation with a period greater than 10 kyr, because there are no known processes other than the geomagnetic field which could affect volcanic records of paleomagnetic inclination in such a periodic manner. A spectral analysis of the HSDP inclination record is required in order to address this question in more detail.

One of the most intriguing aspects of the HSDP inclination data is how short-term variations of the geomagnetic field appear to be superimposed upon long-term trends. For example, the inclination jump in unit 55 (feature C, Figures 3 and 4) occurs during a steady decrease in inclination which persists for at least ~ 50 kyr around this feature. Although not as pronounced, there is also a consistent trend surrounding the large inclination shift recorded by unit 23 (feature A, Figures 3 and 4). These observations indicate that short-term deviations of the geomagnetic field from stable polarity states may not necessarily be related to more subtle, long-term variations.

Summary

The paleomagnetic inclination record obtained from the pilot core of the Hawaii Scientific Drilling Project is the longest continuous volcanic record of geomagnetic field inclination yet reported. This record contains two brief inclination reversals which we tentatively correlate with the Blake and Jamaica/Biwa I/ Pringle Falls events, and an anomalous inclination which may associated with the Laschamp event. These are the first records of these events to be found in the central Pacific region, and provide evidence that they are global features rather than localized perturbations of the geomagnetic field. Long-term variations of the geomagnetic field are recorded in the HSDP core and are significant when conservative estimates of the known uncertainties are included. Two of the sudden inclination shifts (the Jamaica/Biwa I/Pringle Falls and the possible Laschamp records) appear to be superimposed upon these long-term trends. This might suggest that sudden changes of geomagnetic field direction (e.g., excursions or events) and long-term secular variation are caused by two separate processes that produce geomagnetic field variations at different timescales.

Acknowledgements

We would like to thank Jonathan Hagstrum and Edward Mankinen for their thoughtful reviews; Duane Champion, Xavier Quidelleur , Liz Warner Holt and Toshitsugu Yamazaki for helpful discussions, and Warren Sharp for providing radiometric ages soon after obtaining them. We are grateful to Catherine Kissel for spearheading the monumental task of drilling 1132 paleomagnetic samples from the 1 km core. Portions of this work were supported by NSF Grants EAR-9117588 and EAR-9419041. This is California Institute of Technology Contribution no. 5619.

References

Aksu, A.E., Short-period geomagnetic excursions recorded in Pleistocene sediments of Baffin Bay and Davis Strait, *Geology*, *11*, 537-541, 1983.

Audunsson, H. and S. Levi, Magnetic Property Zonation in a Thick Lava Flow, *J. Geophys. Res.*, *97* (B4), 4349-4360, 1992.

Baag, C., C.E. Helsley, S. Xu, and B.R. Lienert, Deflection of paleomagnetic directions due to magnetization of underlying terrain, *J. Geophys. Res.*, *100* (B7), 10,013-10,027, 1995.

Baker, M.B., S. Alves, and E.M. Stolper, Petrography and petrology of the Hawaiian Scientific Drilling Project samples, *J. Geophys. Res.*, this issue.

Beeson, M.H., D.A. Clague, and J.P. Lockwood, Origin and depositional environment of clastic deposits in the Hilo drill hole, Hawaii, *J. Geophys. Res.*, this issue.

Bonhommet, N. and J. Babkine, Sur la presence d'aimantation inversees dans la Chaine de Puys, *C.R. Acad. Sci. Paris*, *264*, 92-94, 1967.

Champion, D.E., M.A. Lanphere, and M.A. Kuntz, Evidence for a new geomagnetic reversal from lava flows in Idaho: Discussion of short polarity reversals in the Brunhes and late Matuyama polarity chrons, *J. Geophys. Res.*, *93* (B10), 11,667-11,680, 1988.

Chauvin, A., R.A. Duncan, N. Bonhommet, and S. Levi, Paleointensity of the earths magnetic-field and K-Ar dating of the Louchadiere volcanic flow (central France) - new evidence for the Laschamp excursion, *Geophys. Res. Lett.*, *16* (10), 1189-1192, 1989.

Constable, C.G. and R.L. Parker, Statistics of the geomagnetic secular variation for the past 5 m.y., *J. Geophys. Res.*, *93*, 11569-11581, 1988.

Courtillot, V. and J.L. Lemouel, Time variations of the earth's magnetic field - from daily to secular, *Ann. Rev. Earth Plan. Sci.*, *16*, 389-476, 1988.

Creer, K.M., P.W. Readman, and A.M. Jacobs, Palaeomagnetic and palaeontological dating of a section at Gioia Tauro, Italy: identification of the Blake event., *Earth Planet. Sci. Lett.*, *31*, 37-47, 1980.

DePaolo, D.J. and E.M. Stolper, Models of Hawaiian volcano growth and plume structure: Implications of results from the Hawaii Scientific Drilling Project, *J. Geophys. Res.*, this issue.

Doell, R.R., Paleosecular variation of the Honolulu volcanic series, Oahu, Hawaii, *J. Geophys. Res.*, *77* (11), 2129-3730, 1972.

Doell, R.R. and A. Cox, The Accuracy of the Paleomagnetic Method As Evaluated from Historic Hawaiian Lava Flows, *J. Geophys. Res.*, *68* (7), 1997-2009, 1963.

Doell, R.R. and A. Cox, Paleomagnetism of Hawaiian Lava Flows, *J. Geophys. Res.*, *70* (14), 3377-3405, 1965.

Doell, R.R. and A. Cox, Pacific Geomagnetic Secular Variation, *Science*, *171*, 248-254, 1971.

Doell, R.R. and A. Cox, The Pacific geomagnetic secular variation anomaly and the question of lateral uniformity in the lower mantle, in *The Nature of the Solid Earth*, edited by E.C. Robertson, pp. 245-284, McGraw-Hill, New York, 1972.

Eardley, A.J., R. Shuey, V. Gvosdetsky, W. Nash, M. Picard-Dane, D. Grey, and G. Kukla, Lake cycles in the Bonneville Basin, Utah, *Geol. Soc. Am. Bull.*, *84*, 211-215, 1973.

Fisher, N.I., T. Lewis, and B.J.J. Embleton, *Statistical Analysis of Spherical Data*, 329 pp., Cambridge University Press, Cambridge, 1987.

Garnier, F., C. Laj, E. Herrero-Bervera, C. Kissel, and D.M. Thomas, Preliminary determinations of the geomagnetic field intensity for the last 450 kyr from the Hawaii Scientific Drilling Project core, Big Island, Hawaii., *J. Geophys. Res.*, this issue.

Hagstrum, J.T. and D.E. Champion, Paleomagnetic correlation of late quaternary lava flows in the lower east rift-zone of Kilauea Volcano, Hawaii, *J. Geophys. Res.*, *99* (B11), 21679-21690, 1994.

Harland, W.B., R.L. Armstrong, A.V. Cox, L.E. Craig, A.G. Smith, and D.G. Smith, *A Geologic Time Scale*, Cambridge University Press, Cambridge, 1989.

Herrero-Bervera, E., C.E. Helsley, A.M. Sarna-Wojcicki, K.R. Lajoie, C.E. Meyer, M.O. McWilliams, R.M. Negrini, B.D. Turrin, J.M. Donnelly-Nolan, and J.C. Liddicoat, Age and correlation of a paleomagnetic episode in the western united-states by Ar-40/Ar-39 dating and tephrochronology - the Jamaica, Blake, or a new polarity episode, *J. Geophys. Res.*, *99* (B12), 24091-24103, 1994.

Holcomb, R., D. Champion, and M. McWilliams, Dating recent Hawaiian lava flows using paleomagnetic secular variation, *Geol. Soc. Am. Bull.*, *97*, 829-839, 1986.

Jacobs, J.A., *Reversals of the Earth's Magnetic Field*, 346 pp., Cambridge University Press, Cambridge, 1994.

Kirschvink, J.L., The least-squares line and plane and the analysis of paleomagnetic data: examples from Siberia and Morocco, *Geoph. J. Royal Astr. Soc.*, *62*, 699-718, 1980.

Levi, S., H. Audunsson, R.A. Duncan, L. Kristjansson, P.Y. Gillot, and S.P. Jakobsson, Late Pleistocene geomagnetic excursion in Icelandic lavas - confirmation of the Laschamp excursion, *Earth Planet. Sci. Lett.*, *96* (3-4), 443-457, 1990.

Levi, S. and R. Karlin, A sixty thousand year paleomagnetic record from Gulf of California sediments: secular variation, late Quaternary excursions and geomagnetic implications, *Earth Planet. Sci. Lett.*, *92*, 219-233, 1989.

Lipman, P.W. and J.G. Moore, Mauna Loa lava-accumulation rates at the Hilo drill site: formation of lava deltas during a period of declining overall volcanic growth, *J. Geophys. Res.*, this issue.

Mankinen, E.A. and D.E. Champion, Broad trends in geomagnetic paleointensity on Hawaii during Holocene time, *J. Geophys. Res.*, *98* (B5), 7959-7976, 1993.

McFadden, P.L. and A.B. Reid, Analysis of palaeomagnetic inclination data, *Geophys. J. R. Astron. Soc.*, *69*, 307-319, 1982.

McWilliams, M.O., R.T. Holcomb, and D.E. Champion, Geomagnetic secular variation from C-14-dated lava flows on hawaii and the question of the pacific non-dipole low, *Philosophical Transactions of the Royal Society of London Series a Mathematicaland Physical Sciences*, *306* (1492), 211-222, 1982.

Negrini, R.M., K.L. Verosub, and J.O. Davis, The middle to late Pleistocend geomagnetic field recorded in fine-grained sediments from Summer Lake, Oregon, and Double Hot Springs, Nevada, U.S.A., *Earth Planet. Sci. Lett.*, *87*, 173-192, 1988.

Peng, L. and J.W. King, A late quaternary geomagnetic secular variation record from Lake Waiau, Hawaii, and the question of the Pacific nondipole low, *J. Geophys. Res.*, *97* (B4), 4407-4424, 1992.

Quidelleur, X. and V. Courtillot, On low-degree spherical harmonic models of paleosecular variation, *Phys. Earth Planet. Inter.*, in press.

Quidelleur, X., J.-P. Valet, V. Courtillot, and G. Hulot, Long-term geometry of the geomagnetic field for the last five million years: An updated secular variation database, *Geophys. Res. Lett.*, *21* (15), 1639-1642, 1994.

Rhodes, J.M., The geochemical stratigraphy of the lava flows sampled by the Hawaii Scientific Drilling Project, *J. Geophys. Res.*, this issue.

Roperch, P., N. Bonhommet, and S. Levi, Paleointensity of the Earth's magnetic field during the Laschamp excursion and its geomagnetic implications, *Earth Planet. Sci. Lett.*, *88*, 209-218, 1988.

Rubin, M., L.K. Gargulinski, and J.P. McGeehin, Hawaiian Radiocarbon Dates, in *Volcanism in Hawaii: USGS Professional Paper 1350*, edited by R.W. Decker, T.L. Wright, and P.H. Stauffer, United States Government Printing Office, Washington, 1987.

Ryan, W.B.F., Stratigraphy of late Quaternary sediments in the eastern Mediterranean, in *The Mediterranean Sea*, edited by D.J. Stanley, pp. 149-169, Dowden, Hutchinson, & Ross, Stroudsburg, Pa., 1972.

Sharp, W.D., J.W. Holt, and P.R. Renne, Correlation of a 226 ±7 ka paleomagnetic excursion in lavas from Mauna Kea, Hawaii with the Pringle Falls excursion (abs.), *Eos Trans. AGU*, in press.

Sharp, W.D., B.D. Turrin, P.R. Renne, and M.A. Lanphere, 40Ar/39Ar and K/Ar Dating of core from the Hilo drill site, Hawaiian Scientific Drilling Project, *J. Geophys. Res.*, this issue.

Smith, D.J. and J.H. Foster, Geomagnetic reversal in Brunhes normal polarity epoch, *Science*, *163* (565-567), 1969.

Stolper, E.M. and M.B. Baker, Hawaii Scientific Drilling Project Core Logs (Summary information; Composite lithologic column; Logs for boxes 1-354), pp. 471, California Institute of Technology, Pasadena, California, 1994.

Stolper, E.M., D.J. DePaolo, and D.M. Thomas, The Hawaii Scientific Drilling Project: Introduction to the Special Section, *J. Geophys. Res.*, this issue.

Thouveny, N. and K.M. Creer, On the brevity of the Laschamp excursion, *Bulletin De La Societe Geologique De France*, *163* (6), 771-780, 1992.

Tric, E., C. Laj, J.P. Valet, P. Tucholka, M. Paterne, and F. Guichard, The Blake geomagnetic event - transition geometry, dynamic characteristics and geomagnetic significance, *Earth Planet. Sci. Lett.*, *102* (1), 1-13, 1991.

Wilson, R.L., Permanent aspects of the Earth's non-dipole magnetic field over upper Tertiary times, *Geophys. J. R. Astron. Soc.*, 1970.

Wilson, R.L., Dipole offset - the time-averaged palaeomagnetic field over the past 25 million years, *Geophys. J. R. Astron. Soc.*, *22*, 491-504, 1971.

Yamazaki, T. and N. Ioka, Long-term secular variation of the geomagnetic field during the last 200 kyr recorded in sediment cores from the western equatorial Pacific, *Earth Planet. Sci. Lett.*, *128*, 527-544, 1994.

Yaskawa, K., Reversals, excursions and secular variations of the geomagnetic field in the Brunhes normal polarity epoch, in *Palaeolimnology of Lake Biwa and the Japanese Pleistocene*, edited by S. Horie, pp. 77-88, Kyoto University, Kyoto, Japan, 1974.

Zhu, R.X., L.P. Zhou, C. Laj, A. Mazaud, and Z.L. Ding, The Blake geomagnetic polarity episode recorded in Chinese loess, *Geophys. Res. Lett.*, *21* (8), 697-700, 1994.

Depth (m)	N-S (m)	E-W (m)	Total (m)	T.A.D. (deg)	P.A.D. (deg)
0	0	0	0	0	
68.28	0.01	-0.59	0.59	0.5	0.5
184.1	-0.18	-2.59	2.6	0.81	0.99
288.65	-1.02	-5.91	6	1.19	1.86
367.28	-1.8	-9.25	9.42	1.47	2.49
457.2	-2.44	-12.52	12.76	1.6	2.12
548.64	-3.26	-15.6	15.93	1.66	1.99
640.08	-3.95	-18.49	18.91	1.69	1.86
731.52	-4.51	-21.42	21.89	1.71	1.87
827.23	-5.51	-24.38	24.99	1.73	1.85
944.88	-6.94	-27.39	28.26	1.71	1.59
1054.61	-8.22	-30.23	31.32	1.7	1.6

Table 1. Measurements of the deviation of the drill hole from vertical, adapted from *Stolper and Baker* [1994]. N-S is deviation in North (+)/South (-) plane; E-W is deviation in East (+)/West (-) plane; total is the resultant of N-S and E-W deviations; T.A.D. is total (average) angular deviation at the measured depth; P.A.D. is partial angular deviation, or the deviation from vertical between successive measurements. The P.A.D. is used in computing the uncertainty of the inclination measurements for paleomagnetic samples.

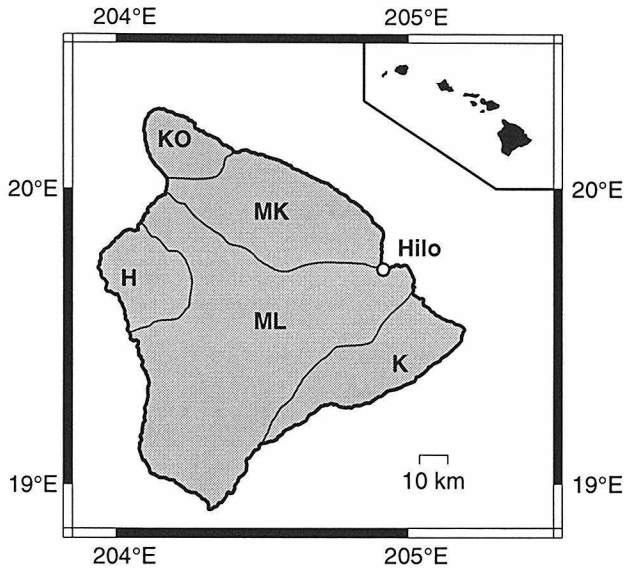

Figure 1. Location map showing the island of Hawaii, largest of the Hawaiian Islands (inset, upper right). The core was drilled near the shore at Hilo (open circle). Boundaries are shown for surficial lava flows from Kohala (KO), Mauna Kea (MK), Hualalai (H), Mauna Loa (ML) and Kilauea (K) Volcanoes in order of general age (after *Rubin et al.* [1987]).

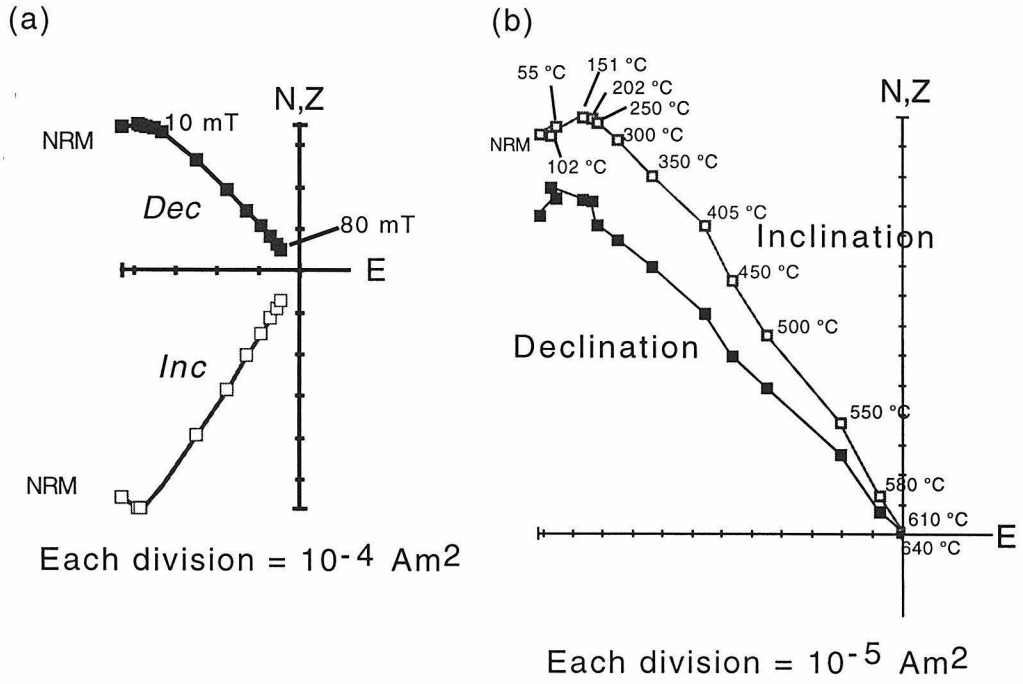

Figure 2. Demagnetization diagrams. Orthogonal projections of declination onto the horizontal plane (solid squares, vertical axis North) and inclination onto the vertical plane (open squares, vertical axis Z or Up). (a) Alternating-field demagnetization of a typical sample with positive inclination. Demagnetization levels are in mT. (b) Thermal demagnetization of a negative-inclination sample from unit 55, showing a partial positive-inclination overprint from the overlying flow, unit 54. Demagnetization levels are in degrees Celcius.

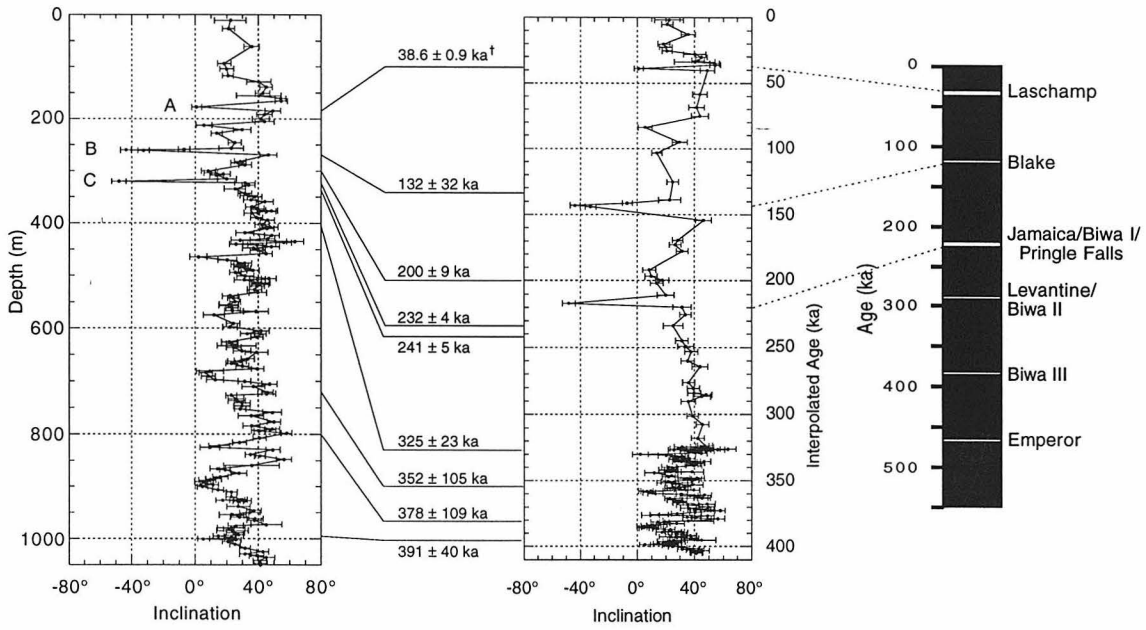

Figure 3. Overall inclination record and interpretation. Mean flow inclinations with ± 1 s error bars calculated from all known uncertainties plotted as a function of depth (left) and interpolated age (middle). All ages are from *Sharp et al.* [this issue], except for (†) from *Beeson et al.* [this issue]. Uncertainty calculations and age interpolations are discussed in the text. Geomagnetic polarity timescale for the past 500 ka (right) is adapted from *Champion et al.* [1988]. The inclination data is available from the HSDP World Wide Web site (http://expet.gps.caltech.edu/Hawaii_project.html) or the Caltech Paleomagnetics Laboratory site (http://www.gps.caltech.edu/MagLab/).

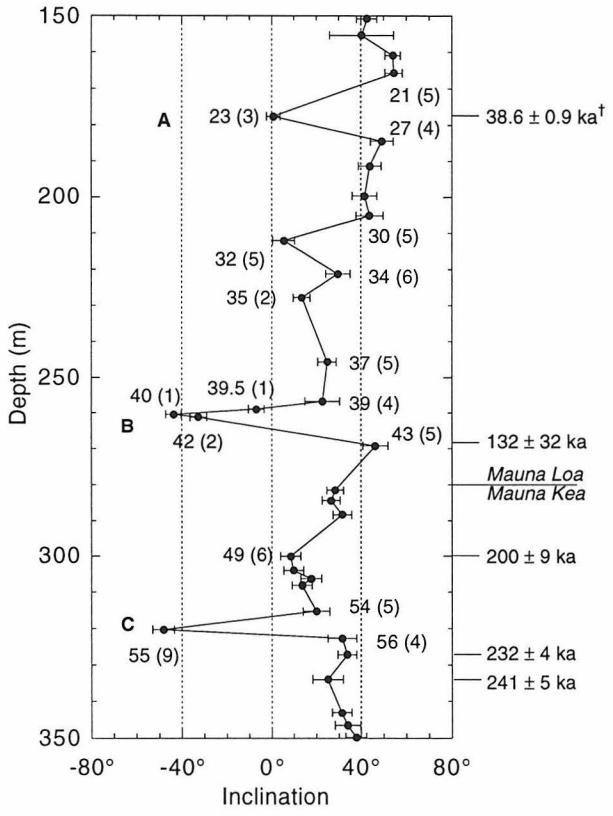

Figure 4. Detail of inclination record from 150 - 350 m depth, spanning inclination features A, B, and C (possibly the Laschamp, Blake, and Jamaica/Biwa I/Pringle Falls events, respectively). Flow unit numbers and the number of paleomagnetic samples from each (in parantheses) are shown for selected units. Ages are discussed in text and in Figure 3. Mauna Loa/Mauna Kea boundary shown for reference [*Stolper et al.*, this issue].

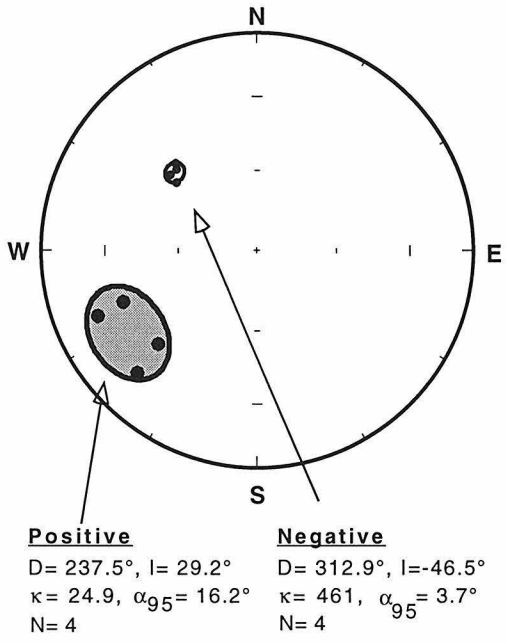

Figure 5. Equal-area diagram showing both overprint directions (solid circles, lower hemisphere projections) and primary directions (open circles, upper hemisphere projections) from samples of unit 55 subjected to stepwise thermal demagnetization (Figure 2b). The α_{95} ellipses for the Fisher means [*Fisher et al.*, 1987] of each component and associated stastistics (D, declination east of north; I, inclination, positive downward; k, precision parameter; N, number of samples) are shown. The relative declination change is 75.4° ± 10°.

II. An age constraint on Gulf of California rifting from Santa Rosalía, Baja California

Paper 5: Age of the Boleo Formation, Santa Rosalía basin, Baja California Sur, Mexico

John W. Holt, Elizabeth W. Holt, and Joann Stock
Division of Geological and Planetary Sciences
California Institute of Technology, Pasadena, CA 91125

To be submitted to:
Geological Society of America Bulletin

Abstract

Marine sedimentary rocks of the Santa Rosalía basin, Baja California Sur, were sampled in a pilot study to determine their suitability for magnetostratigraphy and geochronology with the goal of providing an age constraint on Gulf of California rifting. Progressive demagnetization experiments reveal that sandstones of the Boleo Formation, the earliest formation overlying the deeply-eroded basement, carry two-component magnetizations. The low-coercivity component matches the present-local field direction and is interpreted as a secondary overprint. The high-coercivity component appears to be a stable primary magnetic remanence with stratigraphically-bound normal-and reversed-polarity directions. Samples from the same horizon as a copper ore deposit did not retain a stable high-coercivity component. An $^{40}Ar/^{39}Ar$ isotopic age of 6.76 ± 0.45 Ma (1σ) was obtained for the *cinta colorada*, a tephra deposit within the Boleo Formation. Using the magnetostratigraphic constraints in conjunction with this isotopic age, correlation with the geomagnetic polarity time scale is possible, but depends on the exact age used for the *cinta colorada* and average sedimentation rates for the Boleo Formation. The most likely correlation yields an age of 7.1 ± 0.05 Ma for the base of the Boleo Formation and 6.21 ± 0.06 for the top, with an average sedimentation rate of 28 ± 4 cm/kyr. This is much earlier than the ~ 3.6 Ma commencement of seafloor spreading at the mouth of the Gulf of California and is probably related to an early phase of Gulf rifting caused by a change in Pacific - North America plate motions.

Introduction

The Gulf of California formed as a result of continental rifting and the transfer of crust between the North American and Pacific plates. This process began as early as ~ 12 Ma when the relative motion between the Pacific and North America plates began to change from obliquely convergent to strike-slip [*Stock and Hodges*, 1989]. The role of the offshore subduction zone and other faults associated with the oblique convergence decreased as the plate boundary eventually established itself within the present-day Gulf of California. Seafloor spreading in the southern Gulf began at ~3.6 Ma [*Larson*, 1972; *Curray and Moore*, 1984; *Lonsdale*, 1989], and is usually interpreted as the completion of peninsular transfer to the Pacific plate.

The transfer of the Baja California peninsula to the Pacific plate was a gradual process, however. According to some models [*Lonsdale*, 1989; *Umhoefer et al.*, 1994] , there may have been three distinct stages of development related to this process beginning with extension along the former volcanic arc from ~ 12 to ~ 6 Ma, the development of transform faults and pull-apart basins in from ~ 6 Ma to ~ 3.5 Ma, after which the peninsula was completely transferred to the Pacific plate and its motion relative to North America increased. However, the rate of divergence of Baja California from North America based on spreading lineations in the Gulf is slower than that predicted from global plate circuits since 3.6 Ma [*DeMets*, 1995], indicating that the peninsula was not completely coupled to the Pacific plate at that time.

In addition to seafloor lineations, information about Gulf of California rifting may come from sources on land. A distinctive pre-15 Ma conglomerate channel

deposit was correlated across the Gulf, suggesting ~ 300 km of extension since its deposition [*Gastil et al.*, 1981]. Extension and strike-slip faulting related to rifting has occurred within the Gulf Extensional Province surrounding the Gulf of California [*Gastil et al.*, 1975; *Stock and Hodges*, 1990; *Lee et al.*, 1996]. The faulting in this area gives us much information about the timing of early extension, but its relationship to actual Gulf formation is not clear.

A direct method for constraining the formation of the Gulf of California is the dating of marine sediments exposed along its margin. Numerous localities around the northern Gulf contain Pliocene marine rocks, but in several locations late Miocene, or even middle Miocene, marine rocks crop out or have been recovered from drill holes [summarized by *Smith*, 1991]. There is a caveat, however. This "protogulf" and its related pre-Pliocene extensional structures may have originated by plate boundary motion [*Spencer and Normark*, 1979; *Hausback*, 1984; *Humphreys and Weldon*, 1989; *Stock and Hodges*, 1989], but alternative hypotheses include Basin and Range extension [*Dokka and Merriam*, 1982; *Curray and Moore*, 1984; *Henry*, 1989] and back-arc extension [*Karig and Jensky*, 1972] unrelated to the plate boundary reconfiguration. Whether or not the protogulf is related to plate boundary motions, models which attempt to explain the paleogeography of the Gulf of California must account for the timing of marine sedimentation there. Since the age of marine rocks is yet to be established for many locations around the Gulf, the potential exists to substantially improve these models and perhaps to further our understanding of the rifting process.

Many of the marine sedimentary rocks found in the Gulf margins contain fossil assemblages which aid in correlations, in constraining paleogeography, and, to

some extent, in determining the general age of the rocks. For example, some fossils from sedimentary rocks in the Santa Rosalía area correlate with those found in several marine sequences around the Gulf [*Smith*, 1991], possibly including the Imperial Formation at the northern limit of the Gulf [*Wilson and Rocha*, 1955]. Unfortunately, many of these fossils are mollusks whose chronostratigraphic ranges are not well known [*Smith*, 1991] and may vary with latitude, as studies of some Gulf of California index fossils have suggested [*Natland*, 1950; *McCloy et al.*, 1988]. It is therefore useful to have an independent means by which to correlate and date marine sedimentary rocks around the Gulf margin. In this paper we report on a preliminary paleomagnetic and geochronologic study of early marine sediments from the Santa Rosalía basin, Baja California Sur, Mexico which was undertaken with this goal in mind.

Geologic Setting and Stratigraphy

In the Santa Rosalía area (Fig. 1), basement rocks are overlain by volcanic and sedimentary rocks of both marine and non-marine origin. Marine fossils within these rocks indicate the first transgression of oceanic waters into this area. These rocks are primarily located within the Boleo copper district, an ~ 30 km^2 area surrounding Santa Rosalía (Fig. 2). Due to the economic importance in the copper ore, this area has been mapped in considerable detail [*Wilson and Rocha*, 1955], and mining activities have continued intermittently until the present day. Predominately NNW-SSE striking dextral-normal faults have produced substantial dip in many of the sedimentary sequences, exposing the oldest rocks in arroyos trending at approximately at right angles to the coast (Fig. 2). Bedding dips range from subhorizontal to ~ 50° in the sampled units.

A generalized stratigraphic section for this area is shown in Fig. 3. Forming the basement, but scarcely outcropping in the Santa Rosalía area, is a quartz monzonite of unknown age which is overlain by a succession of andesitic to basaltic volcanic and pyroclastic rocks known as the Comondú volcanics [*Wilson*, 1948; *Wilson and Rocha*, 1955]. These volcanic rocks, dated at 12.3 ± 0.4 Ma and 12.5 ± 0.4 Ma [*Sawlan and Smith*, 1984], are strongly deformed and eroded, with ~450 m of paleorelief.

Unconformably overlying the Comondú volcanics is the Boleo Formation, a deltaic marine sequence with an average thickness of 140 m and consisting of a basal marine limestone overlain by localized gypsum and fossiliferous sandstone lenses, tuffaceous sandstone, and conglomerate [*Wilson*, 1948; *Wilson and Rocha*, 1955]. In places, the basal limestone has a primary dip of up to 30°, overlying topography on the Comondú volcanics. In outcrop, the bulk of the Boleo Formation consists of alternating, thick (3 - 70 m) sandstone and conglomerate layers. The location of the maximum conglomerate thickness moves seaward in progressively higher layers [*Wilson*, 1948], indicating a seaward migration of the depocenter over time. This could be due to concurrent deepening of the protogulf or to local uplift.

The five principal copper-ore-bearing horizons of the Boleo copper district are found within this formation [*Wilson and Rocha*, 1955] just above conglomerates and within tuffaceous sandstone layers. The megafossils of the Boleo Formation are found in localized channel deposits and deposits draping volcanic vents close to the irregular, rugged shoreline in shallow waters [*Wilson*, 1948; *Wilson and*

Rocha, 1955; *Smith*, 1991]. The Boleo Formation has variously been assigned an age of upper Miocene [*Aguilera*, 1906; *Arnold*, 1906] to lower or middle Pliocene [*Hertlein and Jordan*, 1927; *Wilson*, 1948; *Durham*, 1950; *Wilson and Rocha*, 1955] based on its fossil assemblage, and some of its fossils have been correlated to upper middle Miocene strata on Isla Tiburon in the northern gulf [*Smith et al.*, 1985].

A key stratigraphic unit within the Boleo Formation is a reddish to purplish coarse-grained cinder bed known as the "cinta colorada," which, on average, is about 0.5 m thick and ranges from a few decimeters to about 2 m [*Wilson*, 1948; *Wilson and Rocha*, 1955]. This lithic unit is composed largely of volcanic cinders of coarse ash to lapilli size, primarily of andesitic composition, with iron oxide cement (Wilson and Rocha, 1955). Unlike particular conglomerate or sandstone layers, the *cinta colorada* is a true time marker as it was deposited at one time over the entire area. This unit provides an opportunity to obtain a direct isotopic age for the Boleo Formation.

The top of the Boleo Formation is marked by an unconformity separating it from another fossiliferous formation. This unconformity is much more prominent inland than seaward, indicating that uplift of the inland region and/or subsidence of the gulf continued during deposition of the overlying sequence [*Wilson*, 1948], formerly known as the Gloria Formation [*Wilson*, 1948] and renamed Tirabuzón by Carreño [1982]. The Tirabuzón Formation (25 - 185 m thick, avg. 60 m) is composed primarily of fossiliferous marine sandstone and conglomerate. Fossils found within it indicate water depths up to 200 - 500 m [*Applegate and Espinosa*, 1981]. This environment, deeper than that interpreted for the Boleo Fm. [*Wilson and Rocha*, 1955], continued with the Infierno Formation (5-140 m thick, avg. 55

m) which unconformably overlies the Tirabuzón Fm. and also consists of fossiliferous marine sandstone and conglomerate, wedging into nonmarine conglomerate toward the west [*Wilson*, 1948]. The Tirabuzón and Infierno Formations have been regarded as middle and upper Pliocene, respectively, by most authors. The Pleistocene Santa Rosalía Formation unconformably overlies the Infierno Fm., and is comprised of thin fossiliferous sandstone and conglomerate beds.

Paleomagnetism

Sampling

Paleomagnetic sampling was undertaken in arroyos del Boleo and del Montado (Fig. 2). The Comondú Formation was sampled at site C (Fig. 2) where it directly underlies the basal limestone of the Boleo Formation. The basal limestone of the Boleo Fm. was sampled at sites A, B, and C (Fig. 2), the fossiliferous sandstone at site A (Fig. 2), the *cinta colorada* at site E (Fig. 2), and the top of the Boleo Fm. where it unconformably underlies the Tirabuzón Fm. at site G (Fig. 2). The Tirabuzón and Infierno Formations were sampled at sites F and H1-H9, respectively (Fig 2). Fifty-one core samples were drilled and oriented within these formations. The sampling was limited to the fine- to medium-grained units of each formation; the conglomerates are too coarsed-grained for paleomagnetic sampling. Paleomagnetic core samples were collected with a gasoline-powered drill using air-cooled, diamond-tipped, 25 mm diameter coring bits. Sample orientation was determined using a brass orienting sleeve in conjunction with magnetic and solar compasses. In addition, we obtained oriented block samples of the *cinta colorada* for the purposes of paleomagnetic analyses and isotopic age dating.

Measurements

Measurements of magnetization were made using a computer-controlled, magnetically-shielded SQUiD magnetometer with a background noise of 5×10^{-12} Am^2, located within a magnetically-shielded room. After measurements of natural remanent magnetism (NRM), progressive alternating and thermal demagnetization procedures were used in order to isolate the primary magnetic remanence, or characteristic remanent magnetization (ChRM), for each sample. Low-level alternating field (AF) demagnetizations were performed in 1.5 mT steps to a maximum of 17.5 mT, followed by thermal demagnetizations in 50 °C steps to a maximum of 675 °C.

Measurements of rock magnetic properties were also undertaken in order to constrain the carriers of remanence and aid in evaluating magnetization components. Hysteresis parameters and isothermal remanent magnetization (IRM) acquisition characteristics were measured on a vibrating sample magnetometer. The demagnetization of an anhysteritic remanent magnetization (ARM) acquired in a 1 mT biasing field and 100 mT AF was compared with the demagnetization of an IRM acquired in an 800 mT pulsed field. This modified Lowrie-Fuller test [*Lowrie and Fuller*, 1971] yields information on the domain state of the magnetic carriers of remanence.

Magnetizations

Progressive demagnetization revealed that most samples contained two components of magnetization (Figs. 4a,b). For magnetically stable samples a lower

coercivity component is removed after AF demagnetization and thermal demagnetization to 250°C, and a higher coercivity component is removed from ~ 250°C to ~ 600°C. The cinta colorada exhibited three components, two of which are low-coercivity, normal-polarity directions (Fig. 4c). Both normal- and reversed-polarity high-coercivity magnetizations were observed (Figs. 4a-c). Component directions were determined using least-squares principal component analysis [*Kirschvink*, 1980]. The low-coercivity directions are better grouped before tilt correction and their in-situ mean is indistinguishable from the present-local-field (PLF) direction (Fig. 5a). Therefore, we intrepret this component to be a viscous remanent magnetism (VRM) which is a secondary overprint.

Some samples exhibited erratic demagnetization behavior, achieving neither linear nor planar high-coercivity remanent magnetization directions, but these are confined to particular lithofacies or to a discrete stratigraphic horizon. Within the sampled portion of the Boleo Formation, ChRM's were unobtainable from the basal limestone layer (sampled at sites A, B, and C, Fig. 2), the fossiliferous sandstone, and a discrete stratigraphic horizon within the sandstone. Carbonates are typically very weakly magnetized, and the highly contaminated nature of the limestone [*Wilson*, 1948; *Wilson and Rocha*, 1955] probably further precludes the preservation of a primary remanence. The fossiliferous sandstone proved to be too coarse-grained for paleomagnetic analyses, with the possible exception of one sample (normal polarity).

The only samples which did not hold a ChRM within the lowest sandstone unit of the Boleo Formation were in precisely the same stratigraphic horizon as copper ore bed number 4 [*Wilson and Rocha*, 1955] which is found near this sampling location (site D, Fig. 2). The lack of a primary magnetization in these samples

could be the result of hydrothermal fluids related to ore deposition moving through this horizon, but not everywhere producing the copper ore. The confinement of this effect to a discrete horizon (~ 1.5 m) is consistent with the interpretation of copper ore deposition by Wilson and Rocha [1955], in which low-temperature fluids moved along bedding planes, confined by layers of lower permeability. Samples from the Tirabuzón and Infierno Formations showed low-coercivity overprints (included in Fig. 5a) but none contained stable high-coercivity components. These samples were probably too coarse-grained for a depositional remanence within the matrix to overcome the magnetic fields produced by larger grains oriented by other processes.

The high-coercivity directions for all samples which held ChRM's are shown in Fig. 5b. The mean of the tilt-corrected normal-polarity samples from the Boleo Fm. is statistically distinct from the in-situ present local field direction, and is due north, within uncertainty. The four reversed directions are due south within uncertainty. The normal and reversed directions are antipodal, with a positive reversal test [*McFadden and McElhinny*, 1990]. Due to these observations and stratigraphically-bound polarity reversals, we interpret the high-coercivity magnetizations as a primary magnetization, or ChRM.

Rock magnetics

Magnetic hysteresis parameters for a representative sample of the Boleo Fm. (Fig. 6a) suggest that single- or pseudo-single-domain magnetite is the primary carrier of remanence, in support of the Lowrie-Fuller test results which suggested the same domain-state characteristics. The IRM acquisition (Fig. 6b) is indicative of magnetite, due to the remanence becoming nearly saturated in fields of ~ 200

mT. Some higher-coercivity material such as goethite or hematite could be present, however. No difference in ChRM characteristics were observed between samples which yielded normal polarity directions and those of reversed polarity. Many samples held coherent magnetization directions up to 650°C, however (Fig. 4), indicating that at least part of the ChRM may be held by hematite.

Magnetostratigraphy

When the samples are viewed in stratigraphic context, two different geomagnetic polarity zones are observed (Fig. 7) which include three different stratigraphic levels. There is a normal-polarity zone in the basal part of the Boleo Formation, below the *cinta colorada*. The *cinta colorada* and the top of the Boleo Fm. are reversed polarity. The normal- and reversed-polarity samples are antipodal (Fig. 5b), within uncertainties. The possibility exists that more polarity reversals occur in unsampled intervals, but the three magnetostratigraphic control points available from these data, with the ~ 30 m of normal-polarity section at the base of the Boleo Formation, provide useful constraints for correlating this formation to the GPTS, as will be discussed later.

Geochronology

Samples of the *cinta colorada* were collected (site E, Fig. 2) for isotopic dating using the $^{40}Ar/^{39}Ar$ method [*Merrihue and Turner*, 1966; *McDougall and Harrison*, 1988]. A sample was crushed and plagioclase crystals were obtained by conventional heavy-liquid, magnetic, and hand separation techniques. Irradiation was performed at the nuclear reactor at the University of Michigan, with the

Fish Canyon Tuff sanidine [*Cebula et al.*, 1986] as the primary flux monitor, with an assigned age of 27.8 Ma. The J-factor [*Grasty and Mitchell*, 1966] calculated for the irradiation was 7.9696×10^{-4} for this sample. Analyses were performed at the University of California, Los Angeles, on a VG3600 rare gas mass spectrometer operated at ^{40}Ar sensitivity of 1.85×10^{-17} mol/mV with 2% uncertainty. The mass discrimination factor was 0.9934 ± 0.0021, determined by measuring atmospheric argon. Seventeen aliquots of plagioclase (~0.5 to 1.5 mg) were heated by a 5 W continuous laser for 1-3 minutes.

Due to the low amount of radiogenic argon in these aliquots (0.49% - 37.29%, mean 12.6%) model ages are not meaningful. Therefore, the inverse isochron method [*Turner*, 1971; *Roddick*, 1978] is used to determine and evaluate the age (Fig. 7). The points on this diagram should define a mixing line between trapped initial argon and purely radiogenic argon. The regression technique of York [1969] was used for the linear least-squares fitting, yielding an x-intercept of 0.212, with an uncertainty of 1.49×10^{-2}. Measurement blanks were calculated by linear interpolation between calibration blanks. This results in an isochron age of 6.76 ± 0.45 Ma (1-sigma) with a mean squared weighted deviation [MSWD, *McIntyre et al.*, 1966] of 0.98 which is very close to the ideal value of 1 and well within the acceptable range for 17 data points [0.31 - 1.69, *Wendt and Carl*, 1991] indicating that errors are primarily due to ^{40}Ar, the correlated isotope [*McIntyre et al.*, 1966; *York*, 1969].

The trapped $^{40}Ar/^{36}Ar$ ratio is 283.7, slightly less than the atmosphere's $^{40}Ar/^{36}Ar$ ratio of 295.5. This could either be due to the trapped initial argon not being completely equilibrated with the atmosphere or to errors in the analyses. This amount of deviation could easily be accounted for by slight variations in the mass

descrimination factor. This would have an insignificant effect on the age, however, due to the small amount of radiogenic argon, or proximity of the points to the y-axis (Fig. 7).

Discussion

Age of the basin

The *cinta colorada* overlies sedimentary rocks of the lower Boleo Fm. (Fig. 3) and therefore its age of 5.86 - 7.66 Ma (2-sigma) represents a minimum age for deposition in the Santa Rosalia basin. Since the age of the actual base of the Boleo Formation is not known, its age can be estimated given its stratigraphic distance from the cinta colorada and an average sedimentation rate. We do not have any firm constraints on the rate of sedimentation, but we do have other information which may be useful for constraining its age. These include magnetic polarity measurements of the lowest 30 m of the Boleo Fm. (normal), at the *cinta colorada* (reversed) and at the top of the Boleo Fm. (reversed). These constraints can be used in an attempt to match the top and bottom of the Boleo Fm. with reversed- and normal-polarity intervals of the geomagnetic polarity time scale (GPTS), respectively.

As the thickness of the Boleo Fm. varies somewhat and the *cinta colorada* is not at the same stratigraphic position everywhere [*Wilson and Rocha*, 1955], we have used 50 -90 m for the distance between the base of the Boleo Fm. and the *cinta colorada*, and 110 - 180 m for the distance from the *cinta colorada* and the top of the Boleo Formation [*Wilson and Rocha*, 1955]. The age of the top and bottom of the Boleo Formation can then be calculated as a function of sedimen-

tation rate given their stratigraphic distances from the *cinta colorada*. These age curves are essentially constraints on the range of polarity intervals in the GPTS which might correlate with the top and bottom of the Boleo Formation.

However, these calculations are highly dependent on the age used for the *cinta colorada*, so we must consider the available constraints on that age. The isotopic age determination yields a probability density function which is Gaussian [*McDougall and Harrison*, 1988], centered on the mean isochron age of 6.76 Ma with a 2-σ range of 5.86 - 7.66 Ma (Fig. 8a). In addition, the paleomagnetic polarity of this unit may be used to further constrain its age. Given that the *cinta colorada* has a reversed-polarity paleomagnetic direction, it must have been deposited during one of the reversed-polarity intervals of the GPTS. There are 7 such intervals within the isotopic age's 2-sigma range, varying in duration from 34 - 368 kyr (Fig. 8a). The probability that the *cinta colorada's* age falls within a normal polarity interval is zero (Fig. 8a), so the total age probability density function is a combination of the paleomagnetic and isotopic age probabilities (Fig. 8b). Using these criteria, the most likely age of the *cinta colorada* is a small interval surrounding the mean isochron age of 6.76 Ma. When the three ages of highest probability are compared, the probability that the *cinta colorada* is 6.76 $\pm$ 0.18 Ma is 6.5 times higher than the probability at ~7.2 Ma, and 12.4 times higher than the probability at ~6.25 Ma (Fig. 8b).

Age curves for the top and bottom of the Boleo Formation are therefore calculated and compared with the GPTS for three cases, using ages for the *cinta colorada* of 6.76 Ma (Fig. 9a), 7.2 Ma (Fig. 9b), and 6.25 Ma (Fig. 9c). The results are summarized in Table 2. The normal subchrons which may be correlated to the base of the Boleo Fm. are limited to those which allow a sufficient

duration of normal polarity to account for the 30 m of normal polarity section observed there (depicted by the dotted lines in Figs 9a-c). For example, this constraint causes subchron C4n.2n to be eliminated from consideration in the first case (Fig. 9a). Although this subchron appears to be of long duration, it is not long enough to produce 30 m of normal-polarity section at such low sedimentation rates (< 10 cm/kyr). The combined constraints eliminate any sedimentation rates outside of the range 24 - 32 cm/kyr for this case, and yield an age of 7.05 - 7.14 Ma for the base of the Boleo Formation. The top of the Boleo is constrained to be 6.14 - 6.27 Ma.

If the age of the *cinta colorada* is set to 7.17 Ma (Fig. 9b), the best correlation is at low sedimenation rates (7.5 - 12.5 cm/kyr). This yields an age for the base of 7.90 - 8.07 Ma (within subchron C4n.2n), and an age for the top of 5.23 - 5.90 Ma. In the third case, where the *cinta colorada* age is set to 6.26 Ma (Fig. 9c), correlation with the GPTS is possible at sedimentation rates of 30 - 48 cm/kyr, yielding a basal age of 6.45 - 6.57 Ma (within subchron C3An.2n) and an age for the top of the Boleo Fm. within the range 5.65 - 5.90 Ma.

The most likely correlation of the magnetostratigraphy and geochronology of the Boleo Fm. therefore gives an age of 7.1 $\pm$ 0.05 Ma for the base of the Boleo Formation and 6.2 $\pm$ 0.07 Ma for the top. The sedimentation rate required for this correlation (24 - 32 cm/kyr) is reasonable considering the deltaic environment of deposition[*Wilson*, 1948], and comparable to those found during basin formation at Loreto to the southeast [~ 40 cm/kyr, *Umhoefer et al.*, 1994] and in the Imperial Valley at the northernmost Gulf [>50 cm/kyr, *Johnson et al.*, 1983].

Tectonic Implications

The age of 7.1 Ma for the base of the Boleo Formation is useful for constraining models of the evolution of the North America – Pacific plate boundary during the period ~ 12 Ma to ~ 3.5 Ma. According to some models, the Baja California peninsula was essentially a microplate during that period, caught in the boundary zone between the Pacific and North American plates [e.g., *Stock and Hodges*, 1989]. Relative plate motion was partitioned between the boundaries to the west and to the east of the peninsula, and the relative amounts of displacement shifted over time. Strike-slip displacement on faults to the west gradually decreased, accompanied by an increase in extension along NNW-striking faults to the east. Although a change in the direction of relative plate motions and the style of extension may have occurred around 6 Ma [*Lonsdale*, 1989; *Umhoefer et al.*, 1994], the timing of increased extension is not well constrained by seafloor magnetic lineations, however [*Lonsdale*, 1989; *Stock and Hodges*, 1989] The appearance of marine sedimentation on top of highly eroded basement in the Santa Rosalía area at ~ 7.1 Ma suggests a sudden change in base level, perhaps due to an increase in the rate of extension at about that time.

An age of ~ 6.8 ± 0.3 Ma was obtained from pumice lapilli within marine sediments near Puertecitos, in the northern Baja California Gulf margin (Stock, unpublished data). This is nearly identical to our results from the Santa Rosalía basin, suggesting that there was an extensive seaway existing in the Gulf region by ~ 7.0 Ma. This precedes seafloor spreading in the mouth of the gulf by ~ 3.5 myr [e.g., *Lonsdale*, 1989] and indicates that continental rifting progressed quickly after the change in Pacific-America relative motion from strike-slip to obliquely divergent after ~ 12 - 10 Ma [*Stock and Hodges*, 1989].

An additional result of the paleomagnetic data is the observation that negligible vertical-axis rotation has occurred within the sampling area since ~ 7.0 Ma. Mean directions of normal- and reversed-polarity samples from the Boleo Formation (Fig. 5b) are aligned with geographic north and south, respectively, within uncertainty. This is in contrast to results from the Puertecitos volcanic province where as much as 50° of clockwise rotation has been observed in some areas [*Lewis*, 1994] due to block rotation within a dextral shear zone. This implies that the margins of the Gulf Extensional Province may vary considerably in the manner in which extension is accomodated.

Conclusions

Through the combined use of magnetostratigraphy and geochronology, we have found that useful age constraints may be obtained from marine sedimentary rocks in the Gulf of California margin. Although sampling was of a reconnaissance nature, the earliest marine sedimentary rocks in the Santa Rosalía basin were constrained to be 7.1 ± 0.05 Ma (most likely age) using the magnetostratigraphic correlation with the GPTS, which is a tighter constraint than using the isotopic age of 6.76 ± 0.45 Ma from the *cinta colorada* tephra unit alone. The paleomagnetic results also indicate negligible vertical-axis rotation in the sampling area since ~ 7.0 Ma. More detailed sampling could help to further verify the GPTS correlation, and to provide a more useful overall magnetostratigraphy for correlation with rock sequences found elsewhere. When data such as these are available for more locations around the Gulf, our understanding of the paleogeography of the Gulf of California, and hence plate boundary evolution, may be significantly improved.

Acknowledgements

This work was supported by NSF grants No. EAR-9019289, EAR-9419041, and EAR-9296102. We are pleased to thank Joseph L. Kirschvink for use of the Caltech Paleomagnetics Laboratory, Mahmoud Chaudry for preparing mineral separates, Marty Grove at UCLA for performing the argon measurements, Elizabeth Nagy for performing initial argon statistics, Xavier Quidelleur for assisting in blank corrections and additional statistical analyses, and Rob Coe for the use of his rock magnetic facilities at UCSC. Also, muchas gracias to the hombre with the huge tractor who pulled our truck across the flooding river at Colonia San Vicente Guerrero.

References

Aguilera, J.G., Les gisements carboniferes de Coahuila (Mexico), *Proceedings of the International Geological Congress*, 10, (1), 244, 1906.

Applegate, S.P. and L. Espinosa, *The geology and selachian paleontology of Loma del Tirabuzon (Corkscrew Hill), Santa Rosalia, B.C.S.*; in Geology of northwestern Mexico and southern Arizona, Universidad Nacional Autonoma de Mexico, Instituto de Geologia, 1981.

Arnold, R., *The Tertiary and Quaternary pectens of California*, United States Geological Survey, Professional Paper, 47, 1906.

Cande, S.C. and D.V. Kent, Revised calibration of the geomagnetic polarity timescale for the Late Cretaceous and Cenozoic, *Journal of Geophysical Research*, 100, (B4), 6093-6095, 1995.

Carreño, A.L., Biostratigraphy of the Loma del Tirabuzón (Corkscrew Hill), Santa Rosalia, Baja California Sur, Mexico, Third North American Paleontological Convention, 1982.

Cebula, G.T., M.J. Kunk, H.H. Mehnert, C.W. Naeser, J.D. Obradovich and J.F. Sutter, The Fish Canyon Tuff, a potential standard for the $^{40}Ar/^{39}Ar$ and fission-track dating methods, *Terra Cognita*, 6, 139-140, 1986.

Curray, J.R. and D.G. Moore, *Geologic history of the mouth of the Gulf of California*; in Tectonics and Sedimentation along the California Margin, Pacific Section S.E.P.M., 1984.

DeMets, C., A reappraisal of seafloor spreading lineations in the Gulf of California: Implications for the transfer of Baja California to the Pacific plate and estimates of Pacific-North America motion, *Geophysical Research Letters*, 22, (24), 3545-3548, 1995.

Dokka, R.K. and R.H. Merriam, Late Cenezoic extension of northeastern Baja California, *Geological Society of America Bulletin*, 93, 371-378, 1982.

Durham, J.W., *Megascopic paleontology and marine stratigraphy*, Pt. 2 of the E. W. Scripps cruise to the Gulf of California, GSA Memoir, 43, 1950.

Fisher, N.I., T. Lewis and B.J.J. Embleton,*Statistical Analysis of Spherical Data*,Cambridge University Press,Cambridge,1987.

Gastil, G., G. Morgan and D. Krummenacher, *The tectonic history of peninsular California and adjacent Mexico*; in The geotectonic development of California, Prentice-Hall, Englewood Cliffs, New Jersey, 1981.

Gastil, R.G., R.P. Phillips and E.C. Allison, Reconnaissance geology of the state of Baja California, *Geological Society of America Memoir*, 140, 1975.

Grasty, R.L. and J.G. Mitchell, Single sample potassium-argon ages using the omegatron, *Earth and Planetary Science Letters*, 1, 121-122, 1966.

Hausback, B.P., *Cenozoic volcanic and tectonic evolution of Baja California Sur, Mexico*; in Geology of the Baja California Peninsula, Society of Economic Paleontologists and Mineralogists, 1984.

Henry, L.G., Late Cenozoic Basin and Range structure in western Mexico adjacent to the Gulf of California, *Geological Society of America Bulletin*, 101, 1147-1156, 1989.

Hertlein, L.G. and E.K. Jordan, Paleontology of the Miocene of Lower California, *Proceedings of the California Academy of Sciences*, 26 (4th ser.), (19), 605-647, 1927.

Humphreys, E.D. and R.J. Weldon, *Kinematic constraints on the rifting of Baja California*; in The Gulf and Peninsular Provinces of the Californias, Amer. Assoc. Petrol. Geol. Memoir, 1989.

Johnson, N.M., C.B. Officer, N.D. Opdyke, G.D. Woodard, P.K. Zeitler and E.H. Lindsay, Rates of late Cenozoic tectonism in the Vallecito-Fish Creek basin, western Imperial Valley, California, *Geology*, 11, 664-667, 1983.

Karig, D.E. and W. Jensky, The proto-gulf of California, *Earth and Planetary Science Letters*, 17, 169-174, 1972.

Kirschvink, J.L., The least-squares line and plane and the analysis of paleomagnetic data: examples from Siberia and Morocco, *Geoph. J. Royal Astr. Soc.*, 62, 699-718, 1980.

Larson, R.L., Bathymetric, magnetic anomalies, and plate tectonic history of the mouth of the Gulf of California, *Geological Society of America Bulletin*, 83, 3345-3360, 1972.

Lee, J., M.M. Miller, R. Crippen, B. Hacker and J.L. Vazquez, Middle Miocene extension in the Gulf Extensional Province, Baja California: Evidence from the southern Sierra Juarez, *Geological Society of America Bulletin*, 108, (5), 505-525, 1996.

Lewis, C.J., *Constraints on extension in the Gulf Extensional Province from the Sierra San Fermin, Northeastern Baja California, Mexico*, thesis, Harvard University, 1994.

Lonsdale, P., *Geology and tectonic history of the Gulf of California*; in The Geology of North America, Geological Society of America, Boulder, Colo., 1989.

Lowrie, W. and M. Fuller, On the alternating field demagnetization characteristics of multidomain thermoremanent magnetization in magnetite, *Journal of Geophysical Research*, 76, 6339-6349, 1971.

McCloy, C., J. J.C. Ingle and J.A. Barron, Neogene stratigraphy, foraminifera, diatoms, and depositional history of Maria Madre Island, Mexico: evidence of early Neogene marine conditions in the southern Gulf of California, *Marine Micropaleontology*, 13, (3), 193-212, 1988.

McDougall, I. and T.M. Harrison, *Geochronology and Thermochronology by the 40Ar/39Ar Method*, Oxford University Press, New York, 1988.

McFadden, P.L. and M.W. McElhinny, Classification of the reversal test in paleomagnetism, *Geophysical Journal Int.*, 103, 725-729, 1990.

McIntyre, G.A., C. Brooks, W. Compston and A. Turek, The statistical assessment of Rb-Sr isochrons, *Journal of Geophysical Research*, 71, (22), 5459-5468, 1966.

Merrihue, C. and G. Turner, Potassium-argon dating by activation with fast neutrons, *Journal of Geophysical Research*, 71, 2852-2857, 1966.

Natland, M.L., *Report on the Pleistocene and Pliocene foraminifera, part IV of the E.W. Scripps cruise to the Gulf of California*, GSA Memoir, 43, 1950.

Roddick, J.C., The application of isochron diagrams in ^{40}Ar-^{39}Ar dating: A discussion, *Earth and Planetary Science Letters*, 41, 233-244, 1978.

Sawlan, M.G. and J.G. Smith, *Petrologic characteristics, age and tectonic setting of Neogene volcanic rocks in northern Baja California Sur, Mexico*; in Geology of the Baja California peninsula: Pacific Section, SEPM, 1984.

Smith, J.T., *Cenozoic marine mollusks and paleogeography of the Gulf of California*; in The Gulf and Peninsular Provinces of the Californias, The Gulf and Peninsular Provinces of the Californias, 1991.

Smith, J.T., J.G. Smith, J.C. Ingle, R.G. Gastil, M.C. Boehm, J.Q. Roldan and R.E. Casey, Fossil and K-Ar age constraints on upper middle Miocene conglomerate, SW Isla Tiburon, Gulf of California, *Geological Society of America Abstracts with Programs*, 17, (6), 409, 1985.

Spencer, J.E. and W.R. Normark, Tosco-Abreojos fault zone: A Neogene transform plate boundary within the Pacific margin of south Baja California, Mexico, *Geology*, 7, 554-557, 1979.

Stock, J.M. and K.V. Hodges, Pre-Pliocene extension around the Gulf of California and the transfer of Baja California to the Pacific plate, *Tectonics*, 8, 99-115, 1989.

Stock, J.M. and K.V. Hodges, Miocene to recent structural development of an extensional accommodation zone, northeastern Baja California, Mexico, *Journal of Structural Geology*, 12, 315-328, 1990.

Turner, G., ^{40}Ar-^{39}Ar ages from the lunar maria, *Earth and Planetary Science Letters*, 11, 161-191, 1971.

Umhoefer, P.J., R.J. Dorsey and P. Renne, Tectonics of the Pliocene Loreto basin, Baja California Sur, Mexico, and evolution of the Gulf of California, *Geology*, 22, 649-652, 1994.

Wendt, I. and C. Carl, The statistical distribution of the mean squared weighted deviation, *Chemical Geology*, 86, 275-285, 1991.

Wilson, I.F., Buried topography, initial structures, and sedimentation in Santa Rosalia area, Baja California, Mexico, *Bulletin of the American Association of Petroleum Geologists*, 32, (9), 1762-1807, 1948.

Wilson, I.F. and V.S. Rocha, *Geology and Mineral Deposits of the Boleo Copper District Baja California, Mexico*, U. S. Geological Survey, Professional Paper, 273, 1955.

York, D., Least squares fitting of a straight line with correlated errors, *Earth and Planetary Science Letters*, 5, 320-324, 1969.

TABLE 1. PALEOMAGNETIC SAMPLES

Sample Code	Sample No.	Fm	Lith	Loc	Position (m)	GeoDec (deg)	GeoInc (deg)	StratDec (deg)	StratInc (deg)	N	MAD	HTR (°C)	Notes
IFA	9	Inf	FS	H9	33.6								
IFA	8	Inf	FS	H8	29.6								
IFA	7	Inf	FS	H7	23.6								
IFA	6	Inf	FS	H6	17.6								
IFA	5	Inf	FS	H5	15.6								
IFA	4	Inf	FS	H4	10.6								
IFA	3	Inf	FS	H3	06.0								
IFA	2	Inf	FS	H2	03.0								
IFA	1	Inf	FS	H1	00.0								
GFA	5	Tir	FS	F	10.9								
GFA	4	Tir	FS	F	08.4								
GFA	3	Tir	FS	F	03.9								
GFA	2	Tir	FS	F	00.4								
GFA	1	Tir	FS	F	00.0								
BFC	3	Bol	TS	G	03.0	168.1	-40.1	171.7	-21.8	11	5.1	250-575	
BFC	2	Bol	TS	G	02.5	156.2	-32.2	160.4	-14.7	11	8.1	250-575	
BFC	1	Bol	TS	G	00.0	189.7	-57.0	188.8	-37.1	9	3.3	350-575	
CCA	1	Bol	T	E		179.3	-33.5	180.2	-43.5	7	6.0	325-475	
BFB	17	Bol	TS	D	28.3	317.2	-12.9	317.6	7.4	9	20.4	350-575	
BFB	16B	Bol	TS	D	27.8	355.2	10.1	357.5	31.3	5	6.4	500-625	
BFB	16A	Bol	TS	D	27.8	354.8	08.4	356.8	29.7	5	6.1	475-575	
BFB	15	Bol	TS	D	26.6	17.2	-24.8	13.7	-6.6	8	6.1	375-575	
BFB	14	Bol	TS	D	26.5	13.1	04.5	16.1	22.9	8	4.5	375-575	
BFB	13	Bol	TS	D	24.0	339.1	-01.1	339.0	20.0	11	4.5	250-575	
BFB	*12*	*Bol*	*TS*	*D*	*19.0*	*176.8*	*-35.2*	*229.8*	*-62.9*	*7*	*8.8*	*250-500*	likely slumped block
BFB	11	Bol	TS	D	15.8	2.1	28.8	10.4	46.4	7	4.1	250-550	
BFB	10	Bol	TS	D	15.0	11.6	24.0	19.3	39.1	8	3.1	250-500	
BFB	9	Bol	TS	D	14.6	3.8	15.8	8.1	33.5	9	5.4	325-575	
BFB	8	Bol	TS	D	14.2								ore bed horizon
BFB	7	Bol	TS	D	13.7								ore bed horizon
BFB	6	Bol	TS	D	13.0	349.2	14.3	351.1	33.8	9	6.8	325-550	
BFB	5	Bol	TS	D	03.0	323.1	19.3	311.9	45.8	9	5.2	250-500	
BFB	4	Bol	TS	D	02.0	1.4	19.2	5.5	50.8	14	2.6	325-675	
BFB	3	Bol	TS	D	00.3	3.9	09.1	7.4	41.3	14	3.5	325-675	
BFB	2	Bol	TS	D	00.0	350.9	12.3	350.1	44.3	15	2.5	325-675	
BFB	18B	Bol	L	B									
BFB	18A	Bol	L	B									
BFB	1C	Bol	L	C									
BFB	1B	Bol	L	C									
BFB	1A	Bol	L	C									
BFA	1B	Bol	L	A									
BFA	1A	Bol	L	A									
BFA	5B	Bol	FS	A									
BFA	5A	Bol	FS	A									
BFA	4	Bol	FS	A		345.5	40.5	327.5	43.5	10	4.8	325-625	
BFA	3B	Bol	FS	A									
BFA	3A	Bol	FS	A									
BFA	2	Bol	FS	A									
CVA	1	Com	V	C		303.2	49.7	16.3	58.6	13	3.0	250-625	

Table 1: Paleomagnetic samples in relative stratigraphic order (youngest at top). Fm - formation (Inf=Infierno, Tir=Tirabuzón, Bol=Boleo, Com = Comondú); Lith - lithology (FS=fossiliferous sandstone, TS=tuffaceous sandstone, T=tuff, L=limestone, V=andesitic basalt); Loc - location (see Fig. 2); Position - approximate stratigraphic position within formation at sampling location; GeoDec - declination of in-situ ChRM direction; GeoInc - inclination of in-situ ChRM direction; StratDec - tilt-corrected GeoDec; StratInc - tilt-corrected GeoInc; N - number of pts used in least-squares; MAD -maximum angular deviation of linear least-squares fit (Kirschvink, 1980); HTR - high coercivity temperature range. Samples without data were unstable due to coarse-grained nature of rocks unless otherwise noted. Sample BFB-12 (in italics) was not used due to highly suspect bedding indicative of slumping.

TABLE 2. GPTS CORRELATION SUMMARY

Reference age for *cinta colorada* (Ma)	Relative probability*	Sed. rate (cm/kyr)	Boleo top (Ma)	Boleo base (Ma)	Boleo base subchron
6.76	1	28 ± 4	6.2 ± 0.07	7.1 ± 0.05	C3Bn
7.2	0.15	10 ± 2.5 23	5.57 ± 0.34 6.62 ± 0.05	7.99 ± 0.09 7.56	C4n.2n C4n.1n
6.25	0.08	39 ± 9	5.78± 0.13	6.51 ± 0.06	C3An.1n

* With probability of cinta colorada age being 6.76 Ma set equal to 1

Table 2: Summary of possible correlations of magnetostratigraphy and geochronology of the Boleo Formation with the GPTS, as depicted in Fig. 9. Reference ages and weighted probability determinations shown in Fig. 8. Subchron names as defined in Cande and Kent [1995].

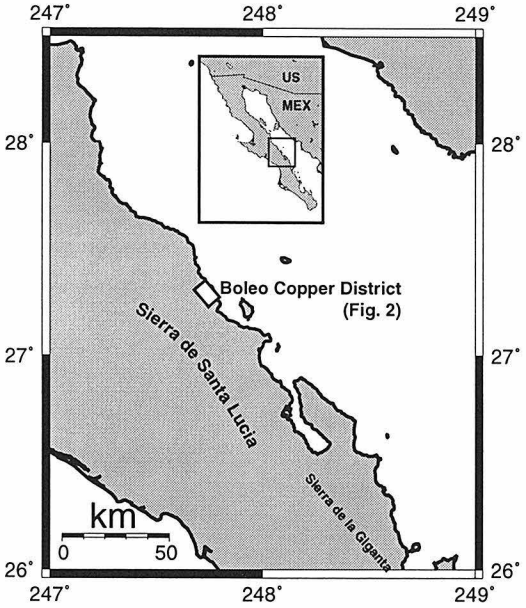

Fig. 1. Santa Rosalía is located within the Boleo Copper District (indicated by box) on the Baja California peninsula. See Fig. 2 for detail of sampling area.

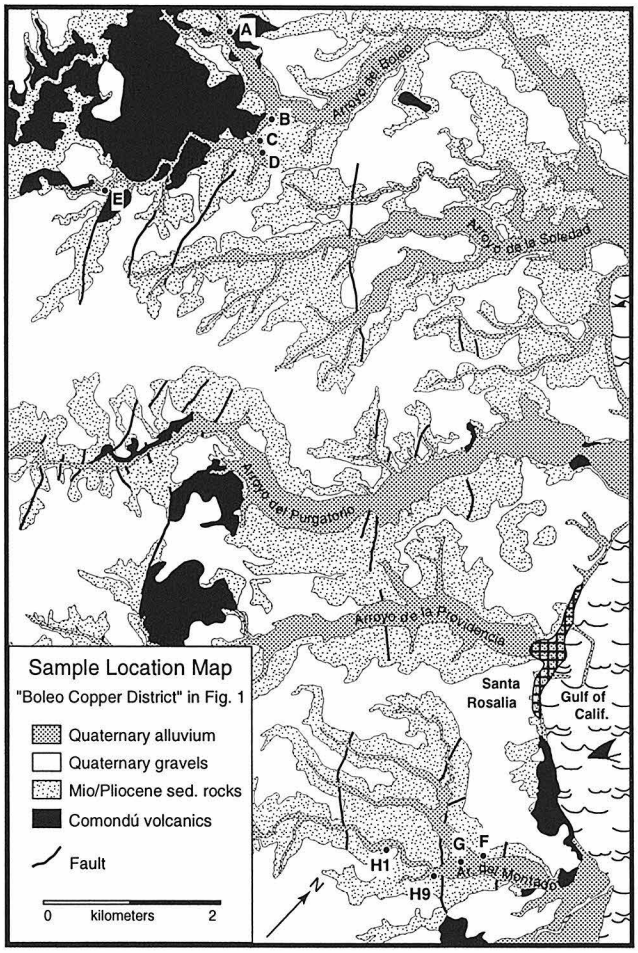

Fig. 2. Map of the Boleo copper district with distribution of rock types and major faults. For location of this area see Fig. 1. Sampling sites are indicated by points marked A - H. "Mio/ Pliocene sed. rocks" includes Boleo, Tirabuzón, and Infierno Formations. Adapted from Wilson and Rocha [1955].

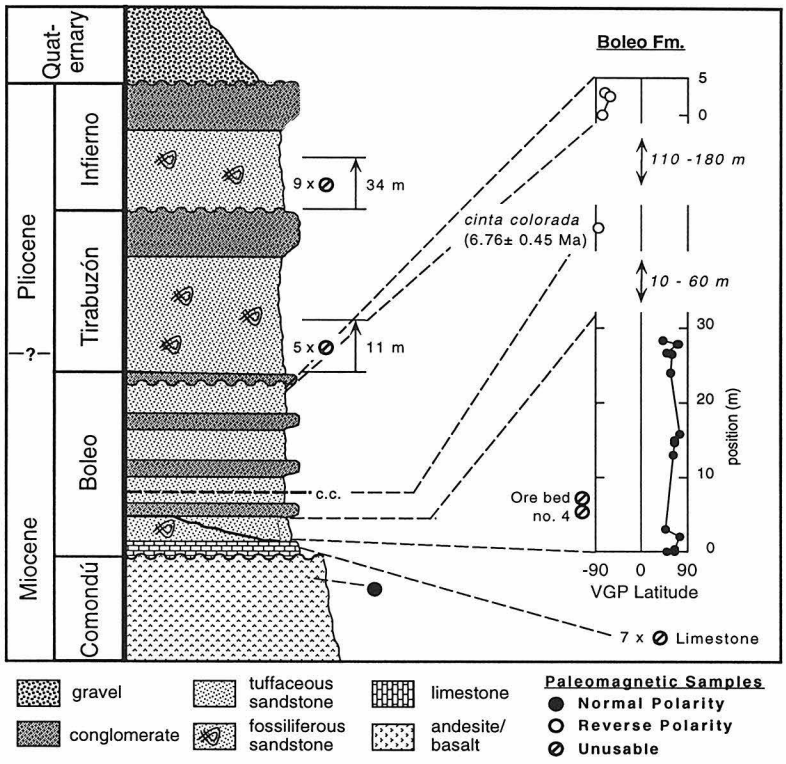

Fig. 3: Generalized stratigraphic column and magnetostratigraphy. Rocks of the Santa Rosalía basin are shown with paleomagnetic polarity (Comondú Fm.) or virtual geomagnetic latitude (VGP, Boleo Fm.). Stratigraphic column adapted from Wilson and Rocha [1955]. Note that only samples from the Boleo Formation and Comondú Fm. yielded stable paleomagnetic directions. One of the samples at 0 m is from the fossiliferous sandstone of the Boleo Formation.

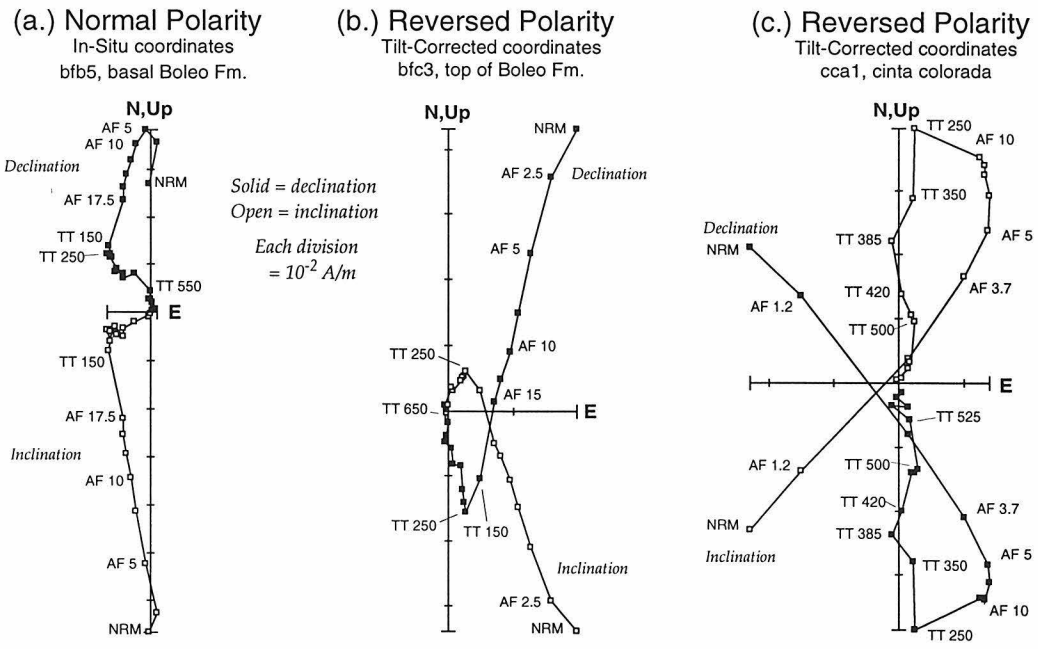

Fig. 4: Orthogonal demagnetization diagrams. Typical demagnetization characteristics for (a) normal polarity sandstone (b) reversed polarity sandstone, and (c) reversed polarity cinder tuff (*cinta colorada*). Declination (solid squares) is projected onto the horizontal plane; inclination (open squares) is projected onto the vertical plane. Demagnetization steps are denoted by AF (alternating field) in milliTeslas or TT (thermal) in °C. The maximum demagnetization step is 650° for these samples.

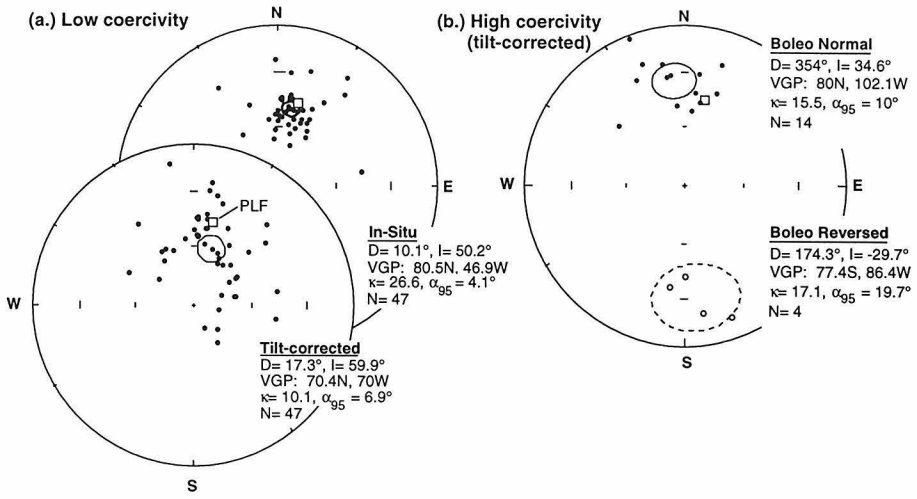

Fig. 5: Equal-area plots of magnetic remanence directions. (a.) Low coercivity and (b.) high coercivity directions. Solid circles represent lower-hemisphere projections, open circles represent upper. The present local field direction (PLF) for the sampling area is indicated by a square (lower-hemisphere projection). Low-coercivity directions are consistent with a PLF overprint acquired after structural tilting. As discussed in the text, this component is removed after low-level AF demagnetization and thermal demganetization to 250°C, and is therefore interpreted as a viscous remanent magnetization (VRM). High-coercivity directions include both normal and reversed polarities which are stratigraphically grouped (see Fig. 3). Parameters of Fisher statistics [*Fisher et al.*, 1987] shown for each grouping (D, declination east of north; I, inclination, positive downward; κ, precision parameter; N, number of samples). Ellipses represent 95% confidence regions (α_{95}).

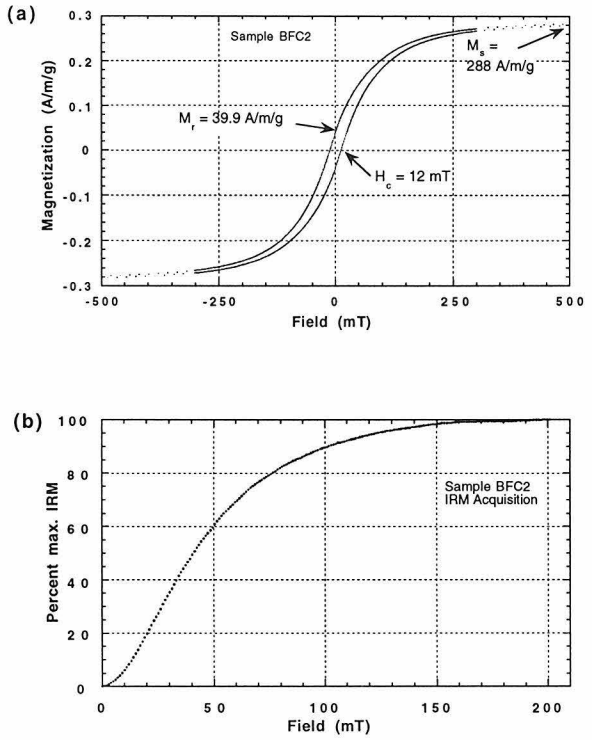

Fig. 6: Rock magnetic experimental results. (a.) Hysteresis parameters (H_C = bulk coercive force; M_S = saturation magnetization; M_r = remanent magnetization). The values of H_C = 12 mT and M_S = 288 A/m/g are consistent with magnetite. (b.) Acquisition of isothermal remanent magnetization (IRM) in pulsed fields of progressively greater strength. The IRM is nearly saturated in a field of 300 mT, consistent with a magnetite carrier of remanence.

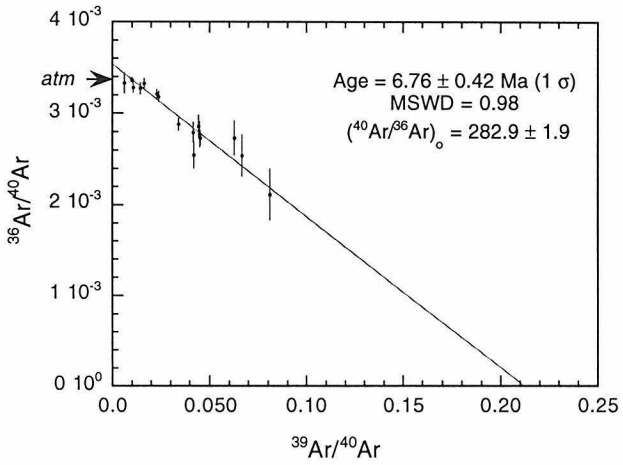

Fig. 7. Inverse isochron plot of *cinta colorada* isotopic age data. X-axis uncertainties are smaller than the data points. Note that the low radiogenic content (points close to y-axis) is the primary cause for uncertainty in the x-intercept, and hence, age of sample. Arrow on vertical axis indicates composition of atmospheric argon.

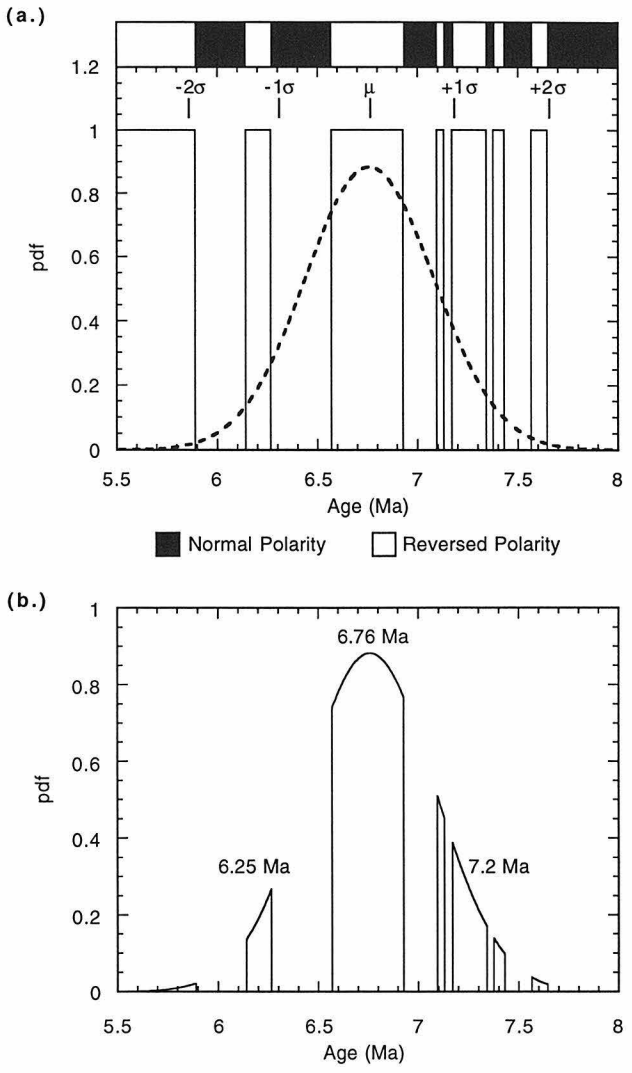

Fig. 8. Constraints on age of *cinta colorada*. (a.) Probability density function of isotopic age determination is shown (dashed line), with its associated mean (μ), 68% confidence interval (± 1σ), and 95% confidence interval (± 2σ). Also shown (solid line) is the probability density resulting from the constraint of reversed magnetic polarity for the *cinta colorada* using the GPTS of Cande and Kent [1995]. Note that the peak of isotopic age probability falls within a reversed-polarity interval. (b.) The combined age probability density function resulting from both constraints (un-renormalized). The probability that the *cinta colorada* falls within a given age interval is proportional to the area under that part of the curve. The area under the peak centered at 6.76 Ma is 6.6 times larger than the next largest area at 7.2 Ma and 12.4 times larger than the area at 6.25 Ma.

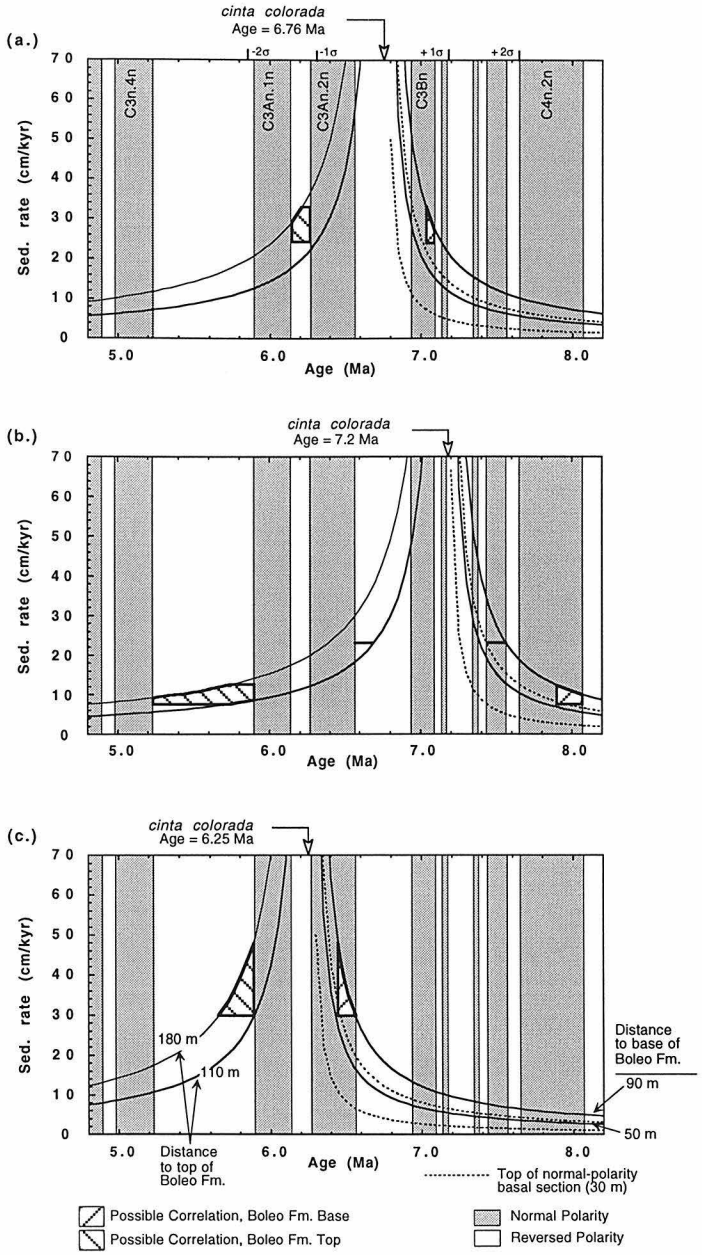

Fig. 9. Correlation of magnetostratigraphy and geochronlogy with GPTS for the three most probable ages of the *cinta colorada* : (a) the mean isochron age of 6.76 Ma , (b) 7.2 Ma, and (c) 6.25 Ma. Curved lines represent age of the top (curved left, toward younger ages) and bottom (curved right, toward older ages) of the Boleo Formation. Dotted lines represent the top of the normal-polarity zone observed at the base of the Boleo Formation. For a given sedimentation rate, the space between a solid line (base) and its associated dotted line must fall entirely within a normal polarity interval of the GPTS., while the top of the section falls within a reversed-polarity interval. Possible correlations are indicated with filled polygons for both the top and bottom of the Boleo Formation. Results summarized in Table 2. GPTS from Cande and Kent [1995].